(12)

ARO 14142.5-EX

the
ohio
state
university

research foundation
1314 kinnear road
columbus, ohio
43212

NON-STEADY VELOCITY MEASUREMENT OF
THE WAKE OF A HELICOPTER ROTOR AT
Low ADVANCE RATIOS

H. Terkel and H. R. Velkoff
Department of Mechanical Engineering

NOV 2 5 1981

A

September, 1981

81 11 24077

REPORT DOCUMENTATION PAGE		READ INSTRUCTIONS BEFORE COMPLETING FORM
1. REPORT NUMBER	2. GOVT ACCESSION NO.	3. RECIPIENT'S CATALOG NUMBER
4. TITLE *(and Subtitle)* ROTOR FLOW FIELD RESEARCH IN LOW SPEED HELICOPTER FLIGHT--Non-Steady Velocity Measurement of the Wake of a Helicopter Rotor at Low Advance Ratios		5. TYPE OF REPORT & PERIOD COVERED Interim July 1, 1979 - April 30, 1981
		6. PERFORMING ORG. REPORT NUMBER 761646/711999
7. AUTHOR(s) H.R. Velkoff and H. Terkel		8. CONTRACT OR GRANT NUMBER(s) DAAG29-79-C-0074
9. PERFORMING ORGANIZATION NAME AND ADDRESS The Ohio State University Research Foundation 1314 Kinnear Road Columbus, Ohio 43212		10. PROGRAM ELEMENT, PROJECT, TASK AREA & WORK UNIT NUMBERS P-14142-E
11. CONTROLLING OFFICE NAME AND ADDRESS U.S. Army Research Office Post Office Box 12211 Research Triangle Park, NC 27709		12. REPORT DATE September, 1981
		13. NUMBER OF PAGES 126
14. MONITORING AGENCY NAME & ADDRESS(if different from Controlling Office)		15. SECURITY CLASS. (of this report) Unclassified
		15a. DECLASSIFICATION/DOWNGRADING SCHEDULE

16. DISTRIBUTION STATEMENT *(of this Report)*

Approved for public release; distribution unlimited.

17. DISTRIBUTION STATEMENT *(of the abstract entered in Block 20, if different from Report)*

NA

18. SUPPLEMENTARY NOTES

The view, opinions, and/or findings contained in this report are those of the author(s) and should not be construed as an official Department of the Army position, policy, or decision, unless so designated by other documentation.

19. KEY WORDS *(Continue on reverse side if necessary and identify by block number)*

Helicopter Rotor
Rotor Flows
Rotor Wake
Hot-wire Anemometry

20. ABSTRACT *(Continue on reverse side if necessary and identify by block number)*

A system was developed which could measure the instantaneous velocities in the wake of a model helicopter rotor operating at low advance ratios. A three-wire hot film probe was mounted on a traverse and placed at many positions in the wake. The output of the probe was fed into an on-line computer operating in an interactive mode. Computer generated vector plots were made of both time averaged velocities and instantaneous velocities for the case of $\mu = 0.06$.

DD $_{1\ JAN\ 73}^{FORM}$ 1473   EDITION OF 1 NOV 65 IS OBSOLETE

Interim Report

Non-Steady Velocity Measurement of
the Wake of a Helicopter Rotor at
Low Advance Ratios

how

H. Terkel

H. R. Velkoff

September 1981

Department of Mechanical Engineering
The Ohio State University
Columbus, Ohio

Abstract

A system was developed which could measure the instantaneous velocities in the wake of a model helicopter rotor operating at low advance ratios. A three-wire hot film probe was mounted on a traverse and placed at many positions in the wake. The output of the probe was fed into an on-line computer operating in an interactive mode. Computer generated vector plots were made of both time averaged velocities and instantaneous velocities for the case of $\mu = 0.06$.

CHAPTER I

INTRODUCTION

Recent requirements for an Advanced Attack Helicopter
(AAH) whose primary missions will be anti-armor in a
battle zone, and low speed terrain flight (Nap-Of-The-
Earth, NOE) has increased the need for data of helicopter
rotor wakes at low advance ratios.

The blade tip vortices constitute the primary distur-
bances in the rotor wake, and contribute significantly to
the dynamic loads and acoustic characteristics of the
helicopter. Various sophisticated theories have been
developed to calculate the velocities of the wake, Refs. (1-6)
the vortex positions, and the resulting dynamic loads.
These have been compared to measured loads, but it is not
known whether the discrepancies are due to nonlinear and
3-dimensional effects or to inaccuracies in the predicted
vortex characteristics. It is, therefore, desirable to
obtain accurate measurements of the rotor wake, the vortex
position, and vortex characteristics.

Early measurements of the flow field used total
pressure tubes (Ref. 7). These results were very useful
in demonstrating the nonuniformity of the time averaged

1

flow. However the instantaneous velocities, which are especially important for accurate loads calculations, were not measured. Hot-film anemometers have been used for rotor wake studies and reported in Refs. 8, 9, and 10. The results of Ref. 8 allowed the structure of a tip vortex to be defined for the hover conditions tested, whereas in Ref. 9 and 10 the averaged velocities at low advance ratios were measured. Photographic techniques have also been used. Ref. 11 and 12 show results from two investigations using Schlieren photography systems. Water and smoke studies using photography are presented in Ref. 13 and 14. Both of these methods are useful for flow visualization, but data reduction is somewhat difficult and accuracy is not high. The first demonstrated use of a Laser Doppler Anemometer (LDA) for rotor investigation was that in Ref. 15. In more recent works with an LDA, such as Ref. 16, instantaneous as well as time averaged velocities were measured. The laser system allows flow measurements to be made very close to the blade, and the vortex velocity distribution and core size were determined.

Very little is known about the transition flight speed $(0 < \mu < 0.2)$ performance. At these speeds, very large wake distortion and very severe vibratory loads occur. The purpose of this work was to develop the instrumentation and the experimental methods needed to measure the instantaneous velocities in the vicinity of a small helicopter rotor

in a wind tunnel operated at low advance ratios and to make measurements of typical flow fields. The measurements were made with a three dimensional hot-film anemometer. The data acquisition was done by a DEC PDP 11/60 minicomputer with a GENRAD Analog to Digital System. A three dimensional traverse system was used to traverse the anemometer probe throughout the rotor wake.

CHAPTER II

BACKGROUND

One can distinguish between two different types of
velocity information at any point in the rotor wake. The
first type is the time-average velocities induced by the
helicopter's rotor in horizontal flight, which is the con-
stant term of the Fourier representation of the wake. The
second type of velocity information is the instantaneous
velocities induced by the rotor.

In a steady-state region of flight, the instantaneous
velocities are periodic with respect to time. The period
is equal to the time required for the rotor to turn through
an angle equal to that between two consecutive blades. In
the consideration of flow around aerodynamic surfaces,
fixed with respect to the helicopter, such as a wing,
stabilizer, or fuselage, instantaneous induced velocities
are usually replaced by the time-average values at a given
point. The smaller the pulsations are in comparison with
their time-average values, the more correct this hypothesis
would be.

The theoretical method of predicting the instantaneous
induced velocities is based on the fundamental assumption

of the linear theory, according to which the transport of
the vortex elements occurs with constant velocity (Ref. 17).
The linear theory gives good results as long as the induced
velocities are small in comparison with those of the undis-
turbed flow approaching the rotor. In that case the velo-
city of the transportation of vortices is not much different
from that of the undisturbed flow. This case is typical for
high speed helicopter flight.

No theoretical treatment is presently available for
low advance ratios, because the phenomenon studied actually
deviates significantly from the linear model. For this
case the magnitudes of the induced velocities are comparable
to those of the flight itself and large downwash angles
occur. Further complicating the problem in the low-speed
flight region are the numerous blade-vortex interactions
that occur (Ref. 18). In order to improve the prediction
accuracy of the rotor's wake in those regimes of flight, it
is desirable to have a better insight in the actual physi-
cal phenomena that occurs. This work is an attempt to
provide the means of producing data for helicopter rotors
in forward flight at low advance ratios.

CHAPTER III

EXPERIMENTAL APPARATUS AND PROCEDURE

3.1 The Test Rig

The tests were conducted in a wind tunnel with a test
section of 8 ft x 4 ft, in The Department of Mechanical
Engineering at The Ohio State University. The flow turbu-
lence is reduced by means of 2 to 1 contraction ratio and
nested 1/8 inch diameter straws. The wind tunnel air
velocity is variable up to 75 ft/sec.

The tests were carried out on a teetering two bladed
rotor with twisted blades. Details of the rotor are in
Table 3.1

Table 3.1   Details of the Rotor

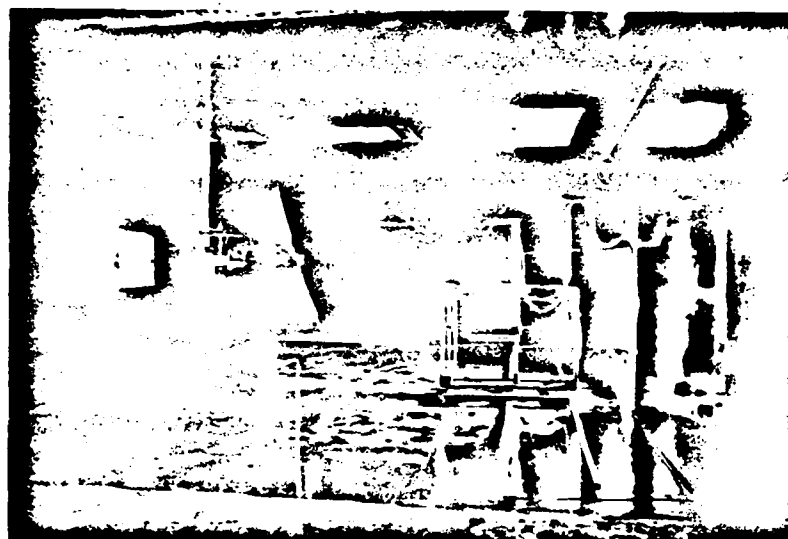|	
Number of Blades	2
Rotor Radius, ft	1.25
Blade Chord, in	2.1875
Rotor Solidity $bc/\pi R$	0.0928
Root Cutout % R	12.08
Blade Taper Ratio	1
Coning Angle	0°
Blade Twist	8° (From 12.08% R to 100% R)
I_B	0.004260 slug-ft^2

Figure 3-1   The Test Section of the Wind Tunnel Looking
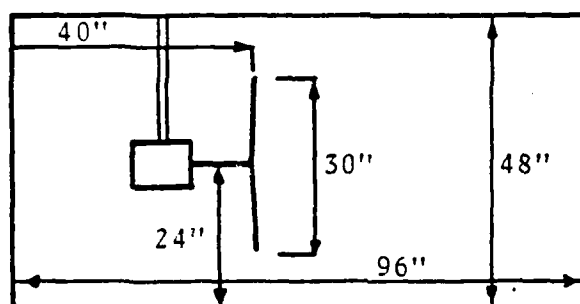from Inlet

Figure 3-2   Dimensions of the Test Section

Airfoil Section   NACA 0012

The rotor is driven by a variable speed electric motor. The speed is variable up to a maximum of 3000 RPM which results in tip speeds up to 400 ft/sec. The collective pitch and the rotor shaft tilt angle are variable but are constant for each case run.

3.2 Data Acquisition System

3.2.1 General Description

The data acquisition system consists of two basic subsystems: 1. the velocity measurement system and 2. the minicomputer and the A/D system.

The velocity measurement system is located at the windtunnel on the first floor of The Mechanical Engineering building and consists of a three-dimensional hot-film probe connected to three constant temperature anemometer circuits. The probe is attached to a traverse mechanism positioned in the wind tunnel enabling the operator to locate the probe at the desired point in the tested volume.

The minicomputer and the A/D are located in the computer room (ADML laboratory) on the second floor of The Mechanical Engineering building. The operator interfaces the computer by means of a alphanumeric terminal. The triggering of the A/D is done from the wind tunnel by a special interface designed and built for this purpose.
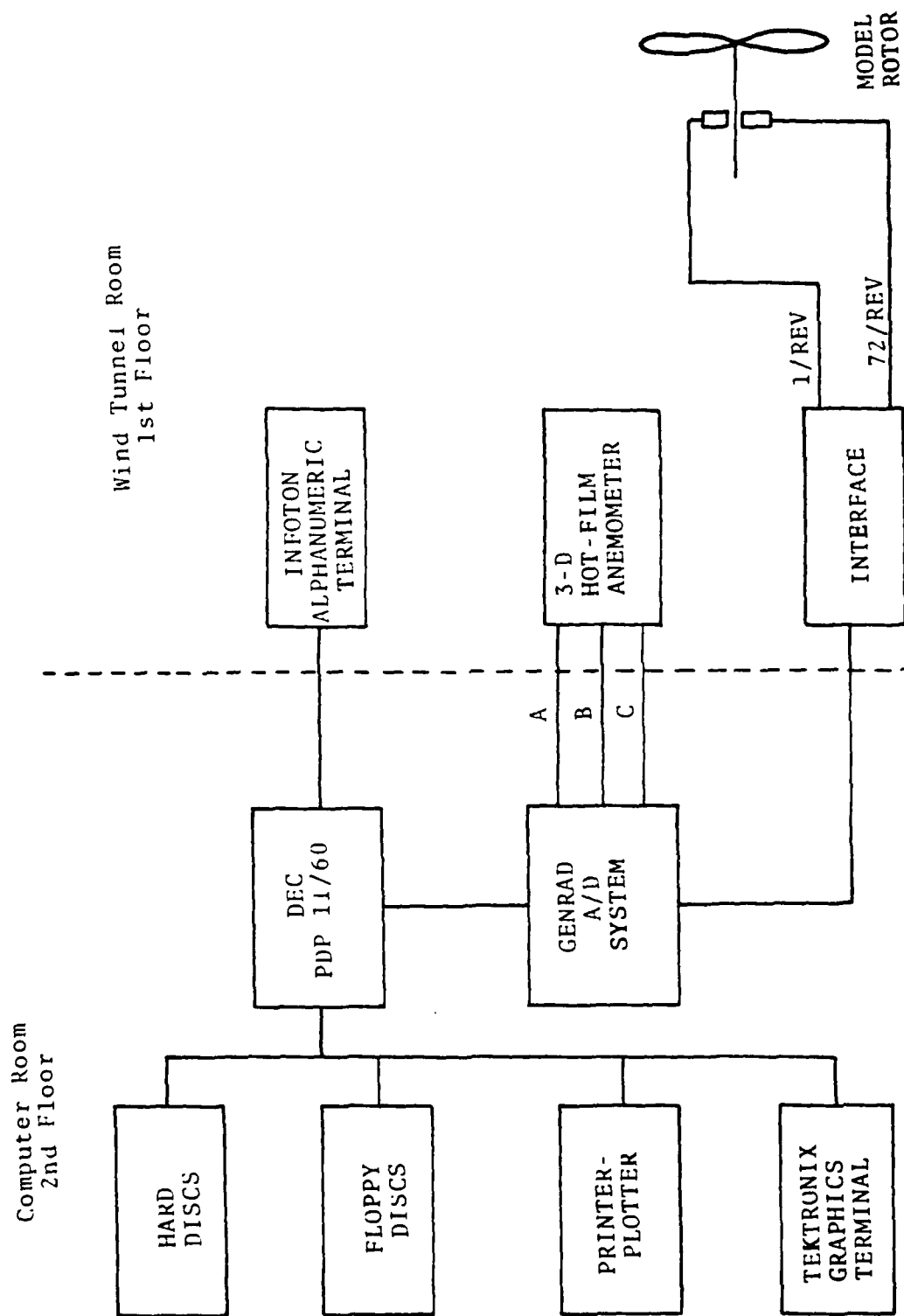
Figure 3-3 Block Diagram of the Entire Measuring System

THREE INDIVIDUALLY
ADJUSTED COMPENSATORS

$$\left[\frac{\tau_A S + 1}{\tau_F S + 1}\right]^2 \quad \bullet E_A$$

$$\left[\frac{\tau_B S + 1}{\tau_F S + 1}\right]^2 \quad \bullet E_B$$

$$\left[\frac{\tau_C S + 1}{\tau_F S + 1}\right]^2 \quad \bullet E_C$$

10

THREE
DANA 2210
DC AMPLIFIER

1A

2B

3C

$e^{-\tau S}$

6 μsec
DELAY LINE

$e^{-2\tau S}$

12 μsec
DELAY
LINE

A   B   C

THREE
DISA
55D05/102C
ANEMOMETERS

TSI 1294-20-18
3-D HOT FILM PROBE

A B C

+ 15VDC

SOLA
83-15-2216
POWER
SUPPLY

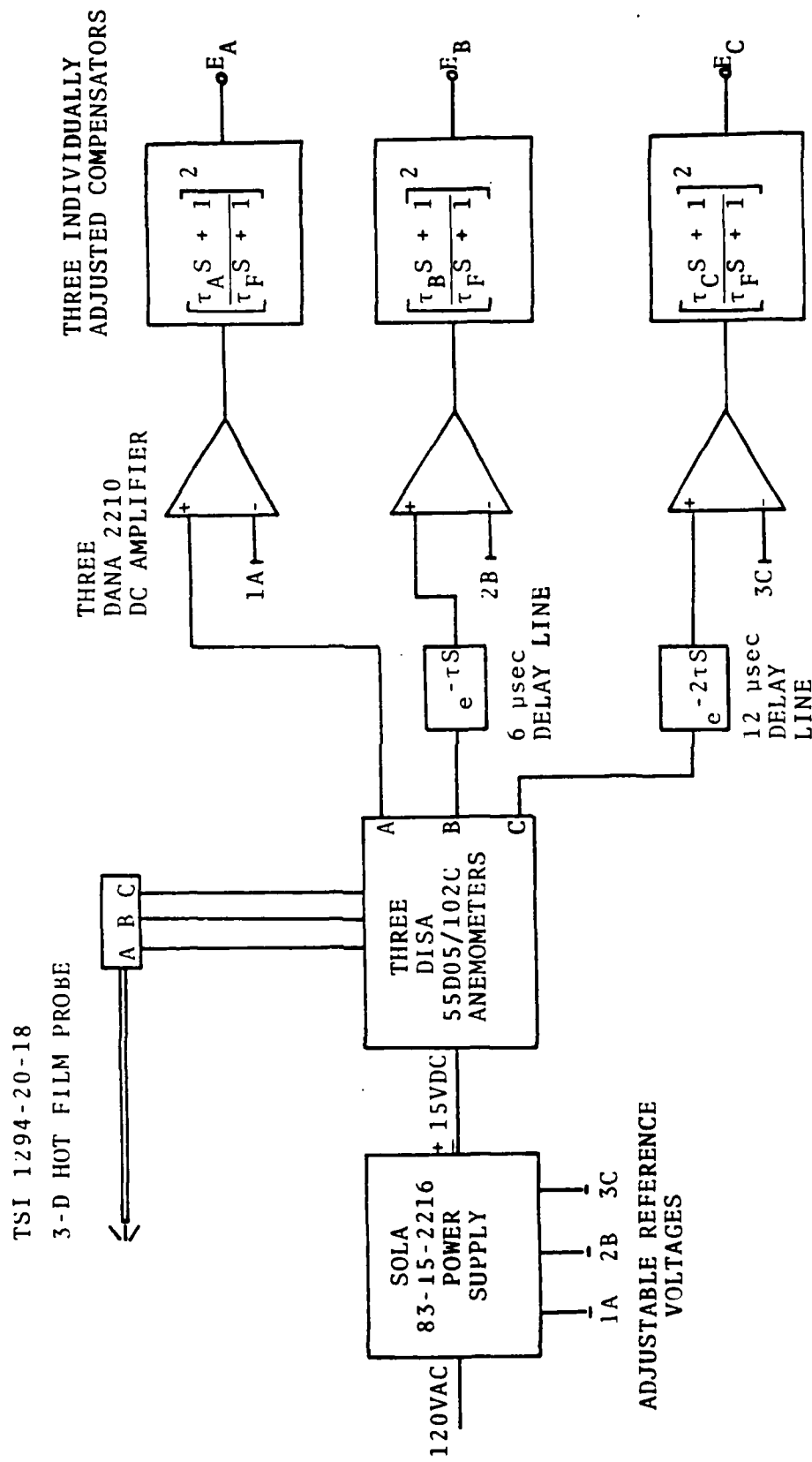120VAC

1A   2B   3C

ADJUSTABLE REFERENCE
VOLTAGES

Figure 3-4 Block Diagram of the Anemometry

Figure 3.3 shows the interconnection of the entire system.

3.2.2 The Velocity Measurement System

The rotor induced velocities were measured by a three dimensional hot-film probe (TSI 1294-20-18) connected to three DISA 55D05/102C constant temperature anemometer circuits with a SOLA 83-15-2216 power supply. In order to improve the frequency response of the hot-film anemometer a lead compensator was added to each channel (Appendix A). Because of the mode of operation of the A/D converter channels B and C had to be delayed, 6 μ sec and 12 μ sec respectively, in order that the computer will "see" the same angle of the rotor in time. The delay lines used were Allen Avionics 1000 ohms impedance 6 μ sec B06P0Z01K. One delay line was used for 'B' and two 6 μ sec delay lines in series were used for 'C' to create the 12 μ sec delay. The output from the anemometer thru the delay lines was connected to three DANA 2210 DC amplifiers. Figure 3.4 shows the complete velocity measuring system including the lead compensators and the delay lines.

3.2.2.1 Directional Sensitivity of Cylindrical Sensors

The basic hot-wire hot-film anemometer output is a voltage which is related to the fluid velocity approximately as:

$$E^2 = A + B\ U^{1/2} \qquad (3\text{-}1)$$

where U is the stream velocity, E is the voltage output
and A, B are constants determined by the electronic circuit,
the physical properties of the sensor and by the fluid
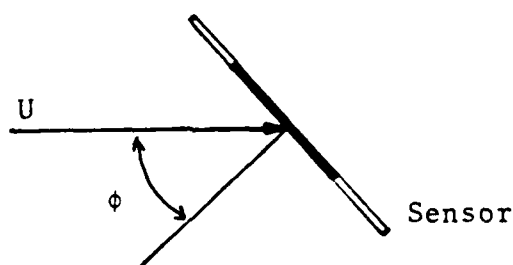properties.

Figure 3-5 Inclined Cylindrical Sensor

If the fluid velocity is not perpendicular to the
sensor, equation (3-1) does not hold, since the heat
transfer from the sensor is reduced. A convenient way to
overcome this problem is to define an "effective cooling
velocity" as the perpendicular velocity which produces the
same cooling effect as the actual, non-perpendicular
velocity and to correlate it to the true stream velocity.
The simplest relationship suggested was:

$$V_{eff} = U \cos \phi \qquad (3\text{-}2)$$

Equation (3-2) neglects the contribution of the flow along the sensor and is not accurate for $\phi > 40^\nu$. More accurate relations have been suggested in References 22, 23, 24. For this work the relationship proposed by Ref. (23) was used after an extensive investigation in Ref. 21.

This relationship is defined by eq. 3-3

$$V^2_{eff} = U^2(\cos^2 \phi + k^2 \sin^2\phi) \qquad (3\text{-}3)$$

where:

V_{eff} is the effective cooling velocity normal to the sensor.

U is the stream velocity.

ϕ is the angle between the free stream and the normal to the sensor.

k is a dimensionless constant.

3.2.2.2 Data Reduction Method for the 3-Dimensional Probe

The three dimensional probe consists of three orthogonal, cylindrical sensors. (Equation 3-3 holds for each sensor.) The effective cooling velocities of the three sensors are:

$$V^2_i = U^2(\cos^2\phi_i + k^2\sin^2\phi_i) \qquad i = 1,2,3 \qquad (3\text{-}4)$$

Adding the three above equations leads to:

$$\Sigma V^2_i = U^2(2 + k^2) \qquad (3\text{-}5)$$

Sensor C

U

γ

α

β

Sensor B

(a)

Sensor A

U_c
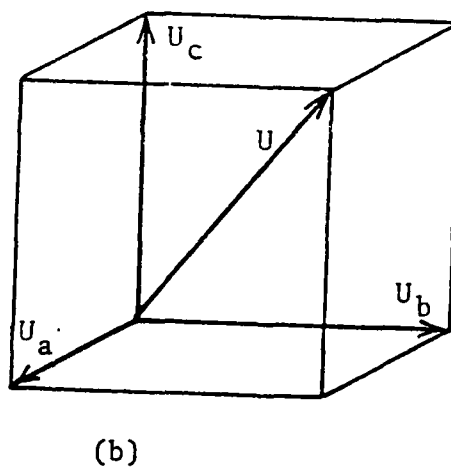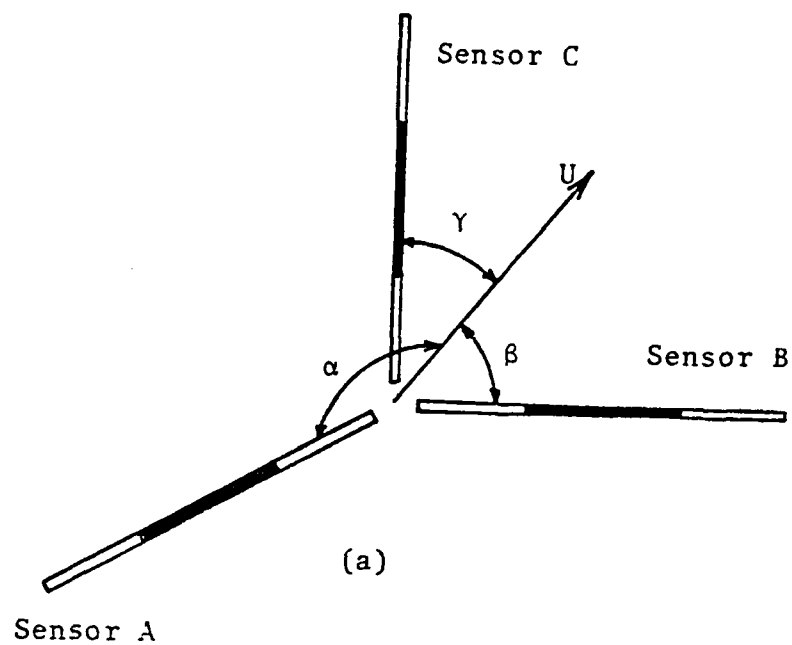
U

U_a

U_b

(b)

Figure 3-6   Geometry of a 3-D Hot-Film Probe
(a) Sensors   (b) Velocities

where the following trigonometric relationships were used:

$$\Sigma \cos^2 \phi_i = 2 \tag{3-6}$$

$$\Sigma \sin^2 \phi_i = 1 \tag{3-7}$$

Solving for the mean velocity:

$$U = \sqrt{\frac{\Sigma V_i^2}{2 + k^2}} \tag{3-8}$$

substituting equations (3-8) in equations (3-4) the directional angles can be obtained

$$\sin \phi_i = \sqrt{[1 - [\frac{V_i}{U}]^2]/(1 - k^2)} \quad i = 1, 2, 3 \tag{3-9}$$

equations (3-8) and (3-9) precisely define the total velocity vector and its direction in the probe system of coordinates.

The above analysis is correct, provided that k^2 is the same for all three wires and that it is not a function of the velocity vector U. Fig. 3.7 shows a typical relationship between k^2 and U. It is apparent that at higher velocities k^2 can be assumed constant whereas at lower velocities this assumption will lead to erroneous results.

To overcome the above stated problem an iterative program was developed to account for the dependency of k^2 on the total velocity vector U. For this case the following analysis was used
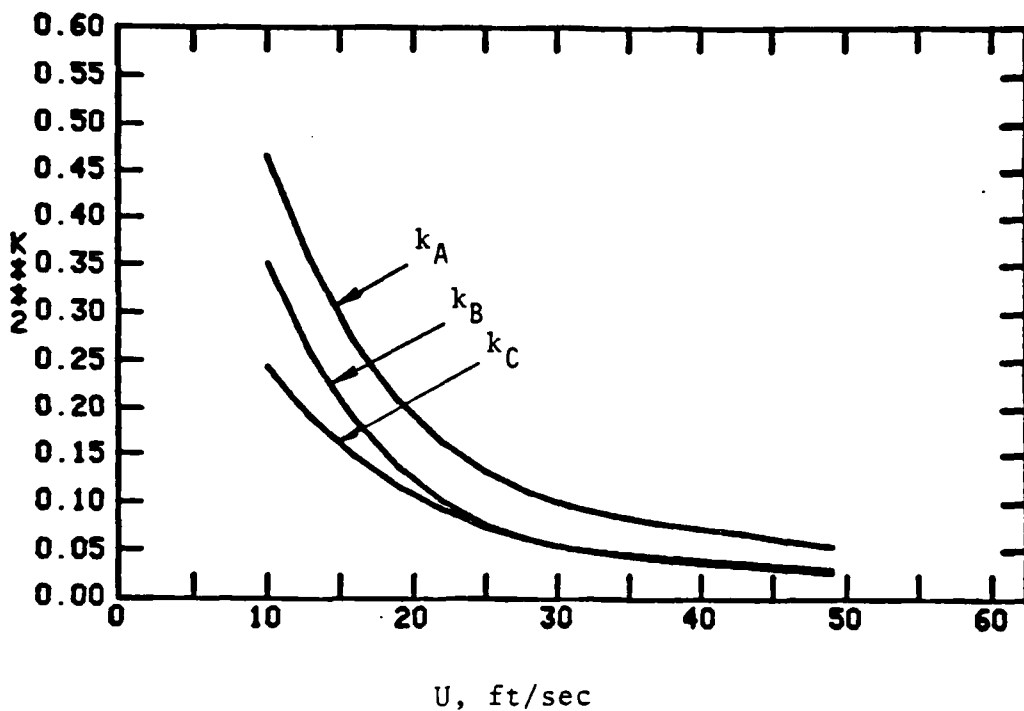
Figure 3-7 Changes of k^2 as a function of U.

(Ref. 25) Eq. (3-4) becomes:

$$V_i^2 = U^2(\cos^2\phi_i + k^2(U)\sin^2\phi_i) \qquad (3\text{-}10)$$

where $k^2(U)$ is now the directional sensitivity constant
dependent on the total velocity, i.e. $k^2 = f(U)$ (3-11)

Equation (3-8) is now:

$$U = \sqrt{\frac{\Sigma V_i^2}{2 + k^2(U)}} \qquad i = 1,2,3 \qquad (3\text{-}12)$$

If one can determine the dependency of k^2 on U, V, k^2 and
ϕ_i can be obtained iterating between equations 3-10, 3-11,
3-12, 3-9.

Extensive investigation on the influence of k^2 on U and ϕ_i showed that k^2 had a negligible effect on the calculations of U, and a significant influence on the angles. Thus, to simplify the iterations a constant value of k^2 (based on the average values of k_A^2, k_B^2, k_C^2 was used in calculating the total vector, and a local value of k_i^2 was used in calculating ϕ_i. The determination of $k^2 = f(U)$ is explained in Section 3.2.2.4.2 and the iterative computer program is shown in Appendix B.

3.2.2.3 Transformation of Velocities from the Probe System of Coordinates to the Tunnel System of Coordinates

The probe used was a T.S.I. 1294-20-18 hot-film probe shown in Figure 3.8. The three sensors are mutually perpendicular and inclined 54.74° to the probe axis. The spatial orientation of the probe in the wind tunnel is shown in Fig. 3.9, and the probe coordinate system is shown in Fig. 3.10, relative to the rotor coordinate system. The orientation of the probe is such that axis C lies in plane $X \div Z$ and plane BOAD is perpendicular to the same plane. For this orientation we can perform the coordinate transformation knowing that:

$$<EOC = 35.26°$$
$$<EOD = 54.74°$$
$$<AOD = <BOD = 45.0°$$

Probe Tip
Detail

Flow

6 Individual
Sensor
Supports

3 Mutually
Perpendicular Sensors
Symmetrically Positioned
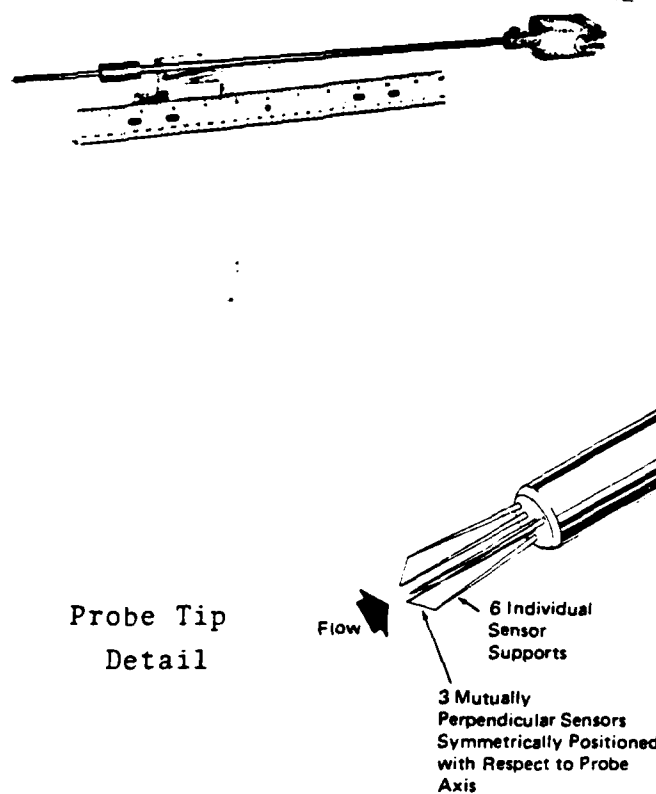with Respect to Probe
Axis

Figure 3-8   TSI 1294-20-18 Three-Dimensional Hot-Film
            Probe
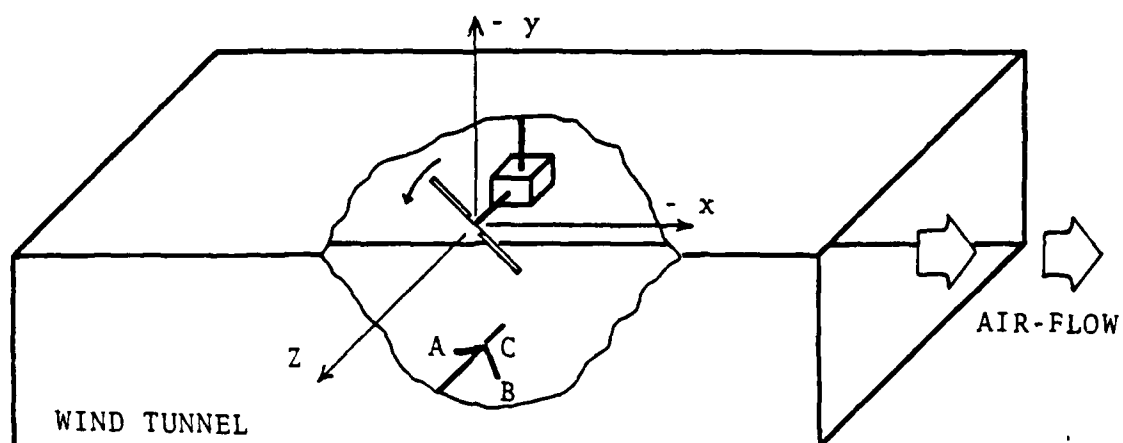
Figure 3-9   The Spatial Orientation of the Probe in the
              Wind Tunnel
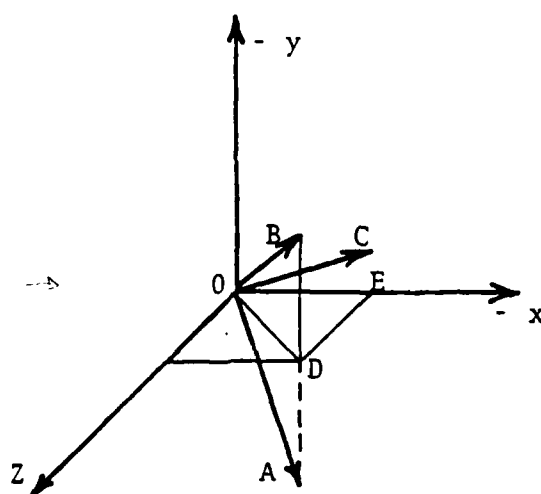

Figure 3-10   Probe Coordinate System Relative to Wind
              Tunnel Coordinate System

Equations 3-13 through 3-16 define this transformation.

$$V_z = + 0.57735(U_a + U_b + U_c) \qquad (3-13)$$

$$V_y' = 0.7071(U_b - U_a). \qquad (3-14)$$

$$V_x = -0.4082(U_a + U_b) - 0.8165U_c \qquad (3-15)$$

3.2.2.4 Calibration of the Three-Dimensional Probe

The calibration of the three-dimensional probe consists of two stages. The first is to obtain the voltage versus velocity curve for each sensor and the second is to determine the dependency of the yaw angle sensitivity constant k^2, on the total vector U.

3.2.2.4.1 The Velocity Calibration

The velocity calibration is performed on a calibrator which consists of a nozzle with exit diameter of 0.75 inches, a turbulence reduction chamber and a probe holder that can vary the angle of the probe relative to the air stream. The air is supplied from a 100 P.S.I. supply line and controlled by a needle valve. An investigation done on this calibrator in Ref. 21 showed that 0.4 inches from the exit plane the jet had a uniform velocity core of 0.6 inches. This location was used to get a correlation curve between the nozzle's velocity and the chamber static pressure. (Fig. 3.11). The same location was used for the hot-film anemometer calibration.
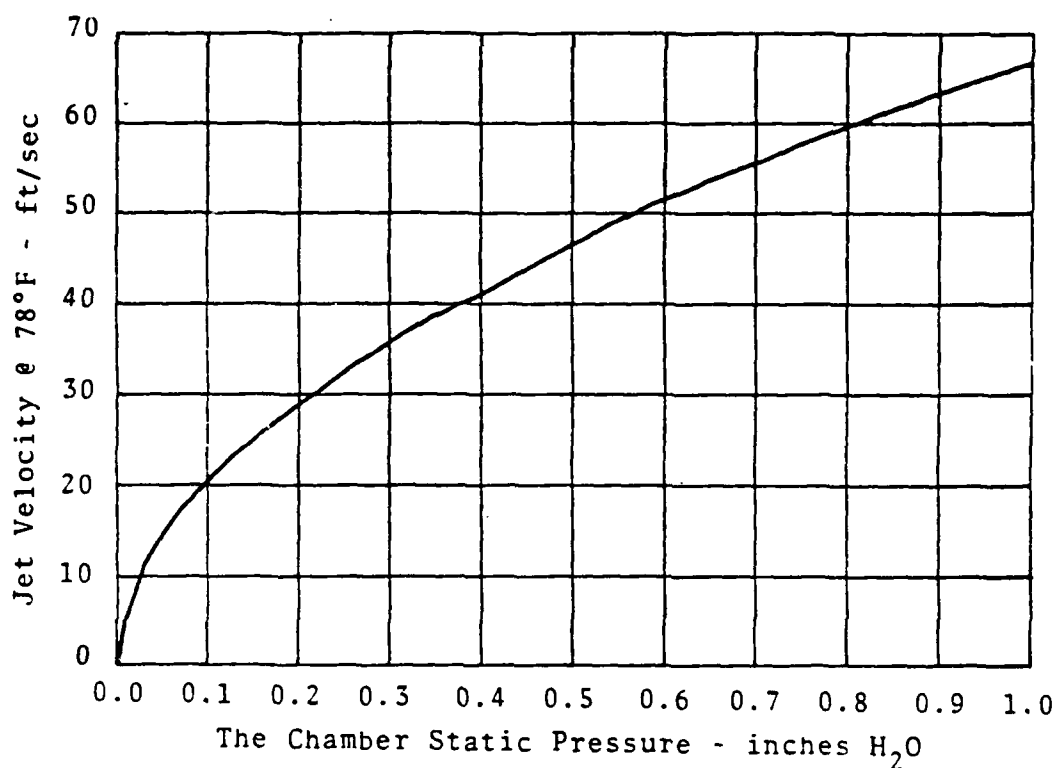
Figure 3-11 *The Calibration Curve for the Velocity Calibrator*

The hot film anemometer was calibrated by adjusting the chamber's static pressure, which corresponds to a specific velocity, and recording the anemometer's output voltage. This calibration was done in the range of 0 to 70 ft/sec.

The author in Ref. 21 has shown that the sensors' prongs do effect the "effective cooling velocity". This velocity is 1 to 3 ft/sec smaller when the prongs are in the plane of the velocity vector than when the prongs are perpendicular to that plane, for the range of 10 to 100 ft/sec. For the probe orientation in the wind tunnel,

sensors A and B had their prongs perpendicular to the total vector, most of the time, and sensor C had its prongs in the plane of the velocity vector. Therefore, sensors A and B were calibrated with their prongs perpendicular to the jet velocity and sensor C was calibrated with its prongs in the plane of the jet. The resulting calibration curves are shown in Fig. 3.12.

Since the calculations of the velocity was done by a computer, a forth order polynomial was fitted to the calibration curves of each sensor. The effective velocities were calculated with this equation, as shown in eq. 3-16.

$$V_{eff} = C_4 E^4 + C_3 E^3 + C_2 E^2 + C_1 E + C_0 \qquad (3-16)$$

The constants of the polynomials were calculated by an existing program using the Method of Least Squares. The curve fit matched the experimental results within $\pm$ 0.4 ft/sec.

3.2.2.4.2 Directional Sensitivity Calibration

The purpose of this calibration was to determine the dependency of k^2 on the velocity vector. An extensive investigation done for this purpose revealed that k^2 is strongly dependent on the wire's Reynolds number where
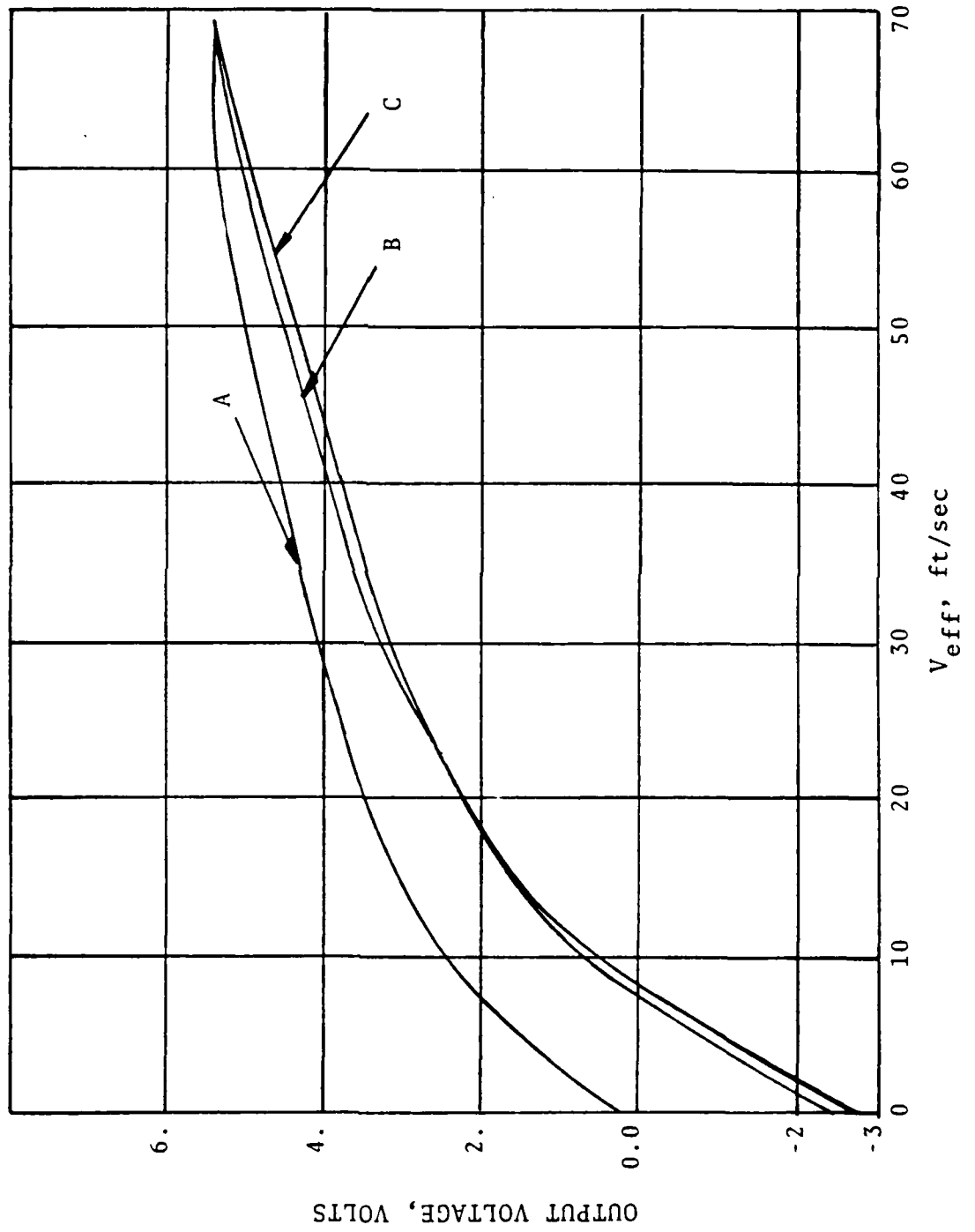
$$Re = \frac{Ud}{\nu} \qquad (3-17)$$

Figure 3-12 Hot Film Anemometer Calibration Curves

However, d and ν are constant for each case, and R_e becomes a function of U alone. Therefore, k^2 was evaluated also as a function of U. For high Reynolds numbers, k^2 is nearly a constant. Thus, only by changing wire diameter (different probes) the values of k^2 would change even though the regime of velocity was not changed. For the TSI 1294-60-18 probe with 0.006 inches wire diameter, a single value of k^2 was adequate, similar to the method discussed in Ref. 21.

However, for the measurements of instantaneous velocities, a finer wire was used in order to improve the system frequency response. For this purpose a TSI 1294-20-18 probe was used with 0.002 inches wire diameter. For this probe k^2 showed a strong dependency on the velocity (lower Reynolds number due to smaller diameter). As seen in Figure 3-7.

In order to determine the correlation between k^2 and U, the following procedure was used. Rewriteing equation (3-3) as:

$$\left(\frac{V_{eff}}{U}\right)^2 = \cos^2\phi + k^2\sin^2\phi \qquad (3\text{-}17)$$

one can obtain the values of k^2 by calculating the coefficients of equation (3-17) when the ratio V_{eff}/U is given for a specific ϕ. This was done by holding U constant and changing ϕ from 0 to 90 degrees. Repeating this procedure for U in the range of 10 to 70 ft/sec. the dependency of k^2 on U was obtained. Then the data obtained was curve fitted so that the relationship $k^2 = f(U)$ could be used in the computer program. Typical correlations are shown in equations 3-18 through 3-20.

For sensor A:

$$k^2_A = 2.546 \times 10^{-7} \times U^4 - 4.533 \times 10^{-5} \times U^3 + 0.003 \times U^2 - .08955 \times U + 1.1042$$

(3-18)

For sensor B:

$$k^2_B = 1.033 \times 10^{-7} \times U^4 - 1.8787 \times 10^{-5} \times U^3 + .001296 \times U^2 - .041 \times U + .54244$$

(3-19)

For sensor C:

$$k^2_C = 2.4781 \times 10^{-7} \times U^4 - 4.2828 \times 10^{-5} \times U^3 + .002755 \times U^2 - .07928 \times U^1 - .9092$$

(3-20)

The incorporation of this relationship with the complete computer program and the iterative computation are shown in Appendix B.

The authors of References 23 and 24 have found that k^2 is dependent of the geometry of the sensor (aspect ratio l/d) and almost independent of other properties of the sensor and the fluid. Therefore, the value of k^2 is not expected to change with time due to contamination and corrosion. Intuitively, a similar assumption can be made about the dependency of k^2 on U, thus the calibration curves obtained in this work for $k^2 = f(U)$ may be used in future applications without recalibration and it is good for the range of velocities of 10 to 70 ft/sec.

3.2.3 The Minicomputer and the A/D System

The new minicomputer, installed in The Department of Mechanical Engineering at The Ohio State University, in the summer of 1978, provided the means of improving the system of average data acquisition and extending the work

to instantaneous velocity measurement.

3.2.3.1 The Minicomputer

The minicomputer is a Digital Equipment Corporation (DEC) PDP 11/60 and is well suited to Fortran based calculations. It has a 256 KBYTES memory (RAM) and 64 KBYTES are available to the user. The PDP hosts graphics (Tektronix 4014-1) and alphanumeric (Infoton) terminals. The terminals are supported by a high speed Printronix Printer-Plotter and a Tektronix hardcopy unit. Data and program storage are provided by a dual floppy disc drive and two cartridge disc drives.

3.2.3.2 The Analog to Digital System (ADS)

Two A/D converters became available during the program. The first was the DEC LPA system which can sample up to 40 KHZ and can be multiplexed up to 16 channels. The second was the GENRAD 4 channel ADS with sampling frequency up to 160 KHZ. Initially the DEC LPA system was used because it was planned to development eventually automate the data acquisition. The computer would control the RPM of the rotor and the x-y-z location of the probe. However, due to hardware problems in the LPA system, the data acquisition system was developed around the GENRAD ADS. (Henceforth referred to as "the ADS").

The ADS is controlled by a canned program using sub-routines available in the PDP's library. The user has to specify the number of channels used and the maximum expected analog voltage. This is done by calling the subroutine SETAD1(IPOINT,NCHAN,IRANGE,KHZ) where: IPOINT specifies the number of points to sample per channel. This number is encoded as shown in Table 3.2. NCHAN is the number of channels to sample. In our case there are three channels. IRANGE is the analog input voltage range encoded as shown in Table 3.3, and KHZ specifies the corner frequency of the antialising filters in the ADS.

Table 3-2 IPOINT Code		Table 3-3 IRANGE Code	
CODE #	IPOINT	CODE #	ANALOG RANGE (+/-) VOLTS
0	128	0	16
1	256	1	8
2	512	2	4
3	1024	3	2
4	2048	4	1
5	4096	5	0.5
6	8192	6	0.25
7	16384	7	0.125

The subroutine SETAD1 initiates the A/D conversion, and now
a second subroutine is called to actually digitize the
analog data. This subroutine is called GETAD(BUFFER) where
BUFFER is an integer array whose dimensions are specified
by the user. The digitizing process continues until the
array BUFFER is filled. If the triggering signals stop
before BUFFER is filled, the computer will wait until the
array is filled.   Thus, the number of triggering signals
always has to be larger than the size of the array. For
our case, it was decided to average the instantaneous data
for 15 revolutions every 5 degrees, thus creating 15 x 72 =
1080 signals. The dimension of BUFFER was selected to be
1024, which indicates that only 14 complete revolutions
will be available for data manipulation.

The ADS is triggered by one pulse sent from the inter-
face (see Appendix C for details). The system then samples
the first channel and after 6 μ sec the next one, until the
number of channels sampled equals the number of channels
specified in the subroutine SETAD1. The 6 μ sec inter-
channel interval caused significant errors in our case,
where the three digitized values had to correspond to the
same instant in space and time. A simultaneous triangular
wave of 2000 Hz had about 10% error when the digitized
values A and C were compared. To overcome this problem
Allen Avionics delay lines were used. Using these delay
lines the analog signal B was delayed by 6 μ sec, and the

analog signal C was delayed by 12 μ sec. The simultaneous triangular wave test conducted with the delay lines showed agreement between channels A and C within 0.26%, which is of the order of magnitude of the noise present in the long cable, connecting the ADS to the wind tunnel.

The analog signals coming out of the constant temperature anemometer were connected by a 500 ft. cable required to get from the wind tunnel room, where the experiments were conducted, to the computer room. An analysis, Appendix A, conducted on the significant frequency content of the wake at a typical point, showed that the significant frequency is contained in the region below 4000 Hz. Fortunately, this frequency was far below the frequency where the reactive elements of the cable became significant. This frequency of the cable was found to be around 20 KHz. However, the triggering signal was a square pulse of 1 μ sec. This short duration makes the frequency content of the pulse on the order of magnitude of 1 MHz which is in the region where the reactive elements of the cable (capacitance and inductance) are significant. We have found that the pulse is attenuated from 10 volts to about 5 volts. The triggering threshold of the ADS is 3 volts, thus the 50% attenuation of the signal did not cause any problem. An additional 0.6 μ sec delay was observed, corresponding to an insignificant rotor rotation, and we concluded that the triggering process was reliable.

3.3 Data Acquisition Method

Prior to starting the data acquisition, the flight conditions are set. This was done by adjusting the collective pitch angle, incidence angle, tip speed and wind velocity. Then the compensators were adjusted according to the procedure outlined in APPENDIX A to yield a flat frequency response of the hot film and data output system up to about 4000 Hz. The next step was to statically calibrate the hot film anemometer (outlined in sections 3.2.2.2 to 3.2.2.4.2). After the calibration constants were obtained, they were entered manually in the programs (Appendix B) and the data acquisition was started according to the type of data of interest, i.e. average velocity using the AVERAGE program or instantaneous data using the INSTVEL program.

The main purpose of this work was to develop a method of measuring instantaneous velocities in the wake of a helicopter rotor. However, once the computer and the ADS were connected to the wind tunnel we used it for average data collection as well. Both programs are similar and the only differences are in the averaging and storage procedures.

3.3.1 Average Data Collection

In this mode of operation the data was averaged over several rotor revolutions, thus the angle azimuth of the rotor was not a variable. The ADS triggering was done directly at the converter by an exact 5 volt square wave obtained from a TTL output of a WAVETECK osci-

lator. Since the estimated significant frequency content was 4000 Hz and a correct reconstruction of a wave required at least two samples of the highest frequency, the sampling frequency was selected to be 8000 Hz. The dimension of the array BUFFER, was 8192 (standard dimensions, see Table 3.2), thus the array was filled within one second, which corresponds to about 40 revolutions for a tip speed of 300 ft/sec.

The data collection was done in a predetermined systematic method, which is basically a three nested do loops, each for one coordinate. The x is changing the fastest, then z, and last to change is y. Each case started at $x = 28$, $y = 20$, $z = 12$ and from this point on, the computer did the bookkeeping and instructed the operator how to proceed. The process is fully continuous from previous days (the data acquisition for one case might take about a week) with no information needed from the operator except defining the status of the new day, i.e. is the present data acquisition a continuation of previous session or not? If the answer is yes, the computer instructs the operator where to locate the probe, and if the answer is no, the computer instructs the operator to locate the probe at the initial point. Once the data collection starts the computer will tell the operator when to change holders and warn him when the probe gets into the area in which the rotor is too close to the sensors.

At each point in the wake, the data was averaged (mean values) for each channel, the effective velocities were calculated and transformed into wind tunnel coordinates. The three components of velocity V_x, V_y, V_z) and the location of the probe (x-y-z) were stored temporarily on the computer's hard discs. At the end of the day the data collected was stored on a floppy disc for safety reasons so that the data might not be accidently erased and lost. After the whole case was completed, the file was transferred to the large AMDAHL 470 computer where SPEAKEASY language was used for vector plots (Appendix B).

3.3.2 Instantaneous Data Collection

Using the assumption that the wake is periodic for each and every rotor revolution the data collected was actually the average instantaneous velocity, which was averaged at every five degrees increment for 14 revolutions. For this case the ADS had to be triggered each time the blade had passed five degrees of rotor revolution. At a tip speed of 300 ft/sec the sampling frequency is about 2750 Hz which is not a sufficient sampling frequency for a

complete wake reproduction. Thus, we have to keep in mind that the values measured are discrete values at five degrees increment of rotor rotation. The five degrees increment triggering signal was supplied by an interface designed and built for this project. A block diagram and elaboration of the mode of operation of this interface are shown in Appendix C.

For the average instantaneous data collected two methods were developed. 1) Computer in real time with the ADS. 2) The analog voltages and the triggering signal recorded on a FM analog recorder and then reproduced at the ADS. The second method was developed as an alternative to the first one. The method is operational but has not been used for actual data acquisition.

3.3.2.1 Computer Mode Operation

The inputs to the interface in this mode of operation were:

1. 1/REV pulse from a magnetic proximity pickup indicating $\psi = 0$.

2. 72/REV pulses from a second magnetic proximity pickup indicating five degrees increments in rotor rotation. The output from the interface was one pulse at each five degree increments for 15 revolutions. (Figure 3.13)

The ADS was initiated by the software, but the digitizing process started only after the operator signaled,
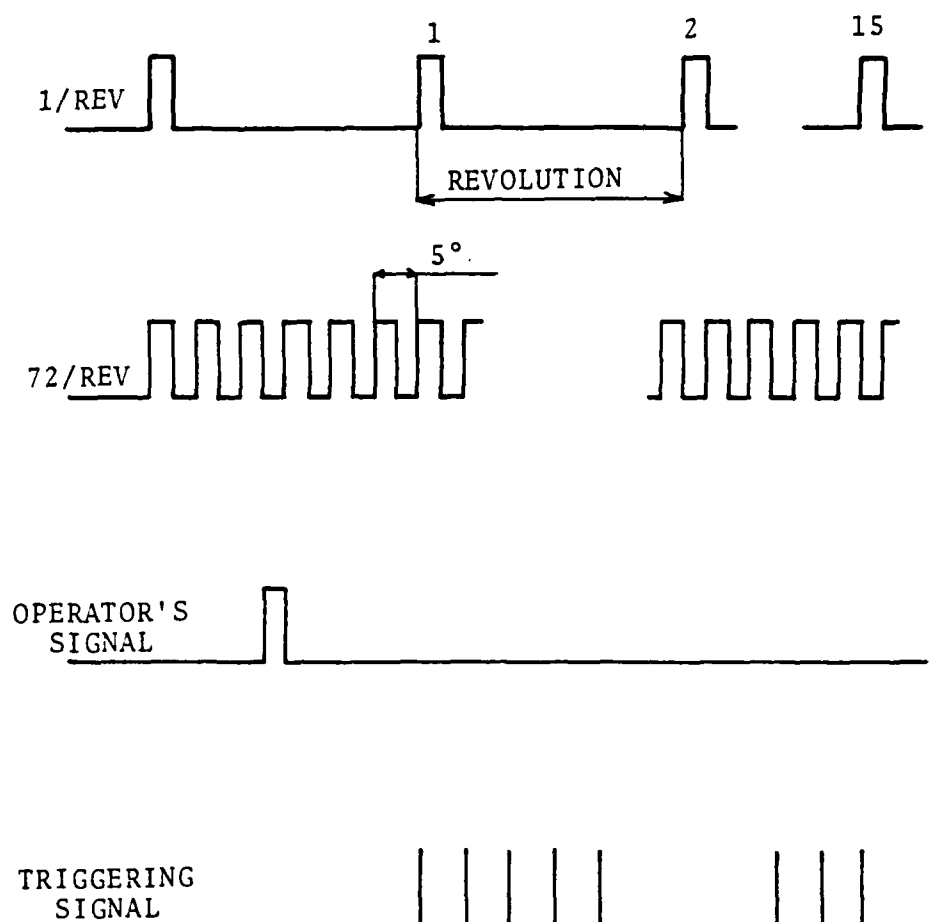
Figure 3-13 Triggering Sequence in Computer Mode

from the interface, that the probe was at the correct loca-
tion. Then, the ADS was triggered every five degrees as
shown in Figure 3.13.

After the digitizing process was completed, the compu-
ter averaged the data for every five degree increments for
14 revolutions. The three average voltages were transformed
into wind tunnel coordinates in the usual manner. These
velocities and the probe location were temporarily stored
in an encoded way, (see Appendix B) on the computer's hard
discs, until the case was completed. The data was then
stored permanently on floppy discs for further use on a
reference.

3.3.2.2 Tape Mode Operation

At this mode of operation, the inter-
face had a dual purpose. When recording the data, it pro-
duced the triggering signals for each five degree increments
and also operated the FM tape recorder. The procedure is
as follows: the operator signaled, from the interface,
that the probe was at the correct location, then the device
started the tape recorder and after 0.5 seconds delay (to
let the tape get to its steady state velocity) the analog
data, stepped down to tape recorder maximum allowable input,
was recorded on three channels. On the fourth channel, a
triggering signal was recorded. After 15 cycles had been counted
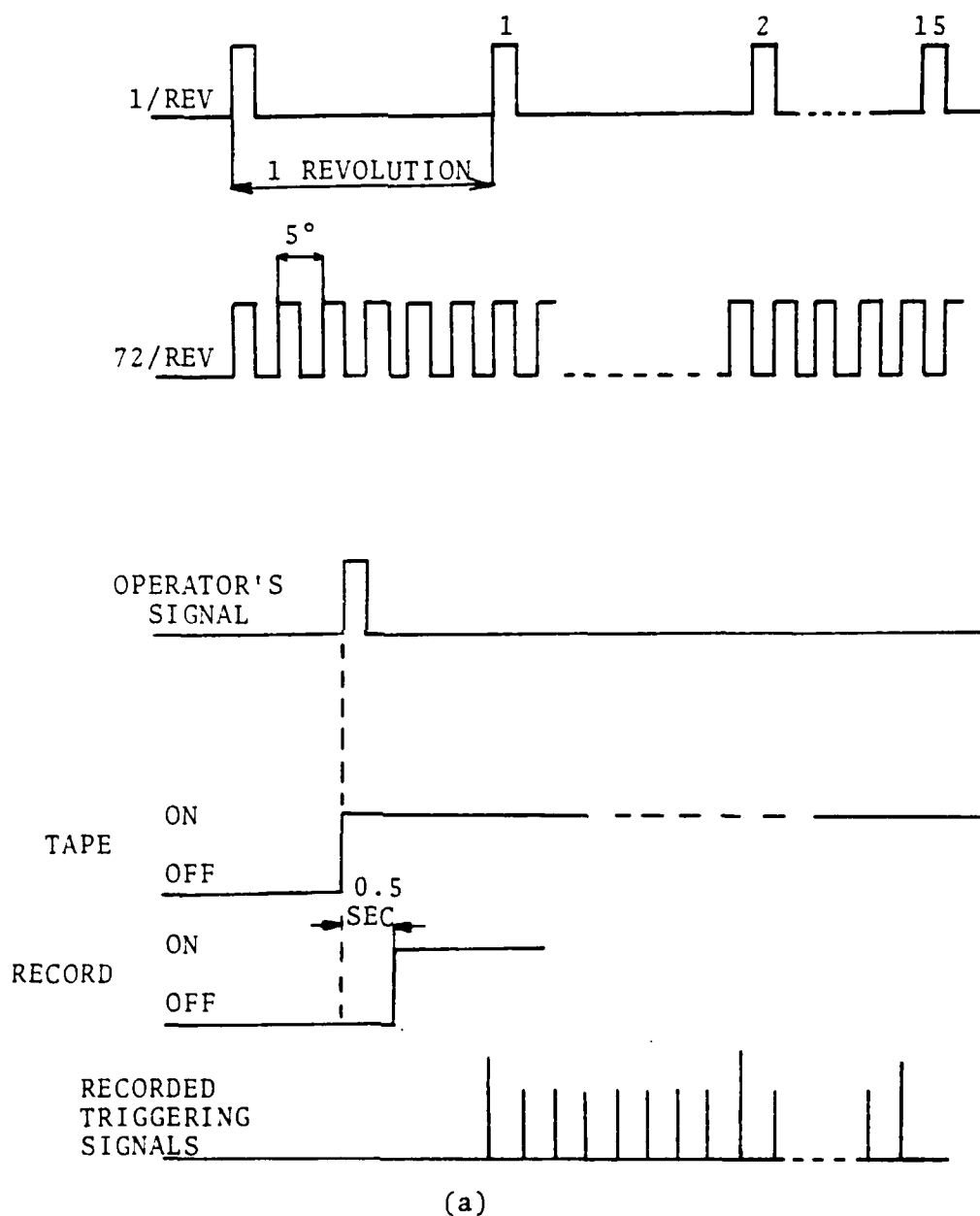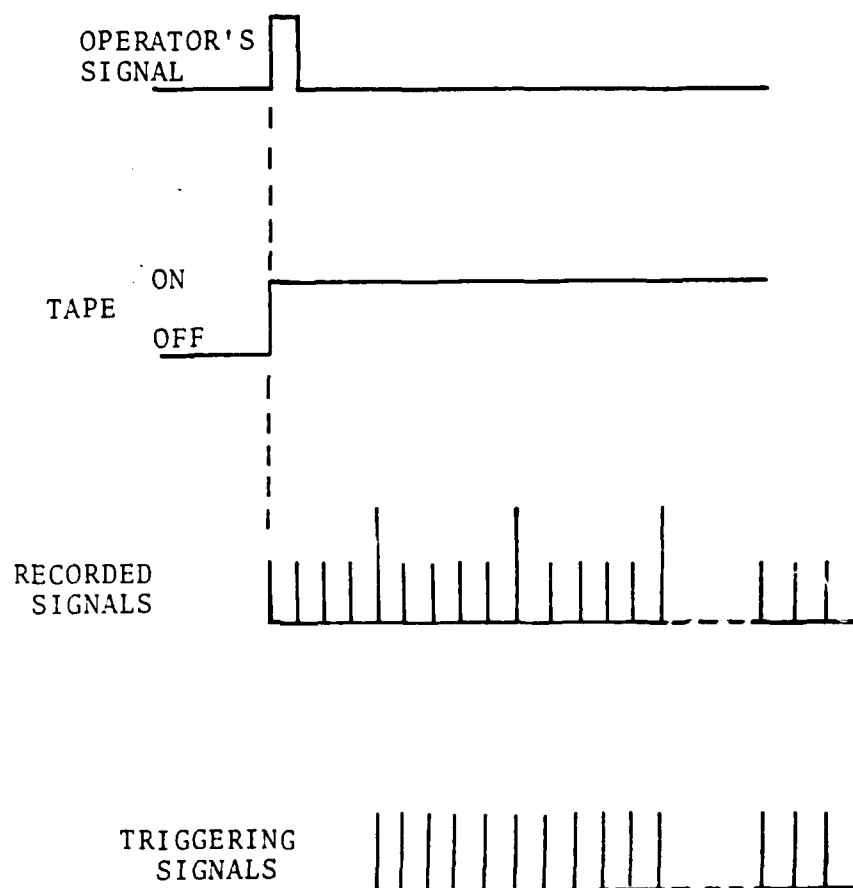the interface stopped the recording and the tape was shut

(a)

Figure 3-1   Recording the Triggering Signals in Tape Mode

OPERATOR'S
SIGNAL

TAPE ON
OFF

RECORDED
SIGNALS

TRIGGERING
SIGNALS

(b)

Figure 3-14   Triggering Sequence in Tape Mode

down (Figure 3.14a). In the reproduction process the three
analog channels were connected to the ADS and the fourth
channel, with the triggering signals, was connected to the
interface whose role was the same as in the computer mode
(Figure 3.14b).

After the digitizing process was completed the data
reduction method is similar to the procedure outlined in
the computer mode.

3.4 Data Presentation

The numerical values of the velocities and their
location were stored on floppy discs and could be displayed
on any terminal or printed out by the PRINTRONIX high
speed printer. However, the vast amount of "numbers"
associated with each case (1188 points x (72 x 3 numbers
per point) = 256608 "numbers" only for velocity presenta-
tion) mode the use of data visualization a necessity.

For data visualization the TEKTRONIX 4014-1 graphics
terminal was used. This terminal has a refresh mode of
operation and animated pictures of any plane (xy, yz, zx)
as the rotor passes by were created. In addition, graph
of velocity vs. rotor position, or velocity vs. probe

location could be obtained by using the PLOT-10 plotting routines available in the PDP's library.

3.5 Measurement Error Analysis

This error was evaluated experimentally, in two stages. First, the velocity calibrator was used to evaluate the velocity and angular errors because of imperfection of the sensors, disturbances due to the prongs, errors in the A/D conversion and errors of the fitted calibration curves. The second error evaluation was done in the wind tunnel, to evaluate the additional errors because of misalignment of the probe in the wind tunnel and because of the vibration of the probe.

3.5.1 Error Evaluation on the Velocity Calibrator

The probe was installed on the probe holder in the calibration nozzle rig so that all the sensors were inside the core of uniform velocity. Then the velocity of the jet was set to velocity values between 10 and 70 ft/sec, and the probe was rotated as to achieve different combinations of ϕ_i. The velocity was varied in steps of 10 ft/sec and combination of the directional angles were set at each velocity. The anemometer's analog voltages were connected to the ADS in the usual way, and the velocities were read from the terminal. These velocities were then compared with the actual velocities determined using the velocity

calibrator's calibration curve. The results showed a maximum velocity error of 1 ft/sec and an angular error of $\pm$ 1°.

3.5.2 Error Evaluation in the Wind Tunnel

For this case the probe was installed in the wind tunnel on its holders. The wind velocity was varied in the same range as on the velocity calibrator. Vertical and horizontal traverses were run and the velocities obtained were compared with the stream velocity. The magnitude of the measured velocity was within 1% of the stream velocity. However, the measured stream vector had a constant 5° error relative to the X axis for all the points measured and for the whole velocity range. This error was due to imperfections in the traverse mechanism and the holders. This error was corrected for in the transformation equation and after that the velocities measured in the wind tunnel had the same order of magnitude of error as on the velocity calibrator.

An extensive investigation done by the author for an undergraduate laboratory design course (ME 581) revealed that the velocity error due to vibration at the sensor is less than 1%.

CHAPTER IV

TEST RESULTS AND THEIR PRESENTATION

The final stage of this work was a preliminary measurement of a z-y plane of the instantaneous velocities in the wake of the model rotor for one flight conditions. The purpose of this stage was to test the instrumentation and mainly to develop an efficient data presentation method, which turned out to b‾ a formidable task. The parameters of the flight condition were as follows:

Blade Tip Speed ft/sec	300
Advance Ratio	0.06
Blade Twist, degrees	8 (from 12.08 to 100% R)
Collective Pitch, (75% R)	8
Rotor Shaft Tilt Angle, degrees	8

The instantaneous velocities were measured for the z-y plane at X/R = - 1.07. This plane contains 66 points and we measured the three components of velocity every five degrees of rotor rotation for each point. Thus, the total number of velocity information for the entire plane was 14256. (For comparison a whole case of average velocity measurement contained "only" 3564 velocity points.)

Therefore it is clear that the task of data presentation was not a simple one.

Our first inclination was to use the vector plots developed for the average data presentation (APPENDIX B) for each azimuth angle. However these vector plots did not transfer to the viewer any information typical to instantaneous velocities that is, high peaks of velocity where vortices were encountered by the sensors. Figure 4-1 shows the vector plots every 20 degrees between 0 and 180 degrees azimuth. The plots are very similar and very little vector movements are apparent between each azimuth angle.

Since the vector plots failed to transfer the desired information, we decided that a presentation of the individual components of velocity at some points of interest was necessary. Thus the plots in Fig. 4-2 and 4-3 were created. These plots show the normal induced velocity (V_z) as a function of the perpendicular coordinate to the rotor at an azimuth angle. For this presentation a complete y traverse was made for two azimuth angles, 0 and 90 degrees. The plots showed a distinct variation of the velocity with y location and also significant changes in the flow pattern were observed between the plots of $\psi = 0$ and $\psi = 90$.

The third type of plots we used, were graphs showing the velocity variation, at a point in the wake, as a function of the azimuthal position of the rotor. These graphs
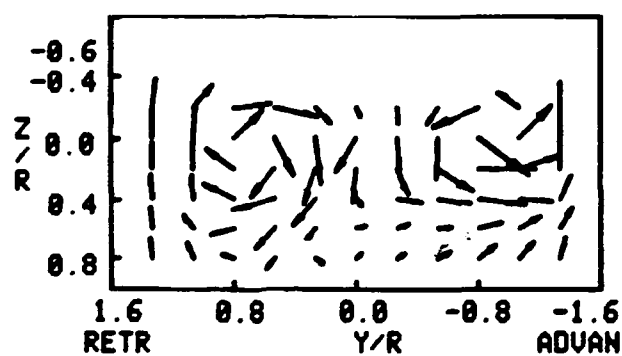
are shown in Figures 4-4, 4-5, 4-6 and are transferring
the most information about the flow.

20 FT/SEC   X/R=-1.07
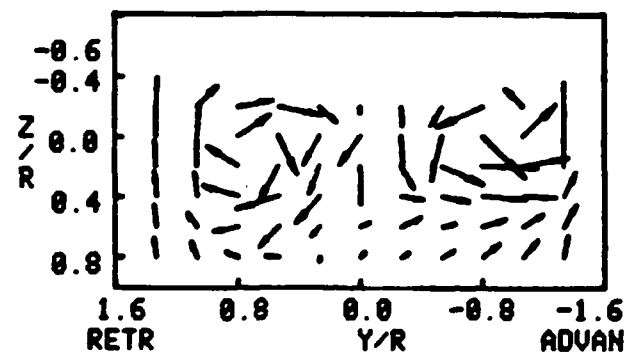
$\psi = 0$

$\psi = 20$
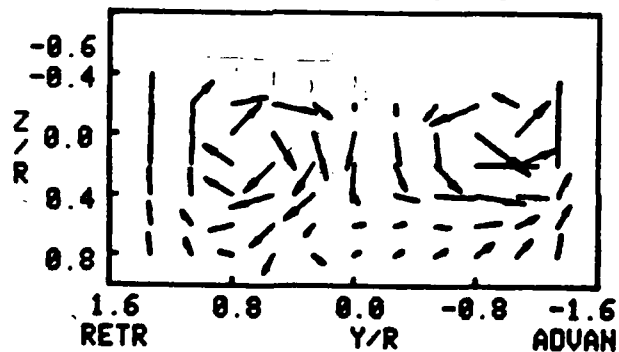
$\psi = 40$
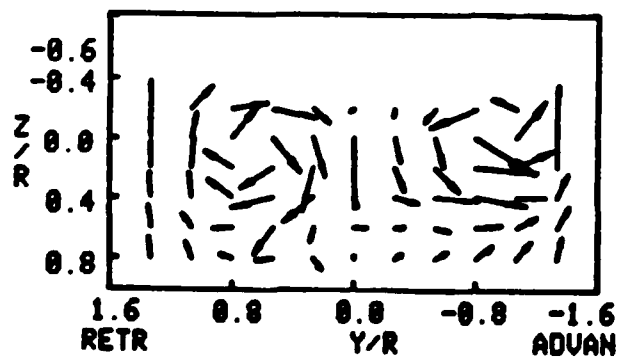
$\psi = 60$

Fig. 4-1   Velocities in Plane z-y

_20 FT/SEC   X/R=-1.07
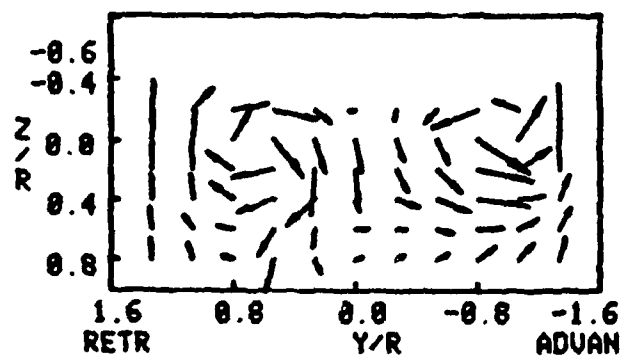
$\psi = 80$
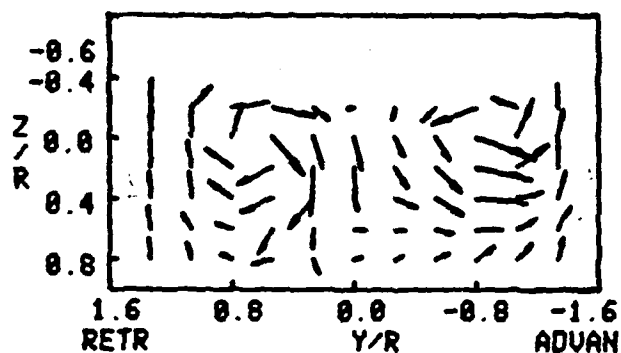
$\psi = 90$
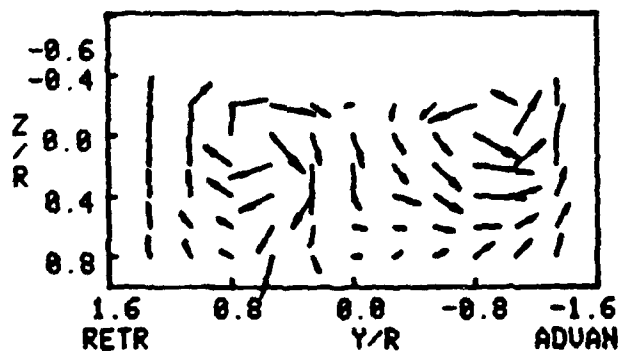
$\psi = 100$
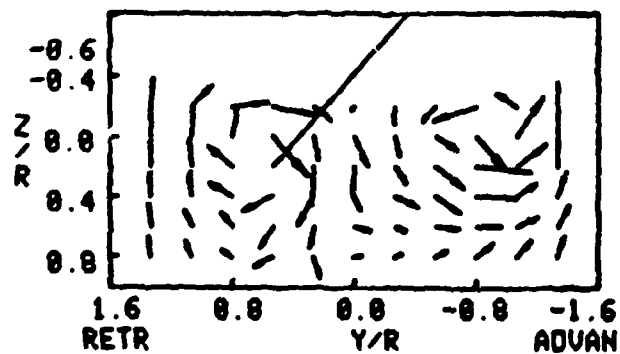
$\psi = 120$

Fig. 4-1 Continued
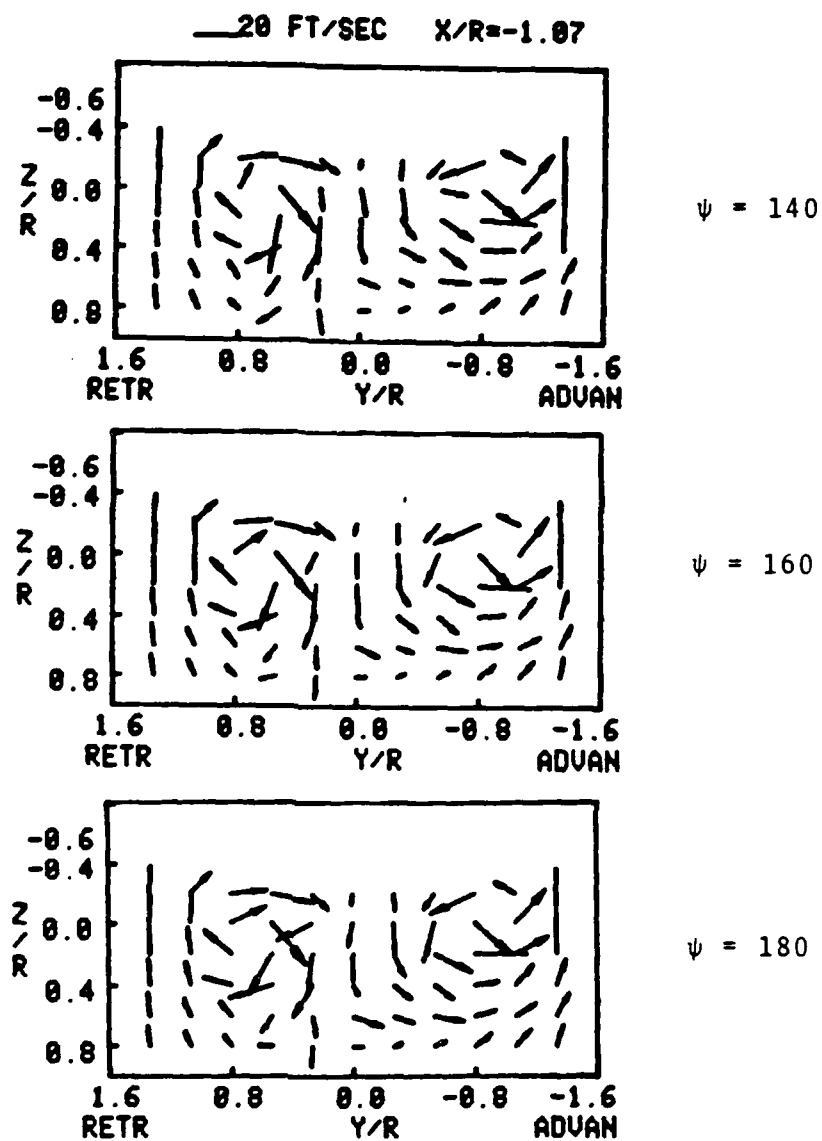
Fig. 4-1   Concluded
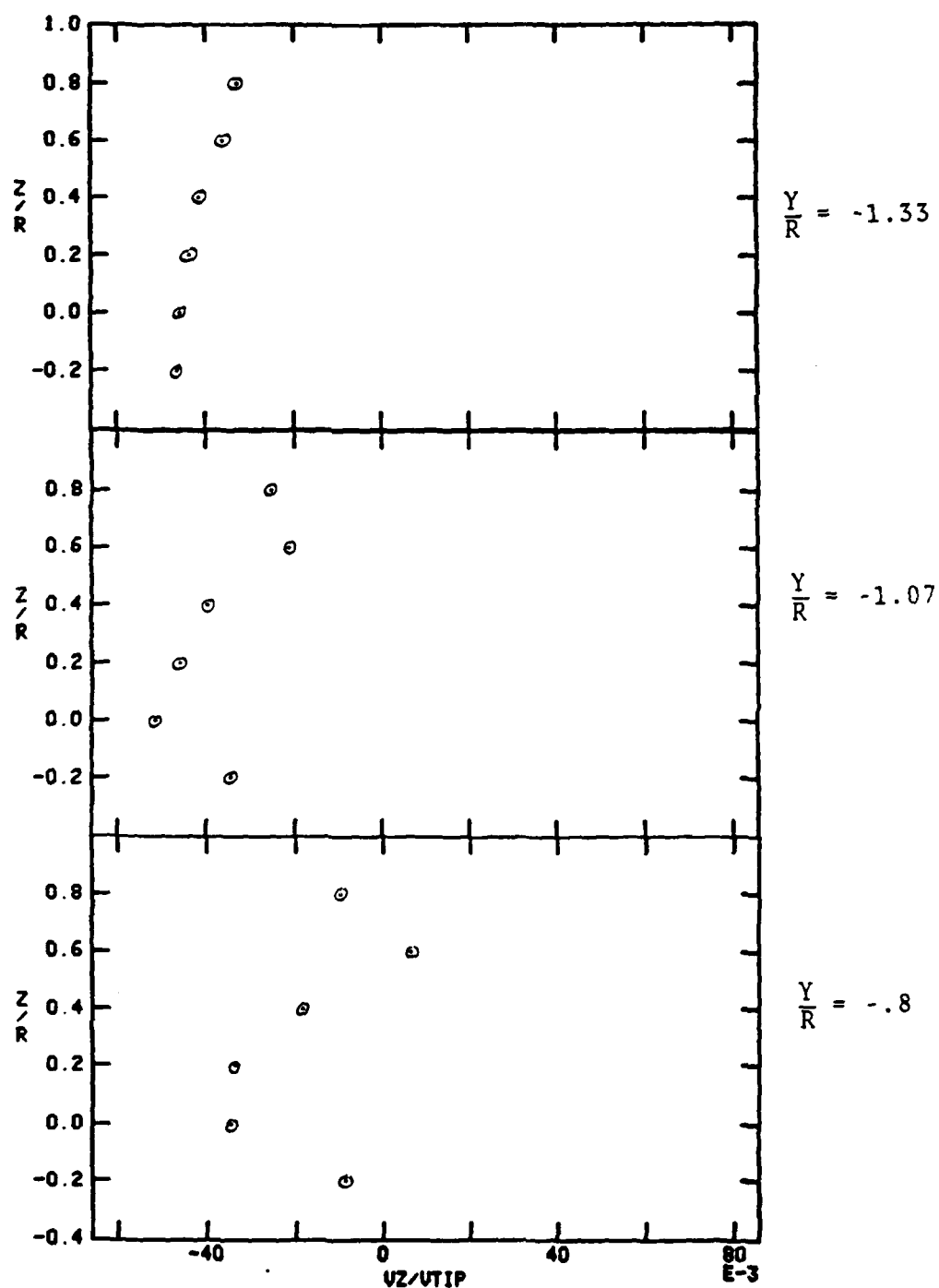
Fig. 4-2 Normal Component of Velocity at Y/R = -1.07
and $\psi = 0$
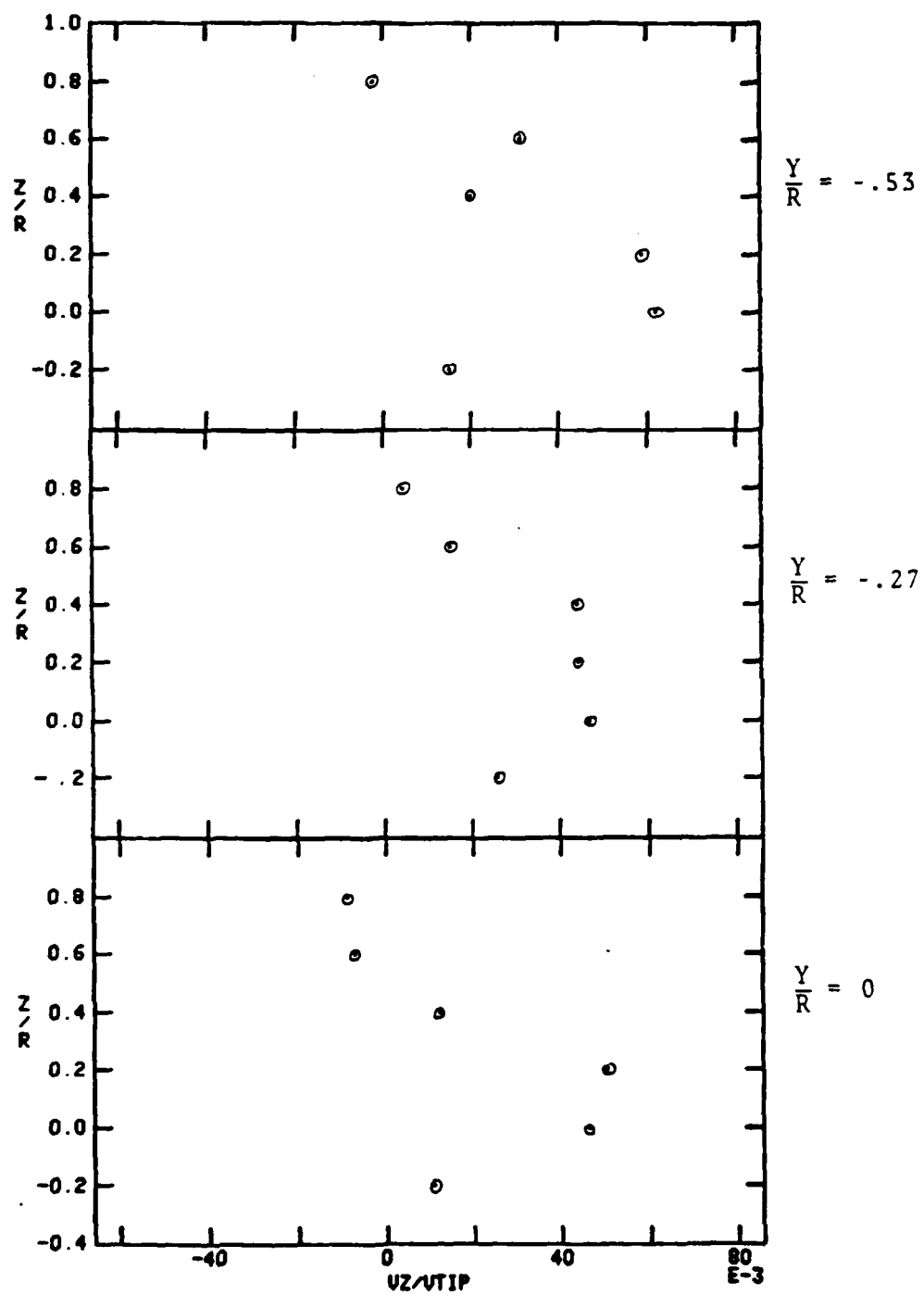
Fig. 4-2 Continued
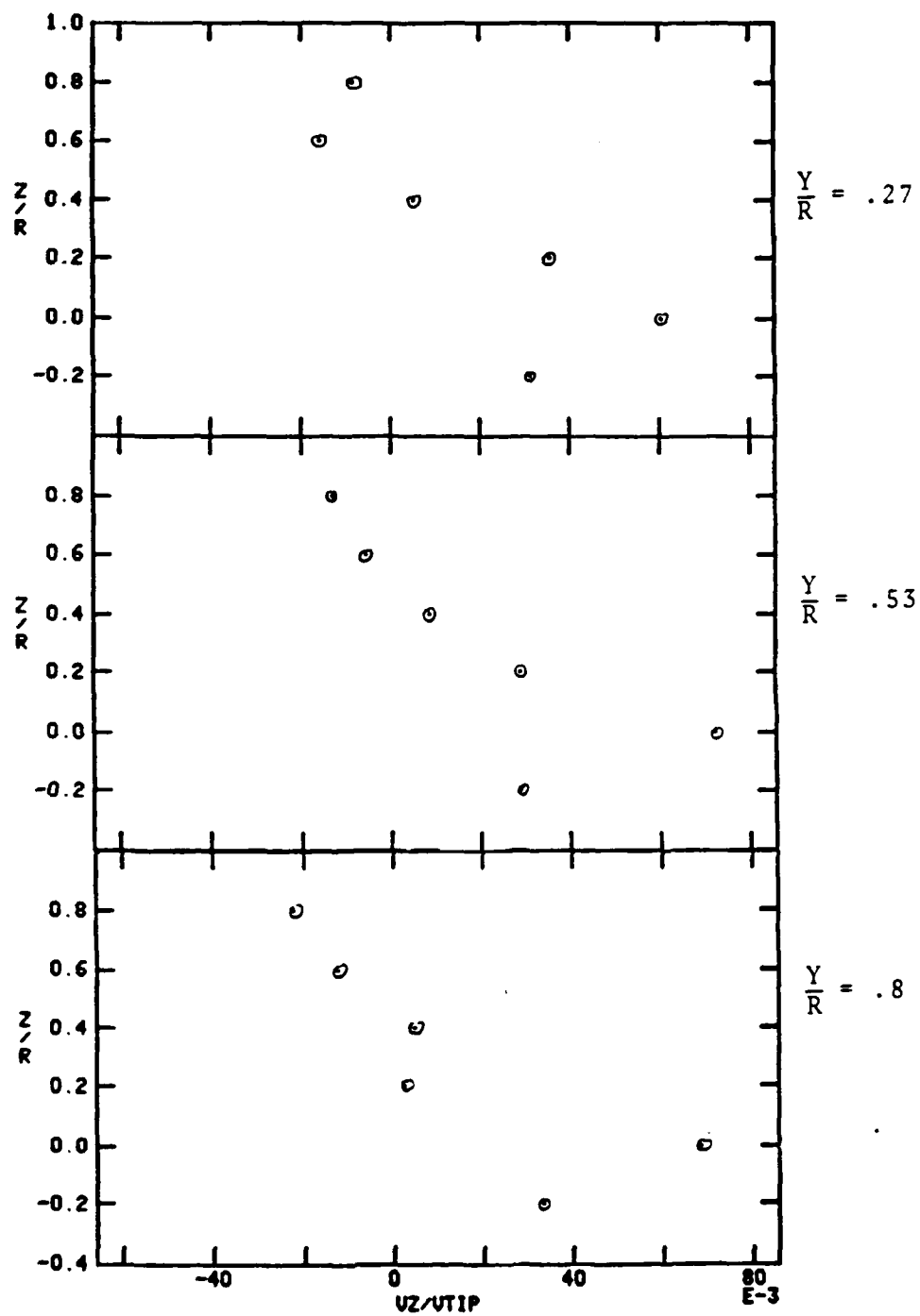
Fig. 4-2 Continued
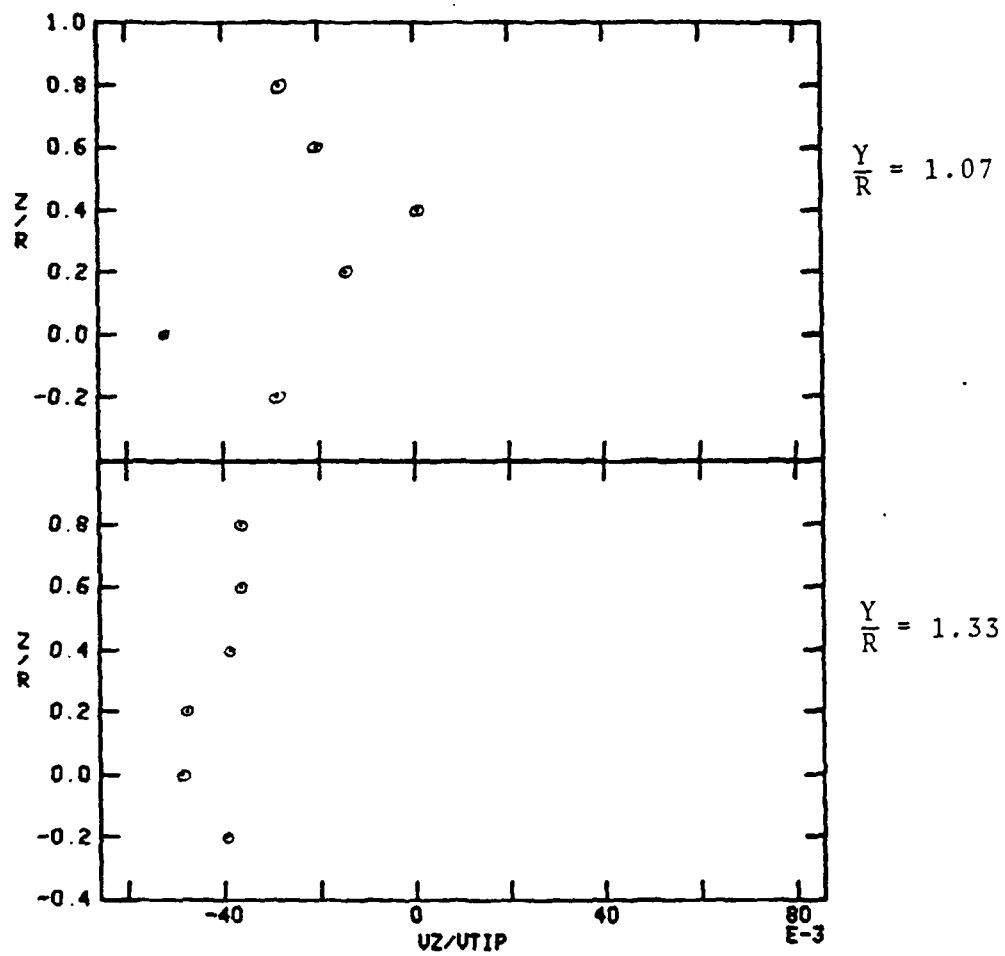
Fig. 4-2 Concluded
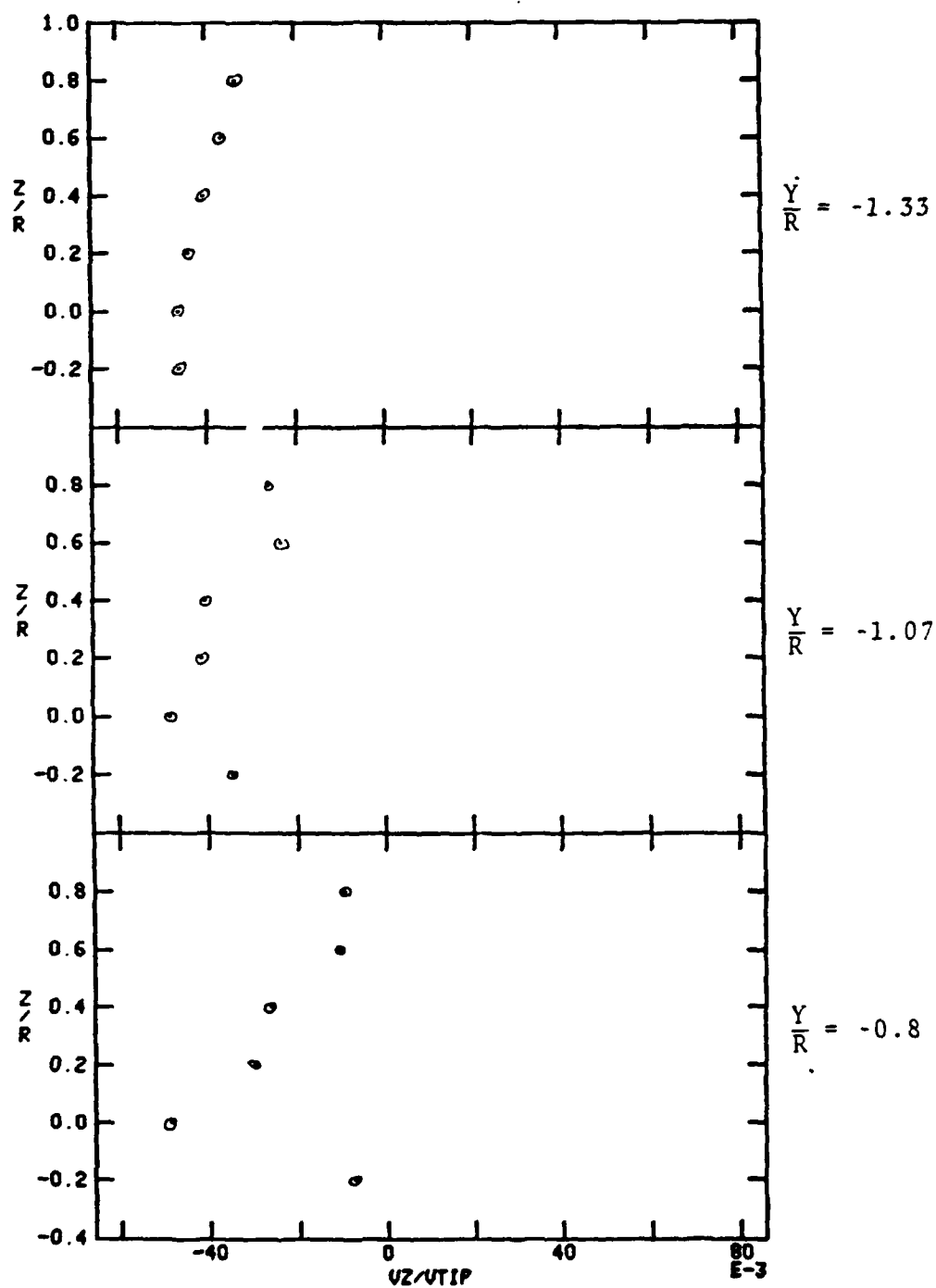
Fig. 4-3   Normal Component of Velocity at Y/R = -1.07 and
ψ = 90
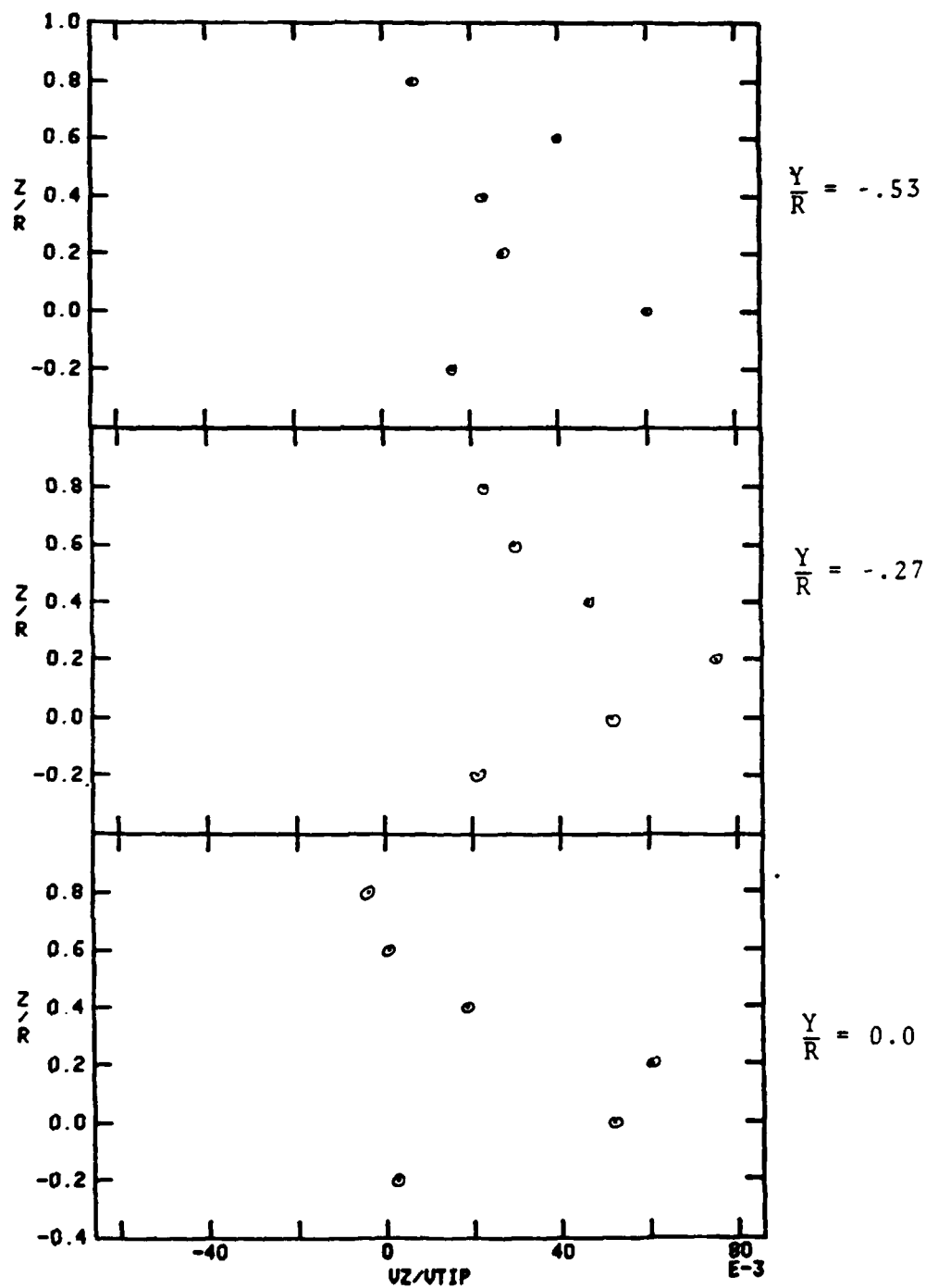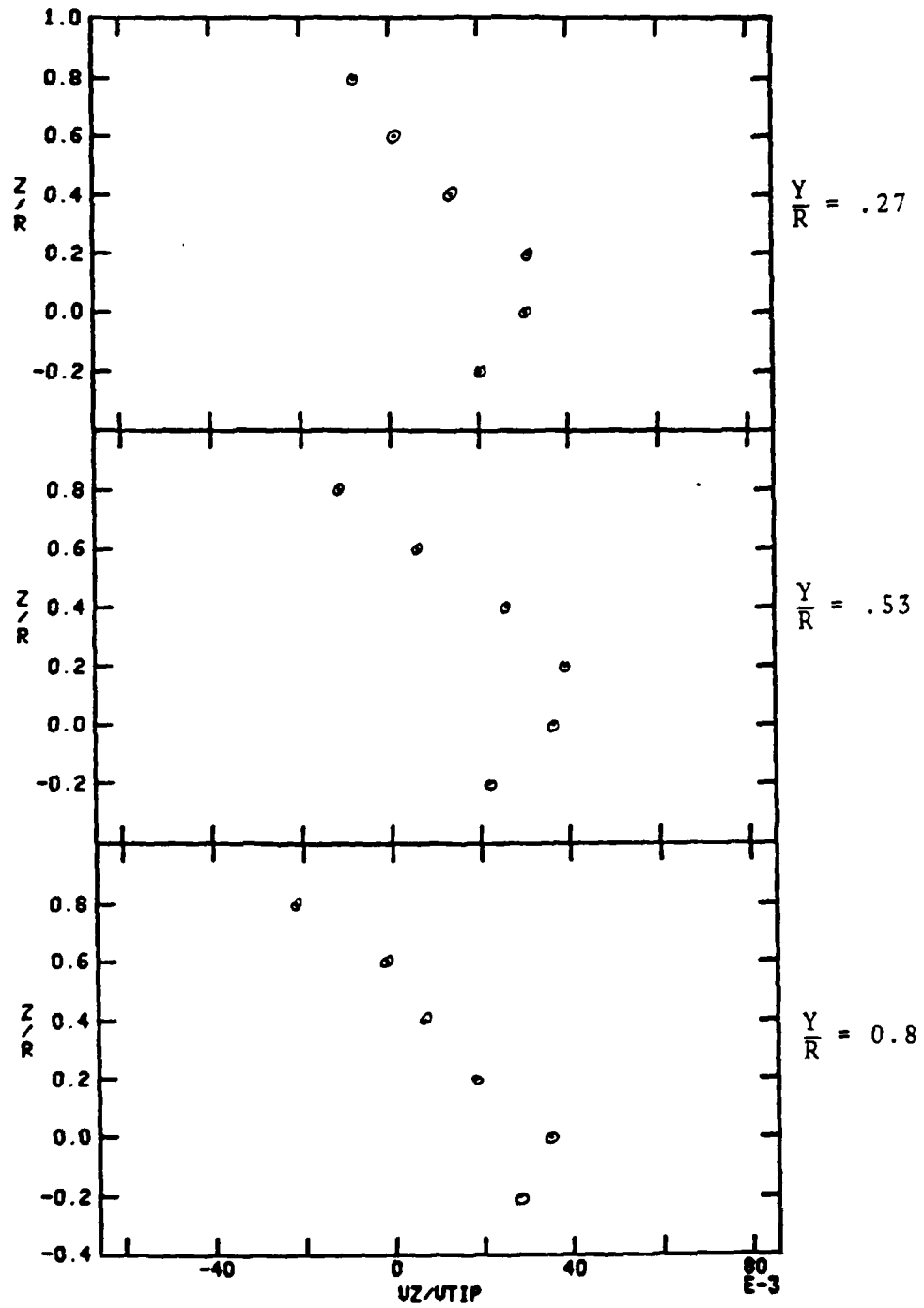
Fig. 4-3 Continued

Fig. 4-3 Continued

54
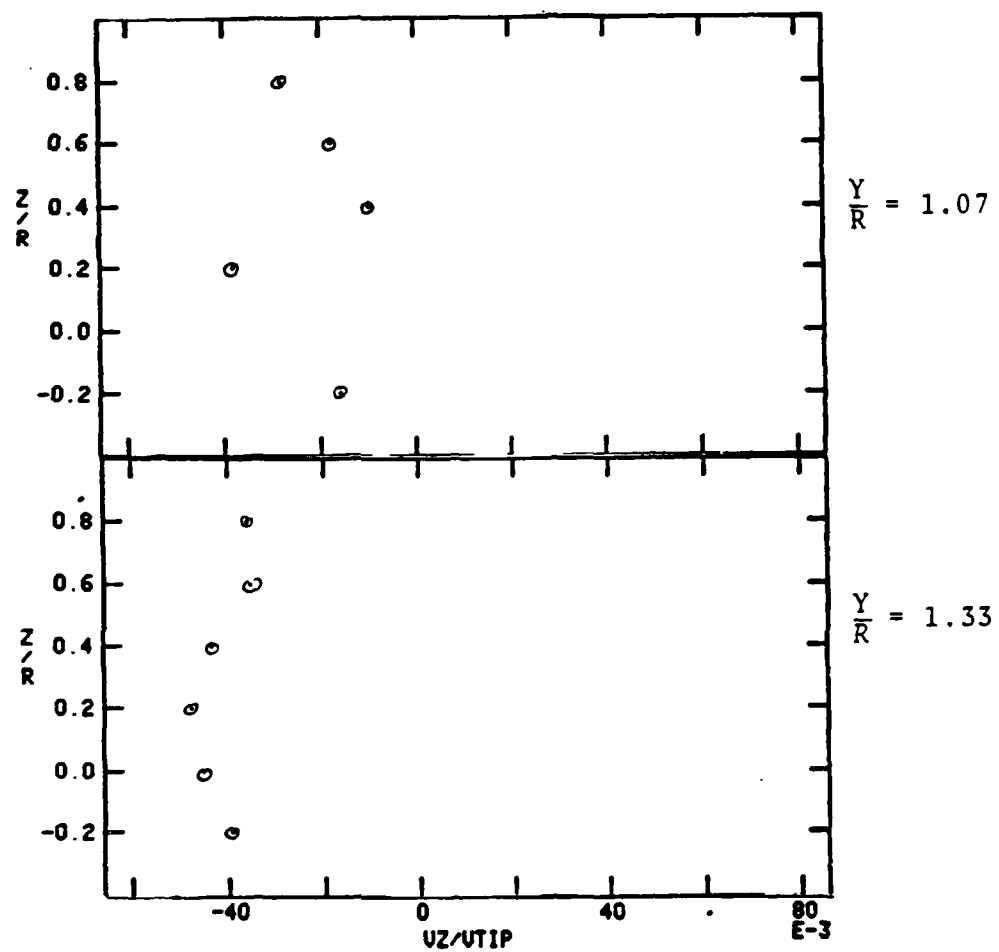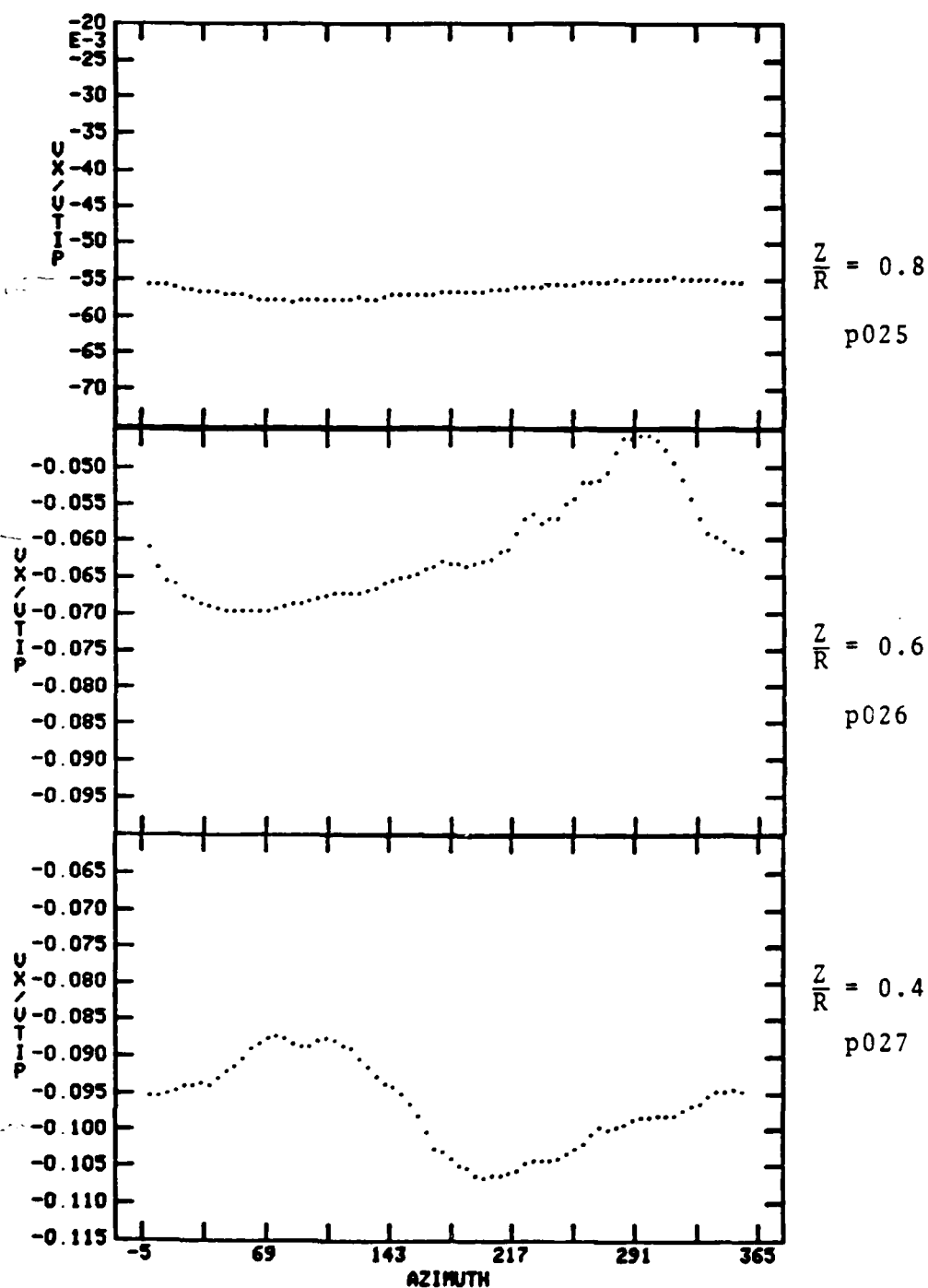
Fig. 4-3 Concluded

Fig. 4-4 Stream Velocity Variation with Azimuth for
          X/R = -1.07 and Y/R = 0.27
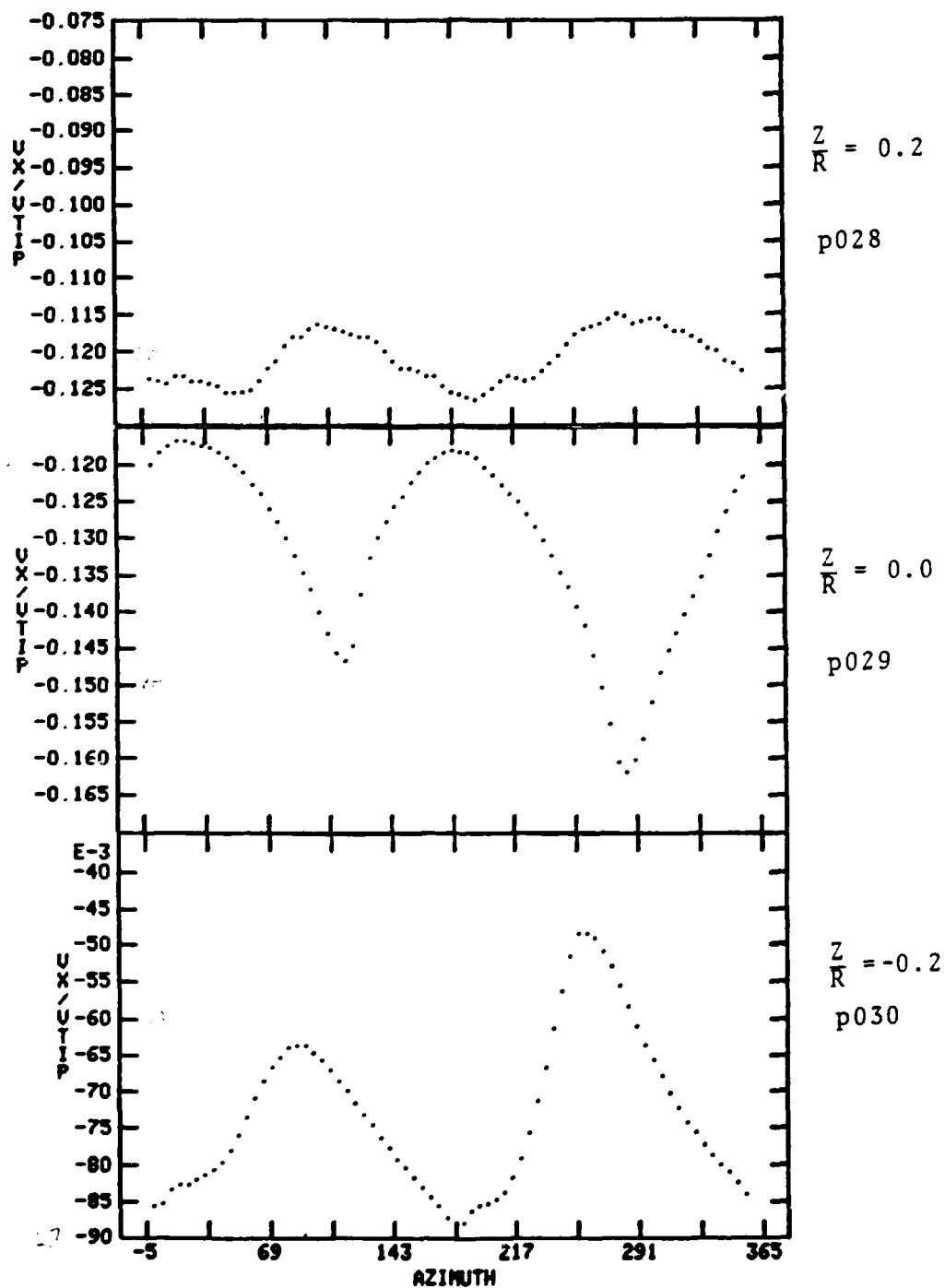
Fig. 4-4   Concluded
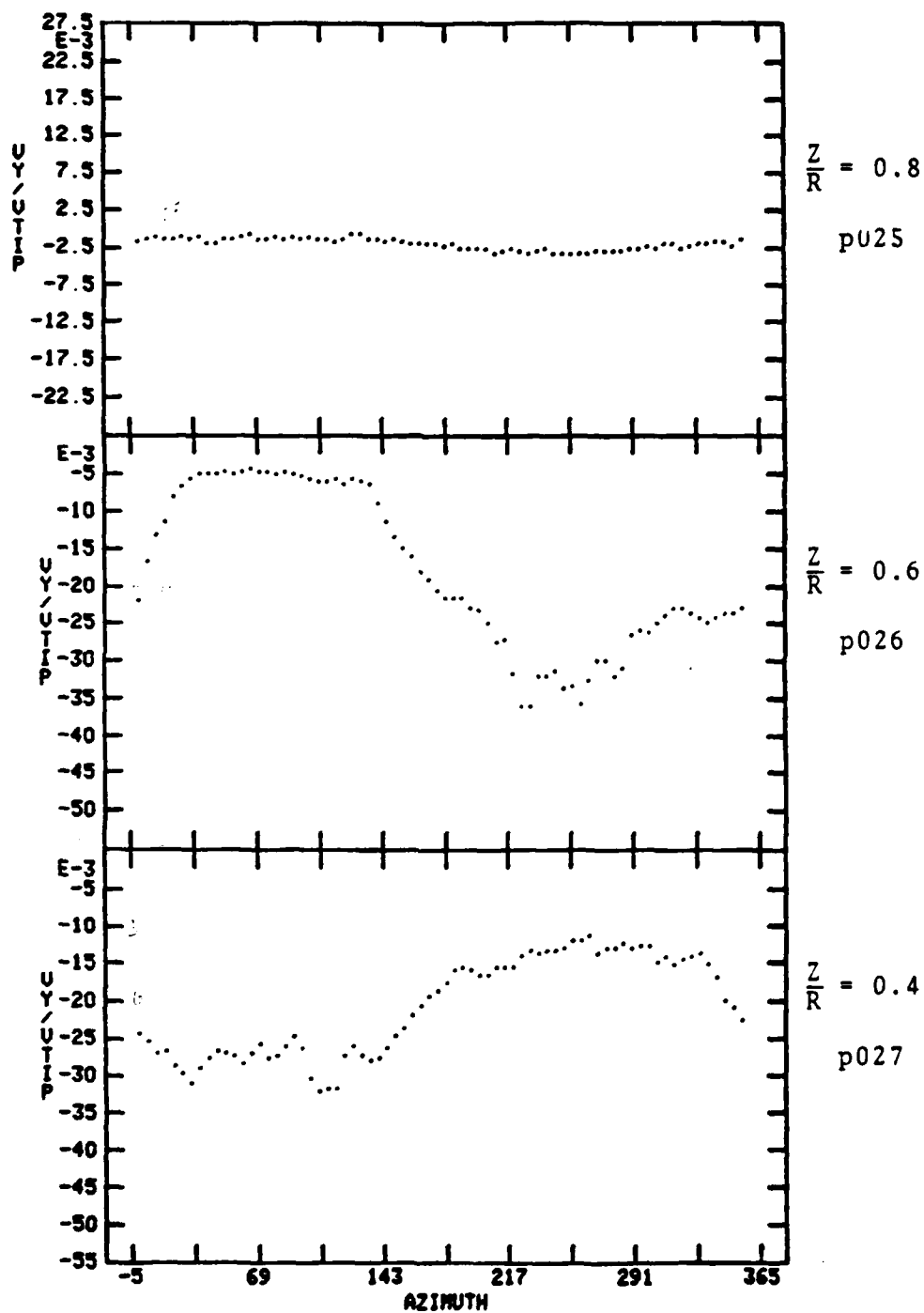
Fig. 4-5 V_y Velocity Variation With Azimuth for $\frac{X}{R}$ = -1.07, $\frac{Y}{R}$ = .27
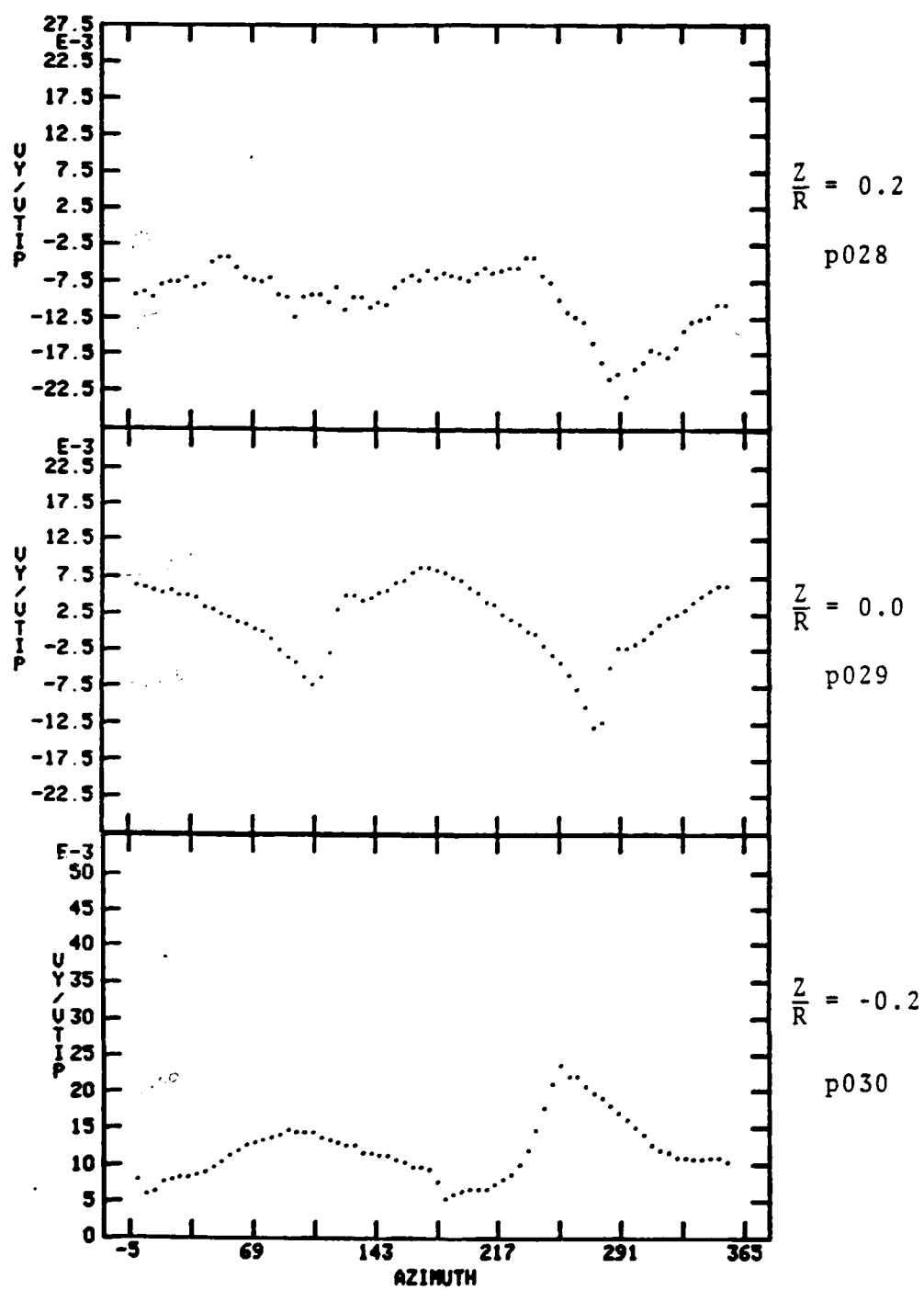
Fig. 4-5   Concluded
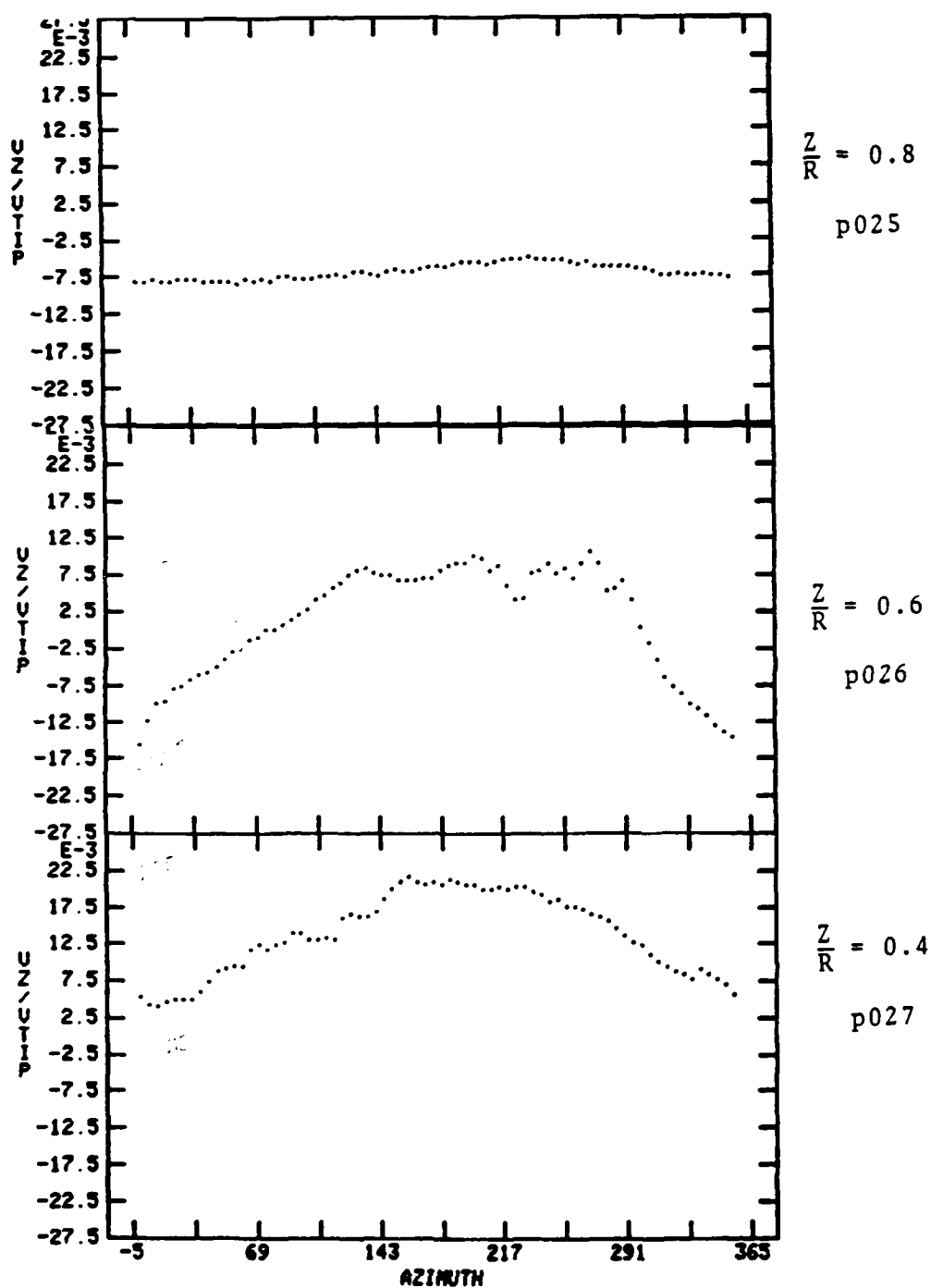
Fig. 4-6 Normal Induced Velocity Variation with Azimuth

$$\frac{X}{R} = -1.07 \quad \frac{Y}{R} = .27$$
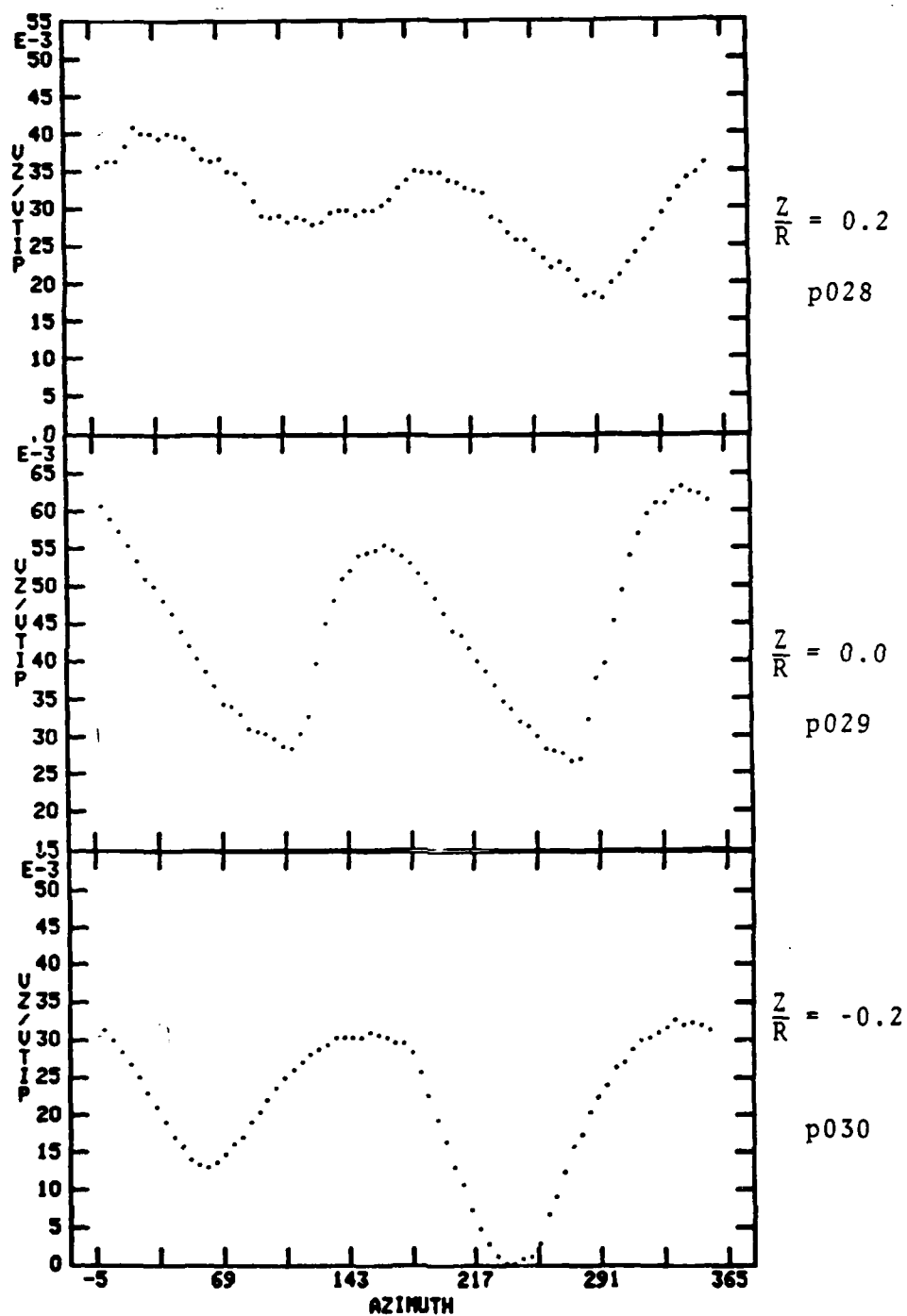
Fig. 4-6 Concluded

CHAPTER V

DISCUSSION OF RESULTS

The plots presented in Chapter IV were a preliminary attempt to check the instrumentation sensitivity and to develop data presentation methods. Therefore, the discussion in this chapter is limited to the plane measured (X/R = -1.07) and to the graphs displayed.

The vector plots shown in Fig. 4-1, displayed flow characteristics similar to the average velocities measured in Ref. 10, that the roll up of the vortex sheet is similar to the roll up of the wake of a low aspect ratio fixed wing. Very little vector movements are apparent between each azimuth position presented. This may probably be attributed to the fact that the tip vortices are rotating in the X-Z plane thus making the velocity component in the Y direction relatively small and its contribution, to the velocity vector in the Z-Y plane, negligible.

Figures 4-2 and 4-3 are a Y traverse at two azimuth angles, $\psi = 0$ and $\psi = 90$ respectively. The flow pattern is similar, i.e. at both azimuth angles the upwash and downwash occur at the same locations. However it was observed that the magnitudes of velocity are larger on the advancing side at $\psi = 90$, and on the retreating side at $\psi = 0$.

Figures 4-4, 4-5 and 4-6 are the time histories of the three components of velocity related to blade azimuth position. Table 4-1 can be used as reference for the figures.

POINT #	X/R	Y/R	Z/R
p025	-1.07	0.27	0.8
p026	-1.07	0.27	0.6
p027	-1.07	0.17	0.4
p028	-1.07	0.27	0.2
p029	-1.07	0.27	0.0
p030	-1.07	0.27	-0.2

The graphs show a distinct variation of the velocity profile with azimuth and normal distance from the rotor. It is clearly observed that 12" (Z/R = 0.8) below the rotor's tip there is no vortex activity indicating that this point (p025) is in the region of uniform flow and outside the rotor's wake boundaries.

Fig. 4-4 at Z/R = 0 and Z/R = -.2 show the distinct 2/REV pulses expected close to the tip of a two bladed rotor. At these points the measured velocities are influenced mainly by the closeness to the tip vortices. As the measured points are further below the rotor there is now a combined influence of the bound vortices, the shed tip vortices and the vortex sheet, creating velocity time histories quite different from the 2/REV measured closer to the blade tip.

The magnitudes of the velocity components V_x, V_y, and V_z as observed at $Z/R = 0.0$ and $Z/R = -0.2$ indicate that the tip vortex rotates in the X-Z plane. (V_x and V_z are much larger than V_y). The change in magnitude of V_x in Fig. 4-4 when traversing the probe from $Z/R = 0.0$ to $Z/R = -.2$ indicates that the vortex rotates in a counter clockwise direction and that the Z coordinate of the vortex core lies between $Z = 0$ (p029) and $Z = -3$ (p030). The reason is that at $Z = 0$ the velocity induced by the tip vortex adds to the stream velocity and at $Z = -3$ (p030) the velocities subtract creating a CCW rotational direction. This conclusion is substantiated by the fact that the tip vortex has to rotate in a CCW direction, from the lower side of the blade (high pressure) to the upper side of the blade (low pressure). Using the CCW direction of rotation of the vortex, as explained above, the velocities' magnitude at $Z = 0$ (p029) and $Z = -3$ (p030) in Fig. 4-6, indicate that the measurements did not traverse thru the core of the vortex, but rather on one side only. The X coordinate of the vortex core lies to the left of the X coordinate of the measured plane ($X/R = -1.07$).

An additional interesting feature that the data revealed was a difference in tip vortex strength. Assuming that the collective pitch and twist of the blade were the same for each blade (our measurements were within $\pm$ 0.5 deg.) the differences in vortex strength could be attributed to differences in plane of rotation between the two blades.

If one of the blades is in a lower plane than the other, the vortices shed by the blades will not be at the same location and the velocities induced by each vortex at a given point in space will be different, such that the furthest one will have lower velocities induced.

CHAPTER VI

CONCLUSIONS AND RECOMMENDATIONS

The instrumentation and the methods developed were found to be a useful tool for measuring the instantaneous velocities in the wake of the model rotor. The results of the preliminary tests show that the instrumentation and the computer were able to handle the vast amount of measurements, and to detect important characteristics of the flow field.

It is recommended to use for data acquisition a graphics terminal (TEKTRONIX 4014) and to make the plotting routines on-line. Such on-line graphics capabilities will enable the operator to concentrate more in the regions of interest and to take less data in areas of low vortex activity.

For better confidence in the collected data it is recommended to have the computer control the RPM of the rotor and the dynamic pressure in the wind tunnel. The data acquisition would be done only when the computer signals that the conditions in the wind tunnel are correct.

65

REFERENCES

1. Goldstein, S., "On the Vortex Theory of Screw Propellers", Royal Society Proceedings, Vol. 123, 1929, p. 440.

2. Coleman, R. P., Feingold, A. M., and Stempin, C. W., "Evaluation of the Induced-Velocity Field of an Idealized Helicopter Rotor", NACA WR L-126, June 1945.

3. ⁴ Drees, J. M., "A Theory of the Airflow Through Rotors and Its Application to Some Helicopter Problems", Journal of the Helicopter Association of Great Britain, Vol. 3, No. 2, July-September 1949, pp. 79-104.

4. Castles, W. and DeLeeuw, J. H., "The Normal Component of the Induced Velocity in the Vicinity of a Lifting Rotor and Some Examples of Its Application", NACA Report 1184, 1954.

5. Miller, R. H., "Rotor Blade Harmonic Air Loading", AIAA Journal, Vol. 2, No. 7, July 1964, pp. 1254-1269.

6. Piziali, R. A. and Du Waldt, F. A., "Computation of Rotary Wing Harmonic Airloads and Comparison With Experimental Results", Proceedings of 18th Annual National Forum, American Helicopter Society, May 1962.

7. Heyson, H. H. and Katzoff, S., "Induced Velocities Near a Lifting Rotor with Nonuniform Disk Loading", NACA Report 1319, 1956.

8. Boatwright, D. W., "Measurement of Velocity Components in the Wake of a Full-Scale Helicopter Rotor in Hover", USAAMRDL TR 72-33, August 1972.

9. Velkoff, H. R. and Horak, D., Rotor Wake Measurements at Very Low Advance Ratios, 35th Annual Forum of the American Helicopter Society, Paper No. 79-G, Washington, D.C., May 1979.

10. Velkoff, H. R., Terkel, H., Shaio, Fu-Kuo, Effect of Changing Rotor Parameters on Rotor Wake Velocities at Very Low Advance Ratios. Fifth European Rotorcraft and Powered Lift Aircraft Forum, Paper No. 32, Amsterdam, The Netherlands, September 1979.

11. Walters, R. E. and Skujins, O., "A Schlieren Technique Applied to Rotor Wake Studies", Proceedings of the Mid East Region Symposium on Status of Testing and Modeling Techniques for V/STOL Aircraft", American Helicopter Society, October 26, 1972.

12. Tanner, W. H. and Wohlfeld, R. M., "Vortex Field, Tip Vortex and Shock Formation on a Model Propeller", Proceedings of Third CAL/USAAVLABS Symposium on Aerodynamics of Rotary Wing and V/STOL Aircraft, Vol. I, June 1969.

13. Landgrebe, Anton J. and Bellinger, Elton D., An Investigation of the Quantitative Applicability of Model Helicopter Rotor Wake Patterns Obtained from a Water Tunnel. United Aircraft Corporation; USAARMRDL Technical Report 71-69; Eustis Directorate, U.S. Army Air Mobility Research and Development Laboratory, Fort Eustis, Virginia, December 1971.

14. Landgrebe, Anton J., An Analytical and Experimental Investigation of Helicopter Rotor Performance and Wake Geometry Characteristics. United Aircraft Corporation; USAAMRDL Technical Report 71-24; Eustis Directorate, U.S. Army Air Mobility Research and Development Laboratory, Fort Eustis, Virginia, June 1971.

15. Sullivan, John P., "An Experimental Investigation of Vortex Rings and Helicopter Wakes Using a Laser Doppler Velocimeter", M.I.T. Aerophysics Laboratory TR-183, June 1973.

16. Biggers, James C. and Orloff, Kenneth L., Laser Velocimeter Measurements, of the Helicopter Rotor Induced Flow Field, Journal of the American Helicopter Society, Vol. 20, No. 1, January 1975.

17. Baskin, V. E., Vil'Dgrube, L. S., Vozhdayev, Y. E. S., and Maykapar, G. I., Theory of Lifting Airscrew, NASA TT F-823, February 1976.

18. Ham, Norman D., An Experimental Investigation of the Effect of a Non-Rigid Wake on Rotor Blade Airloads in Transition Flight, CAL/TRECOM Symposium Proceedings Vol. I, Buffalo, N.Y., June 26-28.

19. Heyson, Harry H., Measurements of the Time-Averaged and Instantaneous Induced Velocities in the Wake of a Helicopter Rotor Hovering at High TIP Speeds, NASA TN D-393, July 1960.

20. Rae, Jr., William H., Limits on Minimum-Speed V/STOL Wind Tunnel Tests, Journal of Aircraft Vol. 4, No. 3, May-June 1967.

21. Horak, D., Development of an Instrumentation System to Measure the Velocities in the Wake of a Rotor, M.Sc. Thesis, The Ohio State University, 1977.

22. Fujita, Hajime and Kovasznay, S. G., Measurement of Reynolds Stress by a Single Rotated Hot Wire Anemometer. The Review of Scientific Instruments. Vol. 39, No. 9, September 1968.

23. Champagne, F. H., Sliecher, C. A., and Wehrmann, O. H., Turbulence Measurement with Inclined Hot-Wires. Journal of Fluid Mechanics. 1967, Vol. 28, part 1, pp. 153-182.

24. Fiehe, C. A. and Schwartz, W. H., Deviations from Cosine Law for Yawed Cylindrical Anemometer Sensors. Journal of Applied Mechanics. Trans. of ASME, December 1968, pp. 655-662.

25. TSI Technical Bulletin No. 8, Data Reduction Method for Model 1294 - 3-D Probes - Orthogonal Sensors.

26. Perry, A. E. and Morrison, G. L., Static and Dynamic Calibrations of Constant Temperature Hot-Wire Systems. Journal of Fluid Mechanics. 1971, Vol. 47, part 4, pp. 765-777.

27. Weidman, P. D. and Browand, F. K., Analysis of a Simple Circuit for Constant Temperature Anemometry. Journal of Physics E: Scientific Instruments. July 1975, Vol. 8, No. 7, pp. 553-560.

28. Bremhorst, K. and Gilmore, D. B., Comparison of Static and Dynamic Hot Wire Anemometer Calibrations for Velocity Perturbation Measurements. Journal of Physics E: Scientific Instruments. December 1976, Vol. 9, No. 12, pp. 1097-1100.

29. TSI Theory and Application Bulletin TB 5: Hot Film and Hot Wire Anemometry.

30. Freymuth, P., Feedback Control Theory for Constant-Temperature Hot-Wire Anemometers, Review of Scientific Instruments, Vol. 38, No. 5, May 1967.

31. Freymuth, P., Noise in Hot-Wire Anemometers, Review of Scientific Instruments, Vol. 39, No. 4, April 1968.

32. Biggers, James C., Lee, Albert, Orloff, Kenneth L., and Lemmer, Opal J., Laser Velocimeter Measurements of Two-Bladed Helicopter Rotor Flow Fields, NASA TM 73238, May 1977.

33. Doebelin, E. O., Measurement Systems. New York, McGraw-Hill, 1975.

Appendix A

A Method of Extending the Frequency Response of Hot
Film Anemometers Beyond Their Natural Capacity

A.1 Determination of the Significant Frequency Content of
the Wake of a Two Bladed Rotor.

The highest frequency that the measuring system
encounters, will be when the vortex sheet or a tip vortex
passes by the sensors. For this case the velocity has an
abrupt change in magnitude, similar to a pulse, and a
high frequency content proportional to the duration of
the pulse. The shorter the pulse is, the higher will be
its frequency content .

In order to get an estimation of what significant
frequencies will be encountered in the wake, a two pulse
per revolution created by the tip vortex of each blade
was simulated by using the measurements of Ref. 32. It
was assumed that the tip vortex is leaving the blade at
some instant and is "travelling" with the wind velocity.
This assumption enabled us to estimate the duration of the
pulse from its length as represented in Ref. 32. The
magnitude of the pulse does not have any effect on its
frequency content. Fig. A-1 shows the wave shape used in
the Fourier analysis to determine the frequency content.
It was assumed also, that between pulses nothing happens

71
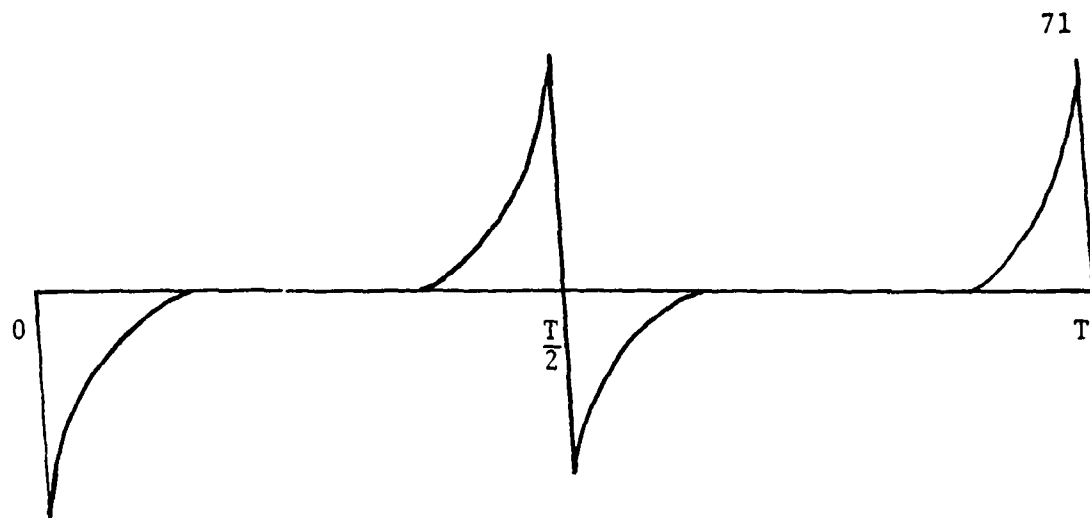
Figure A-1 Simulated 2/REV Vortex (Ref. 32)

a. 100th Harmonics b. 50th Harmonics c. 25th Harmonics
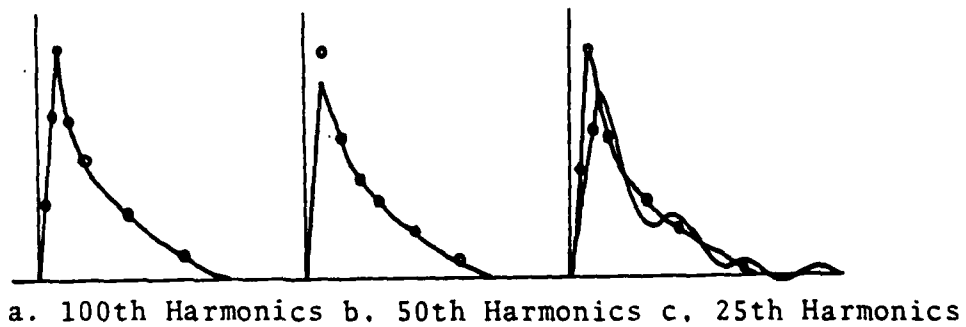
Figure A-2 Harmonics Representation of the Velocity Pulse

in the wake. This assumption, which is not correct, will yield higher harmonics.

The fundamental frequency is the frequency of the rotor, which is 10 Hz in the case of Ref. 32, and each harmonic$ is an integer multiplication of this frequency.

Using a canned Fourier program it was found that using the case of 100th harmonics the spikes were reproduced within 99.9%, the 50th harmonics creates a 10% error only at the peak and the location of the peak is accurate. The 25th harmonics is far from the original shape but it is still quite a good approximation to the velocity pulse. Fig. A-2 shows the positive part of the pulse superimposed on the harmonics representation.

In our case the frequency of the rotor was 37.5 Hz. It was decided to strive for the highest harmonics representation possible, i.e. 100th harmonics. This implied that the required frequency response of the hot film anemometer had to be flat up to 3750 Hz. However, the 0.002" diameter hot film sensor had a flat frequency response up to about 1000 Hz, which is considered high. In order to improve the frequency response of the hot film anemometer it was decided to design a compensator to obtain the desired range of frequency. Sections A-2 and A-3 outline the method and procedures developed.

A.2 Direct Determination of Hot-Film Anemometer Frequency
Response

The method presented here is based on an idea from
Reference 21. Let $G(i\omega)$ be the sinusoidal transfer function
of a dynamic system, $Q_i(i\omega)$ the input spectrum to that
system, and $Q_o(i\omega)$ its output spectrum. Then we can write

$$G(i\omega) = \frac{Q_o(i\omega)}{Q_i(i\omega)} \tag{A-1}$$

A simpler form of equation (A-1) is one using decibel
coordinates, then equation A-1 becomes:

$$20\log_{10}(G(i\omega)) = 20\log(Q_o(i\omega)) - 20\log(Q_i(i\omega)) \tag{A-2}$$

The logic behind this method is to excite the system with
a signal of known frequency spectra to measure the output
spectra, and then to subtract these two spectras. An
additional practical simplification will be, if the input
spectrum is constant, up to a maximum frequency (white
noise), then the output spectrum when normalized represents
actually the sinusoidal transfer function of our system.
This can be written as

$$20\log_{10}G(i\omega) = 20\log_{10}Q_o(i\omega) - N \tag{A-3}$$

where N is the constant input spectrum. In decibals N
just shifts the whole output spectrum up or down.

A special fan was designed and built for this purpose.
The fan is a 4" impeller with 60 blades attached to an
electrical motor with variable speed up to 10000 RPM.
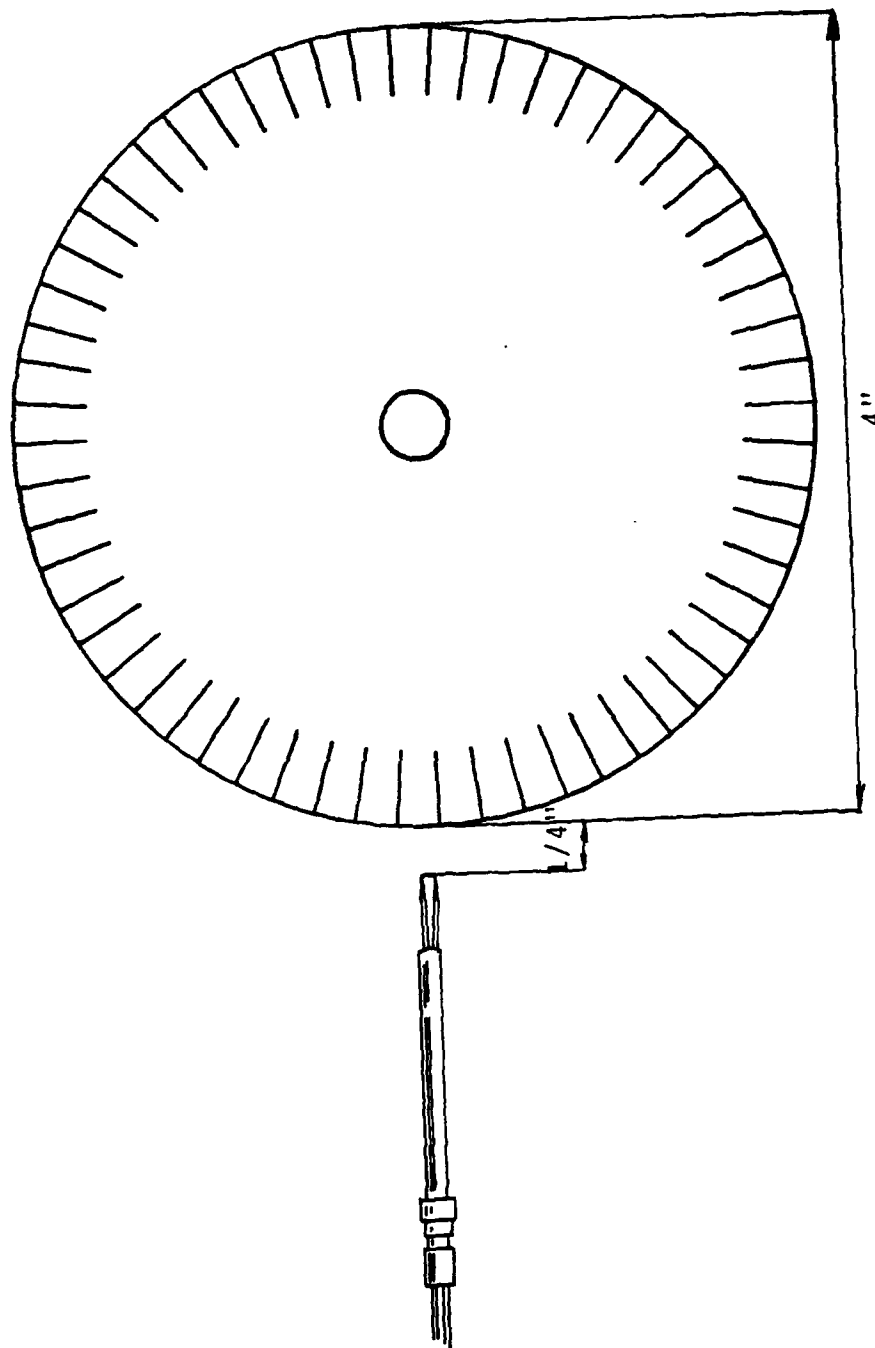
Figure A-3 Velocity White Noise Generator and the Hot-Wire
Sensor
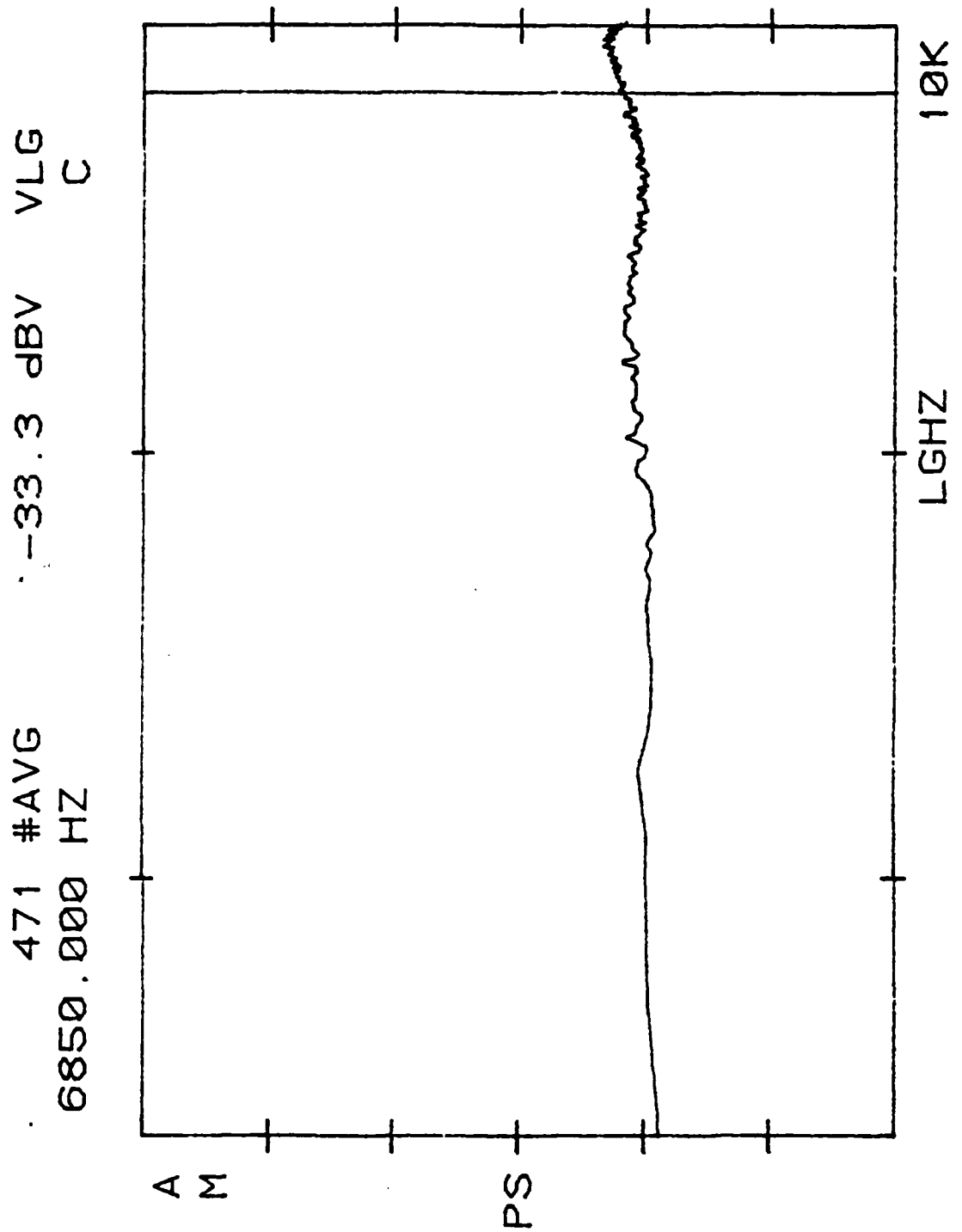
Figure A-4   Reference Spectrum

The impeller produced velocity white noise within $\pm$ 0.5 db up to 10KHz at 10000 RPM. The spectrum was measured by a TSI 0.0004" diameter hot wire with flat frequency response up to 14 KHz measured by an indirect method discussed in Ref. 30. Figure A-3 shows the impeller and the reference hot wire, and Figure A-4 shows the input spectra, calculated by a Nicolet 660-A digital spectrum analyzer.

Once the white noise characteristics of the impeller spectrum was established we proceeded to obtaining the hot film's anemometer break point.

The tested hot film sensor was located at the same location where the references spectrum was obtained. The measured spectrum was the hot film's frequency response as explained before. The point where the assymptote of the flat frequency response meets the assymptote to the roll off indicates the hot film's break point (f_{HF}). (Fig. A-6a)

A.3 The Design of a Lead Compensator to Extend the Frequency Response of the Hot-Film Anemometer

Once the break point of the hot film anemometer was established, as described in Section A-2, a lead compensator was designed to have a roll up to compensate for the hot film's roll off.

The authors of Ref. 27 have shown that the hot film rolls off with a slope of -30 db/DECADE ignoring reactive elements. This kind of slope is very hard to obtain by means of simple operational amplifier circuits. However,

the authors of Ref. 27 have mentioned that the actual slope measured was steeper. Experiments run for this work, using the method described in Section A-2, revealed that the hot film rolls off with a slope of -42 to -47 db/DECADE. This slope is closer to the +40 db/DECADE slope obtainable with OP-AMP circuits. A typical compensator designed and built for this work is shown in Figure A-5.

R_1 = 10 ÷ 250 KΩ R_2 = 15 KΩ
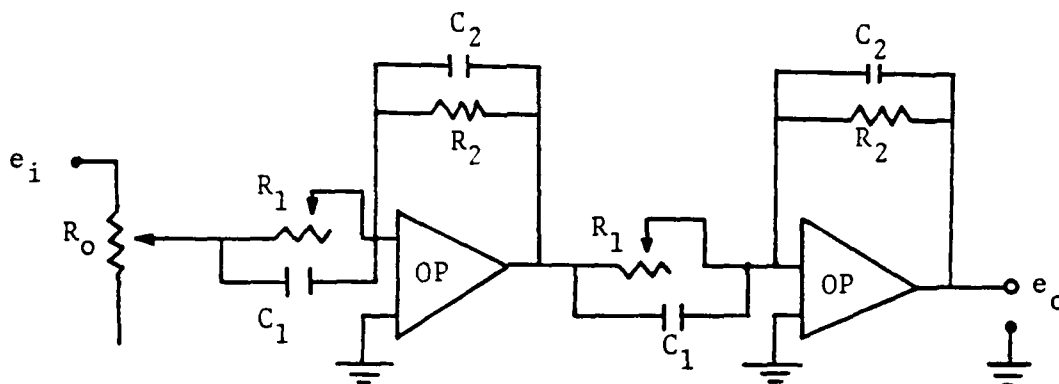
C_1 = 5110 pF C_2 = 90.9 pF

OP = CD471 OPERATIONAL AMPLIFIER

Figure A-5 Lead Compensator Circuit

The transfer function of the compensator is:

$$\frac{\ell_o}{\ell_i}(S) = (\frac{R_2}{R_1})^2 \; [\frac{\tau_1 \, S + 1}{\tau_2 \, S + 1}]^2 \tag{A-3}$$

The numerator is a second order system with damping ratio of one and a roll up of 40 db/DECADE. The denominator is

a second order filter needed to attenuate the high frequency noise associated with differentiators. In addition, three antialising Chebychev filters were used in the ADS to further attenuate the signal for frequencies above 5 KHz. The break point of the compensator is adjustable between 400 to 4000 Hz, according to the measured break point of the hot film anemometer system. The compensator's adjustment is as follows: the hot-film's break point (f_{HF}) is obtained as described in Section A-2. We have found that the best compensation is obtained when the damping ratio of the hot film anemometer system is adjusted to a higher value than the optimum required $(\zeta = 0.7)$ for a good response. This is done by adjusting the offset voltage in the anemometer circuit. The higher damping ratio causes a more sluggish response of the hot film but if the compensator's break point (f_c) is adjusted to approximately 1.5 f_{HF}, the total response is flat within $\pm$ 0.5 db up to 5000 Hz. From the value of f_c, R_1 can now be calculated by means of equation A-4.

$$R_1 = \frac{1}{2\pi f_c\ C_1} = \frac{1}{2\pi (1.5\ f_{HF})\ C_1} \tag{A-4}$$

where $C_1 = 5110 \times 10^{-12}$ F. Any adjustments in R_1 effects the gain of the compensator as shown in equation A-3. The value of R_2 was chosen so that the gain changes between 1:3 to 3:1 at the extreme designated break points of 400 and 4000 Hz. Too high a value of R_1 creates signal to noise

problems where as too low a value saturates the OP-AMP. To overcome these two problems the potentiometer R_o was introduced to increase or decrease the signal according to the existing situation. Figure A-6 shows the response of one of the channels to a velocity white noise, a. without compensation and b. with the lead compensator present.
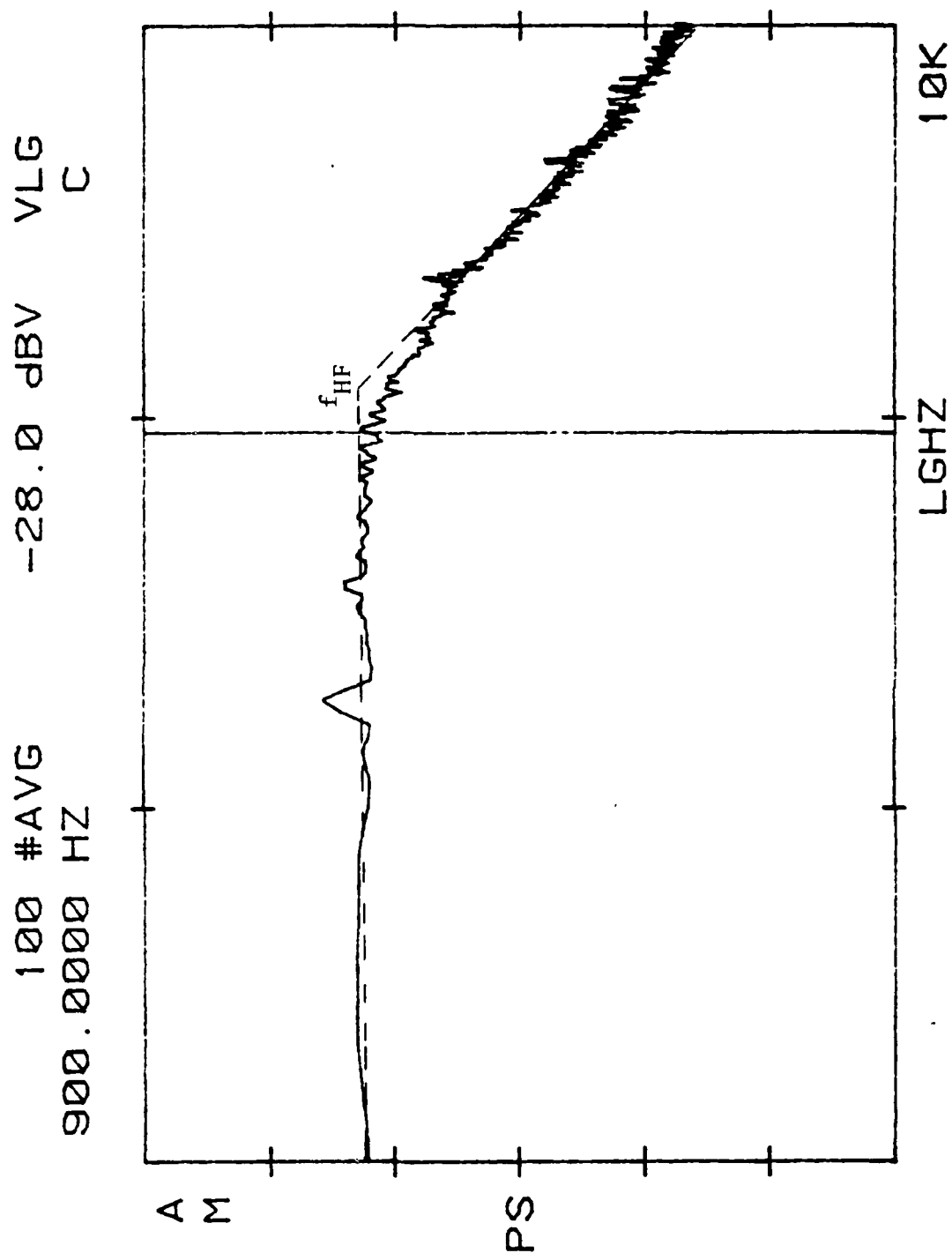
Figure A-6a   Hot Film Anemometer Response Without Compensation
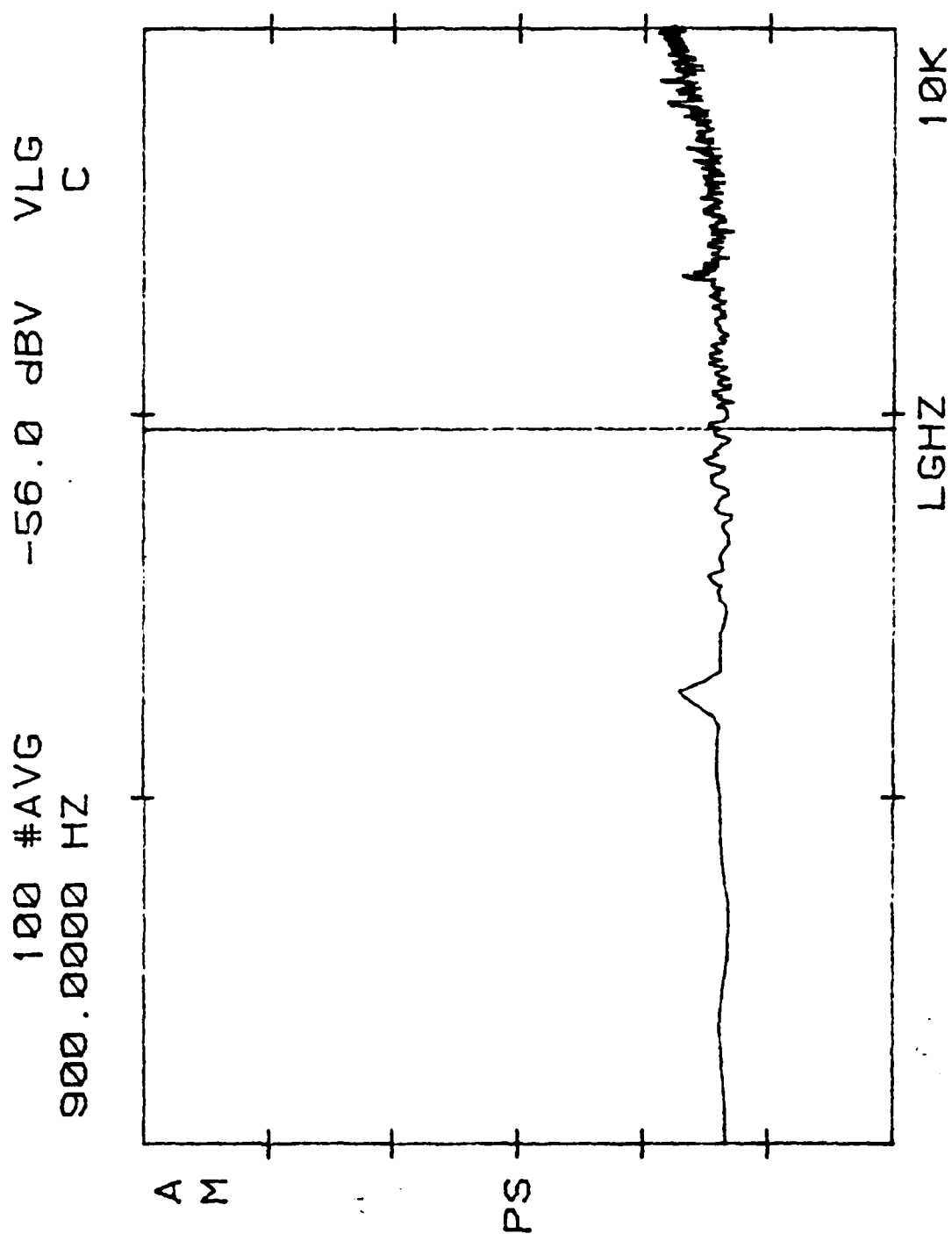
Figure A-6b   Hot-Film Anemometer Response With Compensator

Appendix B

Computer Programs for Instantaneous and
Average Data Acquisition.

B.1 Instantaneous Velocities Acquisition Program (INSTVEL)

INSTVEL is an interactive program used for instantaneous velocities data acquisition. The program controls the analog to digital converter system (ADS) by means of subroutines SETAD1 and GETAD. The ADS sends to the computer the discrete voltage values, as measured by the 3-D hot film anemometer, every five degrees of rotor revolution and for 15 revolutions. The program selects the five degree increment of each revolution from the array BUFFER, averages these values (using the subroutine AVERAG) and then transforms the measured voltages into the effective cooling velocities using the calibration constants of each channel. In the next step the program calculates the total velocity vector (VEL) and its components in the probe coordinate system iterating between VEL, k^2 and ϕ_i using subroutine UKITER and the functions UK1 for sensor A, UK2 for sensor B and UK3 for sensor C. Once the velocity components in probe coordinate system were obtained they are transformed into wind tunnel coordinates. The velocities so obtained are encoded into a one nine digit integer number and stored in a direct access mode. This is done as follows: the three velocity components are multiplied by 10, to make the maximum velocity a

three digit value, and a constant value of 499 is added to
each component to make the velocity positive. Now IVX is
multiplied by 10^6, IVY by 10^3, and the three values are
added. In the program this is done as described below:

$$IVX = IFIX(V_x * 10. + 0.5) + 499$$

$$IVY = IFIX(V_y * 10. + 0.5) + 499$$

$$IVZ = IFIX(V_z * 10. + 0.5) + 499$$

$$NVEL = IVX*10^6 + IVY * 10^3 + IVZ$$

Thus, NVEL is a nine digit integer number which requires
less memory space than the three real values of V_x, V_y, V_z.
In addition, the direct access storage mode compressed the
data even more. This special way of data handling enabled
us to reduce the number of floppy discs required to store
the data for one case, from 6 to one floppy disc. The
location of the probe (x-y-z) was coded and stored in a
similar way. The velocity coding and decoding caused a
maximum error of 0.05 ft/sec which was well within our
measurements error.

B.1.1 Averaging Method for INSTVEL

The averaging was done on the digitized voltages
in order to reduce the number of data points required for
velocity calculations. The computer selected all the data
points at each azimuthal angle (every 72nd element in the
array BUFFER) and calculated the mean of these point using
equation B-1.

$$\overline{E}_{\psi i} = \frac{\sum\limits_{j=1}^{N} E_{\psi j}}{N} \qquad \begin{array}{l} i = 1,2,3\ldots72 \\[6pt] j = 1,2,3\ldots14 \end{array} \qquad \text{(B-1)}$$

Computer printout of the program follows.

```
      INTEGER*4 ARRAY(72),NLOC
     1 ,I,IX,IY,IZ
      INTEGER BUFFER(1024,3)
      DIMENSION EAANG(14),EBANG(14),ECANG(14),V(3),U(3)
     1 ,ASIN(3)

C
C     INITIATE DATA ACQUISION STATUS

      WRITE(5,10)
10    FORMAT(3X,'  IS THIS THE BEGINNIG OF A CASE? ',/,
     1 '  IF YES PRINT A  Y  ,IF NOT PRINT A  N ',')
      READ(5,20) ANS
20    FORMAT(1A1)
      IF(ANS.EQ.'Y') GO TO 30
      OPEN(UNIT=1,NAME='OLDLOC.DAT',TYPE='OLD',ACCESS='DIRECT')
      OPEN(UNIT=2,NAME='ARRAY.DAT',TYPE='OLD',ACCESS='DIRECT')
      OPEN(UNIT=3,NAME='NLOC.DAT',TYPE='OLD',ACCESS='DIRECT')
      READ(1'1) I,IX,IY,IZ,IVCNTS
      GO TO 40
C
30    IX=28
      IY=-20
      IZ=12
      I=1
      IVCNTS=0
      OPEN(UNIT=1,NAME='OLDLOC.DAT',TYPE='NEW',ACCESS='DIRECT'
     1 ,FORM='UNFORMATTED',RECORDSIZE=5)
      OPEN(UNIT=2,NAME='ARRAY.DAT',TYPE='NEW',ACCESS='DIRECT'
     1 ,FORM='UNFORMATTED',RECORDSIZE=72)
      OPEN(UNIT=3,NAME='NLOC.DAT',TYPE='NEW',ACCESS='DIRECT'
     1 ,FORM='UNFORMATTED',RECORDSIZE=1)
      OPEN(UNIT=6,SHARED,NAME='SY:SINE.DAT')
C
C     COMPUTER DETERMINATION OF PROBE LOCATION
C
40    IF(IY.GE.12) WRITE(5,50) IX,IY,IZ
```

```
x

50      FORMAT(3X,' THE PROBE SHOULD BE NOW ON HOLDER  A',/,
        1 ' AT LOCATION:',//,' X= ',I3,/,' Z= ',I3,/,' Y= ',I3)
C
60      IF(IY.LE.8.AND.IY.GE.4) WRITE(5,60) IX,IY,IZ
        FORMAT(3X,' THE PROBE SHOULD BE NOW ON HOLDER B',/,
        1 'AT LOCATION:',//,' X= ',I3,/,' Y= ',I3,/,' Z= ',I3)
C
70      IF(IY.LE.0.AND.IY.GE.-8) WRITE(5,70) IX,IY,IZ
        FORMAT(3X,' THE PROBE SHOULD BE NOW ON HOLDER C',/,
        1 ' AT LOCATION:',//,' X= ',I3,/,' Y= ',I3,/,' Z= ',I3)
C
80      IF(IY.LE.-12) WRITE(5,80) IX,IY,IZ
        FORMAT(3X,' THE PROBE SHOULD BE NOW ON HOLDER D',/,
        1 ' AT LOCATION:',//,' X= ',I3,/,' Y= ',I3,/,' Z= ',I3)
        WRITE(5,90)
90      FORMAT(3X,' WHEN IT IS THERE PRINT OK')
        READ(5,100) LOC
        IF(LOC.NE.'OK') GO TO 40
100     FORMAT(1A2)
C
        MX=(28-IX)/4+1
        MY=(20+IY)/4+1
        MZ=(12-IZ)/3+1
        DO 350  JY=MY,11
        DO 280  JZ=MZ,6
        DO 240  JX=MX,18

C       IND=1
        IF(ABS(IX).LE.12.AND.IZ.LE.3.AND.ABS(IY).LE.12)
        1 CALL ZERO(ARRAY,IND)
        IF(IND.EQ.0) GO TO 170

C       INITIATE A/D CONVERTER
C
110     CALL SETAD1(3,3,1)
        WRITE(5,120)
```

```
      x
120   FORMAT(3X,' NOW PUSH THE SWITCH ON INTERFACE ')
C
C     START A/D CONVERSION
C
      CALL GETAD(BUFFER)
C
C     J COUNTER SELECTS EACH 5 DEGREES INCREMENT
C
      DO 160 J=1,72
      (72=360/5)
C
C     M SELECTS THE CHANNEL
C
      DO 140 M=1,3
      IA=J
C
C     JJ COUNTS THE NO. OF REVOLUTION
C
      DO 130 JJ=1,14
      IF(M.EQ.1) EAANG(JJ)=FLOAT(BUFFER(IA,1))/(32768./8.)
      IF(M.EQ.2) EBANG(JJ)=FLOAT(BUFFER(IA,2))/(32768./8.)
      IF(M.EQ.3) ECANG(JJ)=FLOAT(BUFFER(IA,3))/(32768./8.)
      IA=IA+72
130   CONTINUE
C
C     AVERAGE THE DISCRETE VALUES AT EACH
C     5 DEGREES INCREMENT FOR 14 REVOLUTINS
C
      IF(M.EQ.1) CALL AVERAG(EAANG,AVA)
      IF(M.EQ.2) CALL AVERAG(EBANG,AVB)
      IF(M.EQ.3) CALL AVERAG(ECANG,AVC)
140   CONTINUE
C     VOLTAGE TO VELOCITY CALCULATION
C
C     USE OF CALIBRATION CURVES TO OBTAIN THE CORRESPONDING
C     EFFECTIVE VELOCITIES
```

```
C
C     CALIBRATION CONSTANTS FOR PARTICULAR PROBE
C
      A0=5.74
      A1=-8.7583990
      A2=3.4500208
      A3=-.39423722
      A4=.022448622
      U(1)=A0+A1*AUA+A2*AUA**2+A3*AUA**3+A4*AUA**4
C
      B0=-.34210205
      B1=-.32051355
      B2=.89944941
      B3=-.043491B0
      B4=.004255719
      U(2)=B0+B1*AUB+B2*AUB**2+B3*AUB**3+B4*AUB**4
C
      C0=-.11640930
      C1=-.93899751
      C2=.10894322
      C3=.09231871
      C4=-.00276221
      U(3)=C0+C1*AUC+C2*AUC**2+C3*AUC**3+C4*AUC**4
C
C     CALCULATE MAGNITUDE OF THE ABSOLUTE VELOCITY
      CALL UKITER(U,VEL)
C
C     FIND ANGLES IN PROBE SYSTEM OF COORDINATES
C     USING LOCAL K'S FOR EACH SENSOR
      DO 150 K=1,3
      IF(K.EQ.1) UK=UK1(VEL)
      IF(K.EQ.2) UK=UK2(VEL)
      IF(K.EQ.3) UK=UK3(VEL)
      FF=(1.-(U(K)/VEL)**2.)/(1.-UK)
      IF(FF.LT.0.0) FF=0.0
```

```
C          ASIN(K)=SQRT(FF)
C          IF(ASIN(K).GT.1.)ASIN(K)=1.0
C
C     FIND PERPENDICULAR COMPONENTS OF VELOCITY
C
C          IN PROBE SYSTEM OF COORDINATES
150        U(K)=VEL*ASIN(K)
C
C          IN TUNNEL SYSTEM OF COORDINATES
           UX=-0.57735*(U(1)+U(2)-U(3))
           UZ=0.40825*(U(1)+U(2))+0.8165*U(3)
           UY=-0.70711*(U(2)-U(1))
C
C     ENCODE THE COMPONENTS OF VELOCITY INTO
C     A ONE NINE DIGIT INTEGER NUMBER
C
           IUX=IFIX((UX*10.+0.5)+499
           IUY=IFIX((UY*10.+0.5)+499
           IUZ=IFIX((UZ*10.+0.5)+499
           NVEL=IUX*1000000+IUY*1000+IUZ
           ARRAY(J)=NVEL
160        CONTINUE
C
C     ENCODE THE PROBE'S LOCATION INTO
C     A NINE DIGIT INTEGER NUMBER
C
170        NLOC=(IX+499)*1000000+(IY+499)*1000+IZ+499
C
           WRITE(2'I) (ARRAY(K),K=1,72)
           WRITE(3'I) NLOC
           IF(IND.EQ.0) GO TO 190
           WRITE(5,180)
180        FORMAT(3X,' WAS THE PROBE IN THE CORRECT LOCATION?',//,
          1    ' , IF YES PUSH RETURN ',/,
          2    ' , IF NOT PRINT N ',/)
```

```
      READ(5,20) BACK
      IF(BACK.EQ.'N') GO TO 110

C
C     PROCEED TO THE NEXT POINT OR TERMINATE THE SESSION
C
190   I=I+1
      IX=IX-4
      IF(IX.EQ.12.AND.IZ.LE.3.AND.ABS(IY).LE.12) IND=0
      IF(IND.EQ.0) WRITE(5,200)
200   FORMAT(3X,' YOU ARE NOW IN THE DANGEROUS AREA',//,
     1' MOVE THE PROBE TO Z=6 (78 CNTS),AND THEN TO X=-16')
      IF(IX.LT.-40) IX=28
      IF(IND.EQ.1) WRITE(5,210) IX
210   FORMAT(3X,' MOVE PROBE TO LOCATION',//,
     1' X=',I4)
      IF(IX.EQ.28.AND.IZ.LE.3.AND.ABS(IY).LE.12) WRITE(5,220)
220   FORMAT(3X,' BEFORE YOU MOVE THE PROBE TO X=28',//,
     1' TAKE IT HORIZONTALY TO Z=6 (78 CNTS)')
      WRITE(5,230)
230   FORMAT(3X,' IF YOU WANT TO CONTINUE PUSH RETURN',//,
     1' IF NOT PRINT AN --N--.')
      READ(5,20) ANS
      IF(ANS.EQ.'N') GO TO 360
240   CONTINUE
      MX=1
      IZ=IZ-3
      IF(IZ.LT.-3) IZ=12
      IZCNTS=(12-IZ)*13
      WRITE(5,250) IZ,IZCNTS
250   FORMAT(3X,' MOVE PROBE HORIZONTALY TO',//,
     1' Z=',I4,' EQUIVALENT TO',I4,' (CNTS)')
      WRITE(5,270)
260
270   FORMAT(3X,' PUSH RETURN TO CONTINUE')
      READ(5,20) ZANS
      IF(ZANS.EQ.'N') GO TO 260
280   CONTINUE
```

```
      NZ=1
      IY=IY-4
      IYCNTS=IYCNTS+52
      IF(IY.EQ.8.OR.IY.EQ.0.OR.IY.EQ.-12) IYCNTS=0
      FORMAT(3X,' MOVE THE PROBE VERTICALLY TO ',/,
     1 ' Y=',I4,' EQUIVALENT TO',I4,' (CNTS)',')
      IF(IY.EQ.8) WRITE(5,300)
      FORMAT(3X,' CHANGE PROBE TO HOLDER --B--')
      IF(IY.EQ.0) WRITE(5,310)
      FORMAT(3X,' CHANGE PROBE TO HOLDER --C--')
      IF(IY.EQ.-12) WRITE(5,320)
      FORMAT(3X,' CHANGE PROBE TO HOLDER --D--')
      WRITE(5,290) IY,IYCNTS
      WRITE(5,340)
      FORMAT(3X,' PRINT RETURN TO CONTINUE ',/,
     1 ' YOU CAN NOT TERMINATE THE SESSION FROM HERE')
      READ(5,20) YANS
      IF(YANS.EQ.'N') GO TO 330
      CONTINUE
      WRITE(1'1) I,IX,IY,IZ,IYCNTS
      DO 370 IU=1,3
      CLOSE(UNIT=IU)
      CLOSE(UNIT=6)
      STOP
      END
C     SUBROUTINE ITERATES BETWEEN U & K TO GET VEL-U
C
      SUBROUTINE UKITER(U,VEL)
C
D     DIMENSION U(3),VELI(20)
C     FIRST GUESS FOR K**2 IS 0.06
C
D     VEL=SQRT((U(1)**2+U(2)**2+U(3)**2)/2.06)
D     VELI(1)=VEL
D     DO 77 I=1,19
D     UKA=UK1(VELI(I))
```

290
300
310
320
330
340
350
360
370

```
D        UKB=UK2(VELI(I))
D        UKC=UK3(VELI(I))
D        UK=(UKA+UKB+UKC)/3.
D        VELI(I+1)=SQRT((V(1)*X2+V(2)*X2+V(3)*X2)/(2.+UK))
D77      IF(ABS(VELI(I+1)-VELI(I)).LT.0.01) GO TO 78
D78      CONTINUE
D        VEL=VELI(I)
D        RETURN
D        END

C        FUNCTIONS FOR K=F(U) FOR EACH SENSOR
C
C        SENSOR A
D        FUNCTION UK1(U)
D        UK1=2.219072E-07*U*X4-4.070020E-05*U*X3+.0027199723*U*U-
D        1 0.07945*U+0.9263
D        RETURN
D        END

C        SENSOR B
D        FUNCTION UK2(U)
D        UK2=1.7749664E-07*U*X4-3.4115903E-05*U*X3+.00239459595*U*U-
D        1 .07313832*U+.88759
D        RETURN
D        END

C        SENSOR C
D        FUNCTION UK3(U)
D        UK3=1.7564162E-07*U*X4-3.4339086E-05*U*X3+.0024678740*U*U
D        1 -.078273952*U+.98209
D        RETURN
D        END

C
C        SUBROUTINE AVERAG(A,AV)
```

```fortran
      DIMENSION A(14),SUM(14)
      SUM(1)=A(1)
      DO 9 I=1,13
      SUM(I+1)=SUM(I)+A(I+1)
9     AV=SUM(14)/14.
      RETURN
      END

C     SUBROUTINE TO.SET VX=VY=VZ=0
C     WHEN THE PROBE IS IN THE DANGEROUS REGION
C
      SUBROUTINE ZERO(ARRAY,IND)
      DIMENSION ARRAY(72)
      DO 10 I=1,72
      IVX=499
      IVY=499
      IVZ=499
      NVEL=IVX*1000000+IVY*1000+IVZ
10    ARRAY(I)=NVEL
*     IND=0
      RETURN
      END
```

B.2   Average Velocities Acquisition Program (AVERAGE)

The AVERAGE program is similar in many ways to the INSTVEL program. Thus, only the significant differences are elaborated here.

For the average velocities the azimuth angle of the blades is not relevant. Therefore, the averaging was done over several rotor revolutions. The ADS is triggered continuously by a TTL output from a Waveteck Oscillator until the array BUFFER is filled. A new array (DATA) is defined which includes all the digitized value of one channel at the time. Then, the mean is obtained for each channel and the values are processed in the usual manner.

The three velocity components (V_x, V_y, V_z) and their location are stored in a FORMAT (3I7, 3F7.2) on a hard disc. When the case is completed the whole data set is transferred to a magnetic library available with the large ADMAHL 470 of The Ohio State University, so that the vector plotting routines (Section B.3) could be used.

B.2.1   Averaging Method for AVERAGE

The digitized voltages were averaged so that memory space and computational time could be saved. For this case the data points of each channel were averaged over 40 rotor revolution, which corresponds to 2048 data points. The program selected the first 2048 elements from the array BUFFER for each of the channels and using subroutine AVERAGE the mean was found   by means of equation B-2.

$$\overline{E}_i = \frac{\sum\limits_{j=1}^{n} E_j}{n} \qquad \begin{array}{l} i = 1,2,3 \\ j = 1,2,3\ldots2048 \end{array} \qquad (B\text{-}2)$$

The printout of the computer program AVERAGE fcllows.

```
        INTEGER BUFFER(2048,3)
        DIMENSION DATA(2048)
      1 ,U(3),U(3),ASIN(3)

C       CALL ATTACH
C       INITIATING THE STATUS
C

10      WRITE(5,10)
        FORMAT(3X,' IS THIS THE BEGINNIG OF A CASE? ',/,
      1 ' IF YES PRINT A  Y ,IF NOT PRINT A  N ',)
        READ(5,20) ANS
20      FORMAT(1A1)
        IF(ANS.EQ.'Y') GO TO 90
        OPEN(UNIT=1,SHARED,NAME='OLDLOC.DAT',TYPE='OLD',ACCESS='DIRECT')
        OPEN(UNIT=6,SHARED,NAME='SY:CASE.DAT',TYPE='OLD',ACCESS='APPEND')
        WRITE(5,30)
30      FORMAT(3X,' IF YOU WANT TO CONTINUE FROM PREVIOUS DAY PRINT PRE'
      1 ,/,' IF YOU WANT TO CHOSE THE LOCATION PRINT ICH '
      2 ,//, ' MAKE SURE YOU HAVE DELETED THE BAD DATA '
      3 ,' FROM THE CASE.DAT FILE')
        READ(5,40) PLOC
40      FORMAT(1A3)
        IF(PLOC.EQ.'PRE') READ(1,'1') IX,IY,IZ,IZCNTS
        IF(PLOC.NE.'ICH') GO TO 80
        WRITE(5,50)
50      FORMAT(3X,' PLEASE ENTER X (INTEGER)',/,
      1 ' PLEASE NOTE: IF YOU WANT LOCATION X, PLEASE ENTER X-4 ')
        READ(5,*) IX
        WRITE(5,60)
60      FORMAT(3X,' PLEASE ENTER Y (INTEGER)')
        READ(5,*) IY
        WRITE(5,70)
70      FORMAT(3X,' PLEASE ENTER Z (INTEGER)')
        READ(5,*) IZ
80      IX=IX+4
```

```
      GO TO 100
C
90    IX=-28
      IZ=-20
      IY=12
      IZCNTS=0
      OPEN(UNIT=1,SHARED,NAME='OLDLOC.DAT',TYPE='NEW',ACCESS='DIRECT',
     1 FORM='UNFORMATTED',RECORDSIZE=4)
      OPEN(UNIT=6,SHARED,NAME='SY:CASE.DAT')
C
100   IF(IZ.LE.-12) WRITE(5,110) IX,IZ,IY
C     COMPUTER DETERMINATION OF PROBE LOCATION
C
110   FORMAT(3X,' THE PROBE SHOULD BE NOW ON HOLDER  A',/,
     1 ' AT LOCATION: ',//,' X= ',I3,/,' Z= ',I3,/,' Y= ',I3)
C
120   IF(IZ.LE.-4.AND.IZ.GE.-8) WRITE(5,120) IX,IZ,IY
      FORMAT(3X,' THE PROBE SHOULD BE NOW ON HOLDER B',/,
     1 'AT LOCATION:',//,' X= ',I3,/,' Z= ',I3,/,' Y= ',I3)
C
130   IF(IZ.LE.8.AND.IZ.GE.0) WRITE(5,130) IX,IZ,IY
      FORMAT(3X,' THE PROBE SHOULD BE NOW ON HOLDER C',/,
     1 ' AT LOCATION:',//,' X= ',I3,/,' Z= ',I3,/,' Y= ',I3)
C
140   IF(IZ.GE.12) WRITE(5,140) IX,IZ,IY
      FORMAT(3X,' THE PROBE SHOULD BE NOW ON HOLDER D',/,
     1 ' AT LOCATION: ',//,' X= ',I3,/,' Z= ',I3,/,' Y= ',I3)
150   WRITE(5,160)
160   FORMAT(3X,' LOCATE THE PROBE AT THE GIVEN COORDINATES',/,
     1 ' WHEN IT IS THERE, WRITE OK ')
      READ(5,170) LOC
170   FORMAT(1A2)
      IF(LOC.NE.'OK') GO TO 150
C
      MX=(28+IX)/4+1
      MZ=(20+IZ)/4+1
```

```
      NY=(12-IY)/3+1
      DO 410  JZ=MZ,11
      DO 340  JY=MY,6
      DO 300  JX=MX,18
C
      IND=1
      IF(ABS(IX).LE.12.AND.IY.LE.3.AND.ABS(IZ).LE.12).
     1 CALL ZERO(VX,VY,VZ,IND)
      IF(IND.EQ.0) GO TO 220
C
C     INITIATE A/D CONVERTER
C
180   CALL SETAD1(4,3,1)
C
C     4 means 2048 pnts/cha.
C     3 means 3 channels used
C     1 means a +/-8 volts range
C
C     START A/D CONVERSION
      call getad(buffer)
      DO 200 M=1,3
      DO 190 I=1,2048
      IF(M.EQ.1) DATA(I)=FLOAT(BUFFER(I,1))/(32768./8.)
      IF(M.EQ.2) DATA(I)=FLOAT(BUFFER(I,2))/(32768./8.)
      IF(M.EQ.3) DATA(I)=FLOAT(BUFFER(I,3))/(32768./8.)
190   CONTINUE
C
C     OBTAIN THE MEAN VALUE OF ALL POINTS PER CHANNEL
C
      IF(M.EQ.1) CALL AVERAG(DATA,AVA)
      IF(M.EQ.2) CALL AVERAG(DATA,AVB)
      IF(M.EQ.3) CALL AVERAG(DATA,AVC)
200   CONTINUE
C
C
```

99

```fortran
C
C     USE OF CALIBRATION CURVES TO OBTAIN THE CORRESPONDING
C     EFFECTIVE VELOCITIES
C
C     CALIBRATION CONSTANTS FOR PARTICULAR PROBE
C
      A0=-497.143
      A1=352.93
      A2=-90.328
      A3=9.7716
      A4=-.3556
      U(1)=A0+A1*AVA+A2*AVA**2+A3*AVA**3+A4*AVA**4
C
      B0=-82.799
      B1=-41.06
      B2=-6.4261
      B3=.201
      B4=6.02339
      U(2)=B0+B1*AVB+B2*AVB**2+B3*AVB**3+B4*AVB**4
C
      C0=-281.339
      C1=-188.313
      C2=-45.245
      C3=-4.5344
      C4=-.1426
      U(3)=C0+C1*AVC+C2*AVC**2+C3*AVC**3+C4*AVC**4
C
      WRITE(5,2) (U(IJ),IJ=1,3)
    2 FORMAT(3X,' THE EFF. VEL   ARE',3F7.2)
C
C     CALCULATE MAGNITUDE OF THE ABSOLUTE VELOCITY
C
      CALL UKITER(U,VEL)
D
C     FIND ANGLES IN PROBE SYSTEM OF COORDINATES
C
      DO 210 K=1,3
      IF(K.EQ.1) UK=UK1(VEL)
```

```
*

      IF(K.EQ.2) UK=UK2(UEL)
      IF(K.EQ.3) UK=UK3(UEL)
      FF=(1.-(U(K)/UEL)**2.)/(1.-UK)
      IF(FF.LT.0.0) FF=0.0
      ASIN(K)=SQRT(FF)
      IF(ASIN(K).GT.1.)ASIN(K)=1.0
C
C     FIND  COMPONENTS OF VELOCITY
C
C     IN PROBE SYSTEM OF COORDINATES
210   U(K)=UEL*ASIN(K)
C
C     IN TUNNEL SYSTEM OF COORDINATES
      UX=0.5773S*(U(1)+U(2)-U(3))
      UY=0.4082S*(U(1)+U(2)+0.8165*U(3))
      UZ=0.70711*(U(2)-U(1))
C
C     PROCEED TO NEXT POINT OR TERMINATE THE SESSION
C
      IF(IND.EQ.1) GO TO 240
220   WRITE(5,230)
230   FORMAT(3X,' YOU ARE NOW IN THE DANGEROUS AREA ',/,
     1 ' SET THE PROBE TO THE NEXT SAFE PLACE AT X=16 ',/,
     2 ' WAIT UNTIL THE COMMAND',/,
     3 ' TO MOVE THE PROBE WILL REAPPEAR ')
240   WRITE(5,250)
250   FORMAT(3X,' WAS THE PROBE IN THE CORRECT LOCATION? ',/,
     1 ' IF YES PUSH RETURN',/,
     2 ' IF NOT PRINT N ')
      READ(5,20) BACK
      IF(BACK.EQ.'N') GO TO 180
      WRITE(6,260) IX,IY,IZ,UY,UX,UZ
260   FORMAT(3I7,3F7.2)
      IXX=IX+4
      IF(JX.EQ.18) IXX=-28
      IF(IXX.EQ.-12.AND.IY.LE.3.AND.ABS(IZ).LE.12)
```

```
      1 IND=0
        IF(IND.EQ.0.AND.IXX.EQ.-12) WRITE(5,230)
        IF(IND.EQ.1) WRITE(5,280) IXX
        IF(IXX.EQ.-28.AND.IY.LE.3) WRITE(5,270)
270   FORMAT(3X,' BEFORRE YOU MOVE THE PROBE BACK TO X=-28
     1',/,' TAKE IT BACK HORIZONTALY TO Y=-6 (78 COUNTS)',/,
     2' AND STILL WATCH FOR THE ROTOR! ')
        WRITE(5,290)
280   FORMAT(3X,' MOVE PROBE TO LOCATION ',/,' X= ',I4)
290   FORMAT(3X,' PUNCH IN A RETURN TO CONTINUE SESSION ',/,
     1' PUNCH IN A --N-- TO TERMINATE SESSION ')
        READ(5,20) IANS
        IF(IANS.EQ.'N') GO TO 420
        IX=IX+4
        CONTINUE
        IX=-28
        MX=1
        IY=IY-3
        IF(IY.LT.-3) IY=12
        ICNTS=(12-IY)*13
        WRITE(5,310) IY,ICNTS
310   FORMAT(3X,' MOVE PROBE HORIZONTALLY TO',
     1' Y= ',I4,' EQUIVALEUT TO ',I4,'(CNTS)')
        WRITE(5,330)
330   FORMAT(3X,' PRINT A RETURN TO CONTINUE ',
     1' YOU CAN NOT TERMINATE FROM HERE')
        READ(5,20) YANS
        IF(YANS.EQ.'N') GO TO 320
340   CONTINUE
        MY=1
        IZ=IZ+4
        IZCNTS=IZCNTS+52
        IF(IZ.EQ.-8.OR.IZ.EQ.0.OR.IZ.EQ.12) IZCNTS=0
        FORMAT(3X,' MOVE THE PROBE VERTICALLY TO ',/,
     1' Z= ',I4,' EQUIVALENT TO',I4,' (CNTS)')
350   IF(IZ.EQ.-8) WRITE(5,360)
```

```
      *
  360 FORMAT(3X,' CHANGE PROBE TO HOLDER --B--')
      IF(IZ.EQ.0) WRITE(5,370)
  370 FORMAT(3X,' CHANGE PROBE TO HOLDER --C--')
      IF(IZ.EQ.12) WRITE(5,380)
  380 FORMAT(3X,' CHANGE PROBE TO HOLDER --D--')
      WRITE(5,350) IZ,IZCNTS
  390 WRITE(5,400)
  400 FORMAT(3X,' PRINT RETURN TO CONTINUE ',/,
     1 ' YOU CAN NOT TERMINATE THE SESSION FROM HERE')
      READ(5,20) ZANS
      IF(ZANS.EQ.'N') GO TO 390
  410 CONTINUE
  420 WRITE(1'1) IX,IY,IZ,IZCNTS
      CLOSE(UNIT=1)
      CLOSE(UNIT=6)
      STOP
      END
C
C     SUBROUTINE ITERATES BETWEEN U & K TO GET VEL-U
C
      SUBROUTINE UKITER(V,VEL)
C
C
      DIMENSION VELI(21),V(3)
C     FIRST GUESS FOR K**2 IS 0.06
C
      VEL=SQRT((V(1)**2+V(2)**2+V(3)**2)/2.06)
      VELI(1)=VEL
      DO 77 I=1,20
      UKA=UK1(VELI(I))
      UKB=UK2(VELI(I))
      UKC=UK3(VELI(I))
      UK=(UKA+UKB+UKC)/3.
      VELI(I+1)=SQRT((V(1)**2+V(2)**2+V(3)**2)/(2.+UK))
      IF(ABS(VELI(I+1)-VELI(I)).LT.0.01) GO TO 78
   77 CONTINUE
   78 VEL=VELI(I)
      RETURN
```

```
      END
C
C     FUNCTIONS FOR K=F(U) FOR EACH SENSOR
C
C     SENSOR A
      FUNCTION UK1(UU)
      UK1=2.219072E-07*UU*X4-4.0700208E-05*UU*X3+
     1 .00272*UU*UU-.079*UU+0.926
      RETURN
      END
C
C     SENSOR B
      FUNCTION UK2(UU)
      UK2=1.7749664E-07*UU*X4-3.4115903E-05*UU*X3+.0023945995*
     1 UU*UU-.07331383Z*UU+.88759
      RETURN
      END
C
C     SENSOR C
      FUNCTION UK3(UU)
      UK3=1.7564162E-07*UU*X4-3.4339086E-05*UU*X3+.0024678400*
     1 UU*UU -.0782739952*UU+.98209
      RETURN
      END
C
C
      SUBROUTINE AVERAG(A,AV)
      DIMENSION A(2048),SUM(2048)
      SUM(1)=A(1)
      DO 9 I=1,2047
    9 SUM(I+1)=SUM(I)+A(I+1)
      AV=SUM(2048)/2048.
      RETURN
      END
C
```

```
C     SUBROUTINE TO SET UX=UY=UZ=0
C     FOR THE DANGEROUS LOCATIONS
C     AROUND THE ROTOR

      SUBROUTINE ZERO (UX,UY,UZ,IND)
      UX=0.
      UY=0.
      UZ=0.
      IND=0
      RETURN
      END
```

B.3 SPEAKEASY Programs for Average Velocities Vector Plots

The SPEAKEASY language proved to be a very useful and convenient means of data presentation. The following sections shows the programs and the vector plots obtained. The only difference between each program is the number of vectors used for the plot according to the planes plotted, and the indicator (I) used to select the proper vectors.

B.3.1 Vector Plots of Z-X planes.

For this plane I is defined as:

$$I = GRID(1,1188,18)$$

and 66 vectors were used for each plot. Figure B-1 shows these planes plotted, and the additional information printed, by the computer on each graph.

`:%`

```
EDITING ARROWZX
  1.0 PROGRAM
  2.0 MODEPRINT(OFF)
  3.0 GET CORTW
  4.0 XX=CORTW(I,)
  5.0 FREE CORTW
  5.5 AA=2/3
  6.0 X=-XX(,2)*AA
  7.0 X1=X-(XX(,4)+5.06)/5*AA
  7.5 WHERE(XX(,4).EQ.0) X1=X
  8.0 Q=-XX(1,1)/15
  9.0 Q=ROUNDED(Q,3)
 10.0 Q=BASE(Q,10)
 11.0 Q=CHARACTER(Q)
 12.0 Z=XX(,3)*AA
 13.0 Z1=Z+(XX(,6)-5.57)/5*AA
 13.5 WHERE(XX(,6).EQ.0) Z1=Z
 14.0 B=.6;C=.7
 15.0 FREE XX
 16.0 DZZ1=ABS(ABS(Z)-ABS(Z1))
 17.0 DXX1=ABS(ABS(X)-ABS(X1))
 18.0 X2=X+B*DXX1
 19.0 X3=X+C*DXX1
 20.0 Z2=Z+C*DZZ1
 21.0 Z3=Z+B*DZZ1
 22.0 WHERE(X.GT.X1) X2=X-B*DXX1
 23.0 WHERE(X.GT.X1) X3=X-C*DXX1
 24.0 WHERE(Z.GT.Z1) Z2=Z-C*DZZ1
 25.0 WHERE(Z.GT.Z1) Z3=Z-B*DZZ1
 26.0 HSCALE=(-40,40)
 27.0 VSCALE=(-30,30)
 28.0 TEK(120)
 29.0 JOIN(X1,Z1,X2,Z2)
 30.0 JOIN(X1,Z1,X3,Z3)
```

```
31.0 JOIN(X,Z,X1,Z1)
31.5 FREE X X1 Z Z1 X2 X3 Z2 Z3
32.0 JOIN(-10,-16,-10,16)
33.0 JOIN(-10,-16,8,-16)
34.0 JOIN(8,-16,8,16)
35.0 JOIN(8,16,-10,16)
36.0 XTIC=ARRAY(5:)-10
37.0 XTIC1=XTIC+.5
38.0 N=GRID(0,4,1)
39.0 ZTIC1=ARRAY(5:)-16+12%N%AA
40.0 JOIN(10,-11,10,-11+20/5%AA)
41.0 JOIN(XTIC,ZTIC1,XTIC1,ZTIC1)
42.0 ZTIC1=ARRAY(5:)-8+6%N%AA
43.0 XTIC=ARRAY(5:)-16;XTIC1=XTIC+.5
44.0 JOIN(ZTIC1,XTIC,ZTIC1,XTIC1)
45.0 D=-12;E=-20
46.0 TEXTPUT("1.6",D,-17)
47.0 TEXTPUT("0.8",D,-9)
48.0 TEXTPUT("0.0",D,-1)
49.0 TEXTPUT("-0.8",D,6)
50.0 TEXTPUT("-1.6",D,13)
51.0 TEXTPUT("RETR",D-2,-17.5)
52.0 TEXTPUT("ADVAN",D-2,12)
53.0 TEXTPUT("Y/R",D-2,0)
54.0 TEXTPUT("-0.8",-9,E-1)
55.0 TEXTPUT("-0.4",-5,E-1)
56.0 TEXTPUT("0.0",-1,E)
57.0 TEXTPUT("0.4",3,E)
58.0 TEXTPUT("0.6",5,E)
59.0 TXT1=ARRAY(3,1:"Z/R")
60.0 TEXTPUT(TXT1,0,E-2)
61.0 TXT2="X/R",Q
:%
```

```
 62 TEXTPUT(TXT2,10,5)
 63 TEXTPUT("20 FT/SEC",10,-8)
 64 I=I+1;PRINT MAX(I)
*66 FREE TECK
:%
```
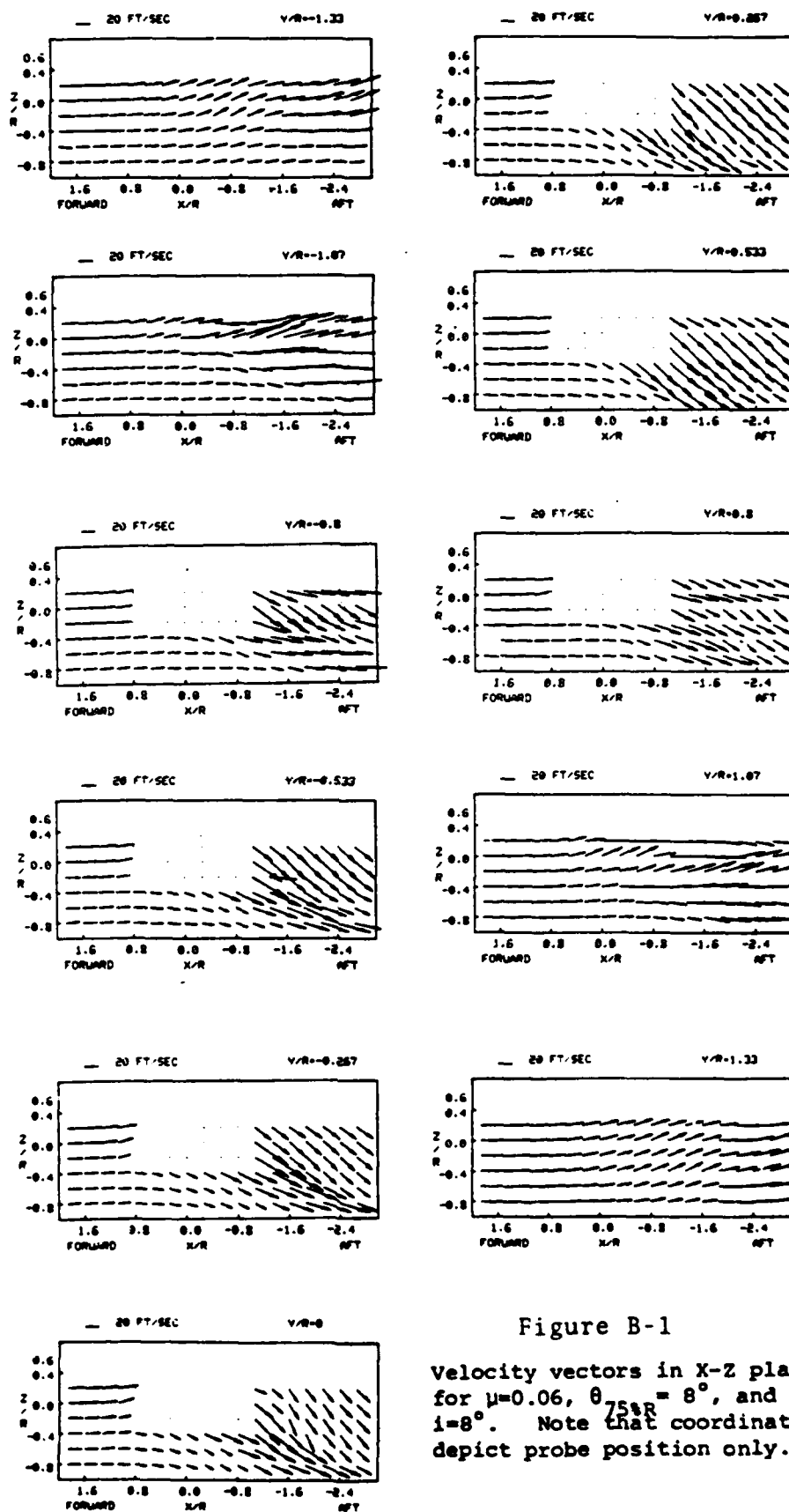
Figure B-1

Velocity vectors in X-Z plane for $\mu=0.06$, $\theta_{75\%R} = 8°$, and $i=8°$. Note that coordinates depict probe position only.

B.3.2 Vector Plots of X-Y Planes.

For this case the initial I is defined as:

$$I = GRID(1,108,1)$$

and 108 vectors were used for each plot. Figure B-2 shows these plots.

```
EDITING ARROWXY
  1 PROGRAM
  2 MODEPRINT(OFF)
  3 GET CORTW
  4 XX=CORTW(I,)
  5 FREE CORTW
  6 AA=2/3
  7 Q=XX(1,3)/15
  8 Q=ROUNDED(Q,3)
  9 Q=BASE(Q,10);Q=CHARACTER(Q)
 10 TEK(120)
 11 X=-XX(,2)%AA
 12 X1=X-(XX(,4)+5.06)/6%AA
 13 WHERE(XX(,4).EQ.0) X1=X
 14 Z=XX(,1)%AA
 15 Z1=Z+XX(,5)/6%AA
 16 WHERE(XX(,4).LT.-90) Z1=Z
 17 B=.6;C=.7
 18 FREE XX
 19 DZZ1=ABS(ABS(Z)-ABS(Z1))
 20 DXX1=ABS(ABS(X)-ABS(X1))
 21 X2=X+B%DXX1
 22 X3=X+C%DXX1
 23 Z2=Z+C%DZZ1
 24 Z3=Z+B%DZZ1
 25 WHERE(X.GT.X1) X2=X-B%DXX1
 26 WHERE(X.GT.X1) X3=X-C%DXX1
 27 WHERE(Z.GT.Z1) Z2=Z-C%DZZ1
 28 WHERE(Z.GT.Z1) Z3=Z-B%DZZ1
 29 HSCALE=(-35,45)
 30 VSCALE=(-30,30)
:%
```

```
31 JOIN(X1,Z1,X2,Z2)
32 JOIN(X1,Z1,X3,Z3)
33 JOIN(X,Z,X1,Z1)
34 FREE X Z X1 Z1 X2 Z2 X3 Z3
35 FREE DXX1 DZZ1
36 JOIN(-10,-20,-10,30)
37 JOIN(-10,-20,8,-20)
38 JOIN(-10,30,8,30)
39 JOIN(8,30,8,-20)
40 XTIC=ARRAY(6:)-10
41 XTIC1=XTIC+.5
42 N=GRID(0,5,1)
43 ZTIC1=ARRAY(6:)-16+12*N*AA
44 JOIN(XTIC,ZTIC1,XTIC1,ZTIC1)
45 N=GRID(0,4,1)
46 ZTIC1=ARRAY(5:)-8+6*N*AA
47 XTIC=ARRAY(5:)-20;XTIC1=XTIC+.5
48 JOIN(ZTIC1,XTIC,ZTIC1,XTIC1)
49 JOIN(10,-16,10,-16+20/6*AA)
50 D=-12;E=-24
51 TEXTPUT("1.6",D,-17)
52 TEXTPUT("0.8",D,-9)
53 TEXTPUT("0.0",D,-1)
54 TEXTPUT("-0.8",D,6)
55 TEXTPUT("-1.6",D,14)
55 TEXTPUT("-2.4",D,22)
57 TEXTPUT("FORWARD",D-2,-18.67)
58 TEXTPUT("X/R",D-2,0)
59 TEXTPUT("AFT",D-2,24)
60 TXT10=ARRAY(3,1:"Z/R");TEXTPUT(TXT10,0,E-2)
61 TEXTPUT("20 FT/SEC",10,-11)
:%
```

```
62 TEXTPUT("-0.8",-9,E-1);TEXTPUT("0.8",-1,E)
63 TEXTPUT("-0.4",-5,E-1);TEXTPUT("0.4",3,E)
64 TEXTPUT("0.6",5,E)
65 TXT12="Y/R=",Q
66 TEXTPUT(TXT12,10,16)
67 I=I+108
68 PRINT MAX(I)
$69 FREE TECK
:%
```
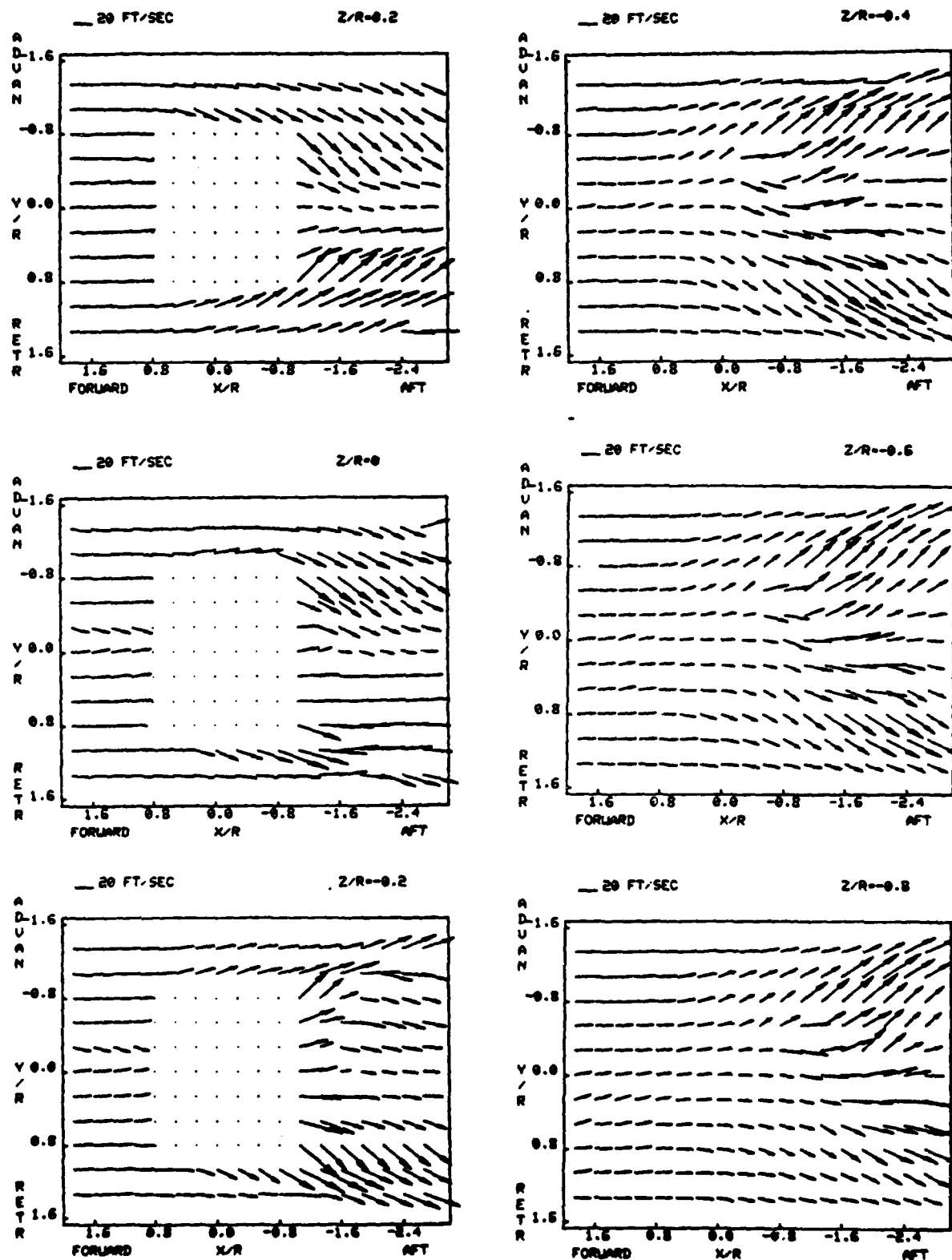
Figure B-2
Velocity vectors in X-Y plane
for $\mu=0.06$, θ_{75eR} = 8°, and
i=8°.   Note that coordinates
depict probe position only.

B.3.3 Vector Plots of Z-Y Planes.

For these planes the indicator I was more complex since the needed points were the first 18 points then 108 had to be shipped and so on, therefore the simple GRID statement could not be used. A small computer program was written to create the I for this case, and it was stored on our magnetic library for future use.

Figure B-3 shows the Z-Y planes obtained by the plotting program.

```
EDITING ARROWZY
  1.0 PROGRAM
  2.0 MODEPRINT(OFF)
  3.0 AA=2/3
  4.0 GET CORTW
  5.0 XX=CORTW(I,)
  6.0 FREE CORTW
  7.0 Q=XX(1,2)
  8.0 Q=-Q/15
  9.0 Q=ROUNDED(Q,3)
 10.0 Q=BASE(Q,10)
 11.0 Q=CHARACTER(Q)
 12.0 X=XX(,3)*AA
 13.0 X1=X+(XX(,6)-5.57)/6*AA
 13.5 WHERE(XX(,6).EQ.0) X1=X
 15.0 Z=XX(,1)*AA
 16.0 Z1=Z+XX(,5)/6*AA
 18.0 B=.6;C=.7
 19.0 FREE XX
 20.0 DZZ1=ABS(ABS(Z)-ABS(Z1))
 21.0 DXX1=ABS(ABS(X)-ABS(X1))
 22.0 X2=X+B*DXX1
 23.0 X3=X+C*DXX1
 24.0 Z2=Z+C*DZZ1
 25.0 Z3=Z+B*DZZ1
 26.0 WHERE(X.GT.X1) X2=X-B*DXX1
 27.0 WHERE(X.GT.X1) X3=X-C*DXX1
 28.0 WHERE(Z.GT.Z1) Z2=Z-C*DZZ1
 29.0 WHERE(Z.GT.Z1) Z3=Z-B*DZZ1
 30.0 HSCALE=(-35,45)
:%
```

```
31  VSCALE=(-30,30)
32  TEK(120)
33  JOIN(X1,Z1,X2,Z2)
34  JOIN(X1,Z1,X3,Z3)
35  JOIN(X,Z,X1,Z1)
36  FREE X,Z,X1,Z1,X2,X3,Z2,Z3
37  JOIN(-16.67,-20,-16.67,30)
38  JOIN(-16.67,-20,16.67,-20)
39  JOIN(-16.67,30,16.67,30)
40  JOIN(16.67,30,16.67,-20)
41  XTIC=ARRAY(6:)-16.67
42  XTIC1=XTIC+.5
43  N=GRID(0,5,1)
44  ZTIC1=ARRAY(6:)-16+12*N*AA
45  JOIN(XTIC,ZTIC1,XTIC1,ZTIC1)
46  XTIC=ARRAY(6:)-20;XTIC1=XTIC+.5
47  ZTIC1=ARRAY(6:)-16+12*N*AA
48  JOIN(ZTIC1,XTIC,ZTIC1,XTIC1)
49  JOIN(20,-16,20,-16-20/6*AA)
50  D=-18;E=-24
51  TEXTPUT("1.6",D,-17)
52  TEXTPUT("0.8",D,-9)
53  TEXTPUT("0.0",D,-1)
54  TEXTPUT("-0.8",D,6)
55  TEXTPUT("-1.6",D,14)
56  TEXTPUT("-2.4",D,22)
57  TXT7="FORWARD";TEXTPUT(TXT7,D-2,-18.67)
58  TXT8="X/R";TEXTPUT(TXT8,D-2,0)
59  TXT9="AFT";TEXTPUT(TXT9,D-2,24)
60  TXT10=ARRAY(3,1:"Y/R");TEXTPUT(TXT10,0,E-2)
61  TXT11="20 FT/SEC";TEXTPUT(TXT11,20,-15)
:%
```

```
62 TEXTPUT("1.6",-16,E);TEXTPUT("0.8",-8,E)
63 TEXTPUT("0.0",0,E);TEXTPUT("-0.8",8,E-1)
64 TEXTPUT("-1.6",16,E-1)
65 TXT12=ARRAY(5,1:"ADVAN")
66 TEXTPUT(TXT12,18,E-2)
67 TXT13=ARRAY(4,1:"RETR")
68 TEXTPUT(TXT13,-13,E-2)
69 TXT14="Z/R=",Q;TEXTPUT(TXT14,20,16)
70 I=I+18;PRINT MAX(I)
*71 FREE TECK
:%
```
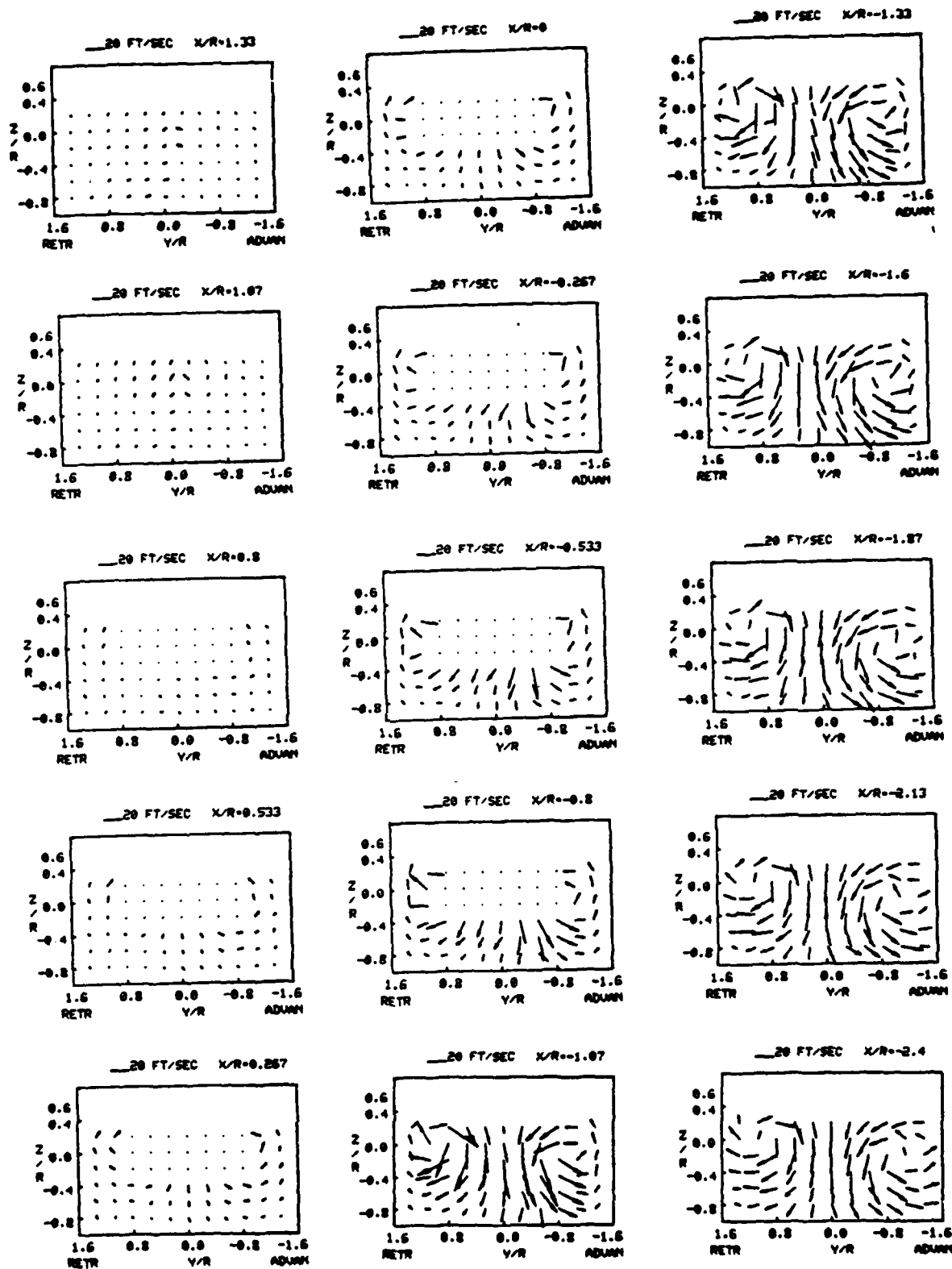
Figure B-3

Velocity vectors in Y-Z plane
for μ=0.06, θ_{75%R} = 8°, and
i=8°. Note that coordinates
depict probe position only.

Appendix C

ADS and Tape Recorder Triggering Circuit - Interface

The purpose in designing and building this device, was to provide a simple method of measuring the rotor's azimuthal angle at five degree increments and to trigger the ADS at each increment for a predetermined number of revolutions. An additional mode of operation wad designed also, that can be used when the analog data is recorded first on a FM analog tape recorder.

As mentioned, there are two modes of data acquisition: 1. Computer Mode, 2. Tape Mode. The modes of operation are selected by the switch SW as shown in Figure C-1. Prior to starting data acquisition the number of revolutions (N) is set, for the case presented in this work, N was 15.

In the computer mode the inputs to the interface are a 1/R and a 72/R signals from two proximity magnetic pickups. The comparators, C1 and C3 are shaping the approximately sinusoidal pulses from the magnetic pickups, into positive square pulses whose duration is the duration of the pulses from the pickups. The role of the monostables, MS1 and MS2, is to create a pulse of constant duration and height whenever there is an output pulse from the comparators. The operator signals that the digitizing process can start by pushing the push button PB. This signal energizes the flip flop (FF) FF2 which sends a constant binary 1 to

the nand gates (N) N1 and N2. N1 energizes, initially, FF1 and also sends the 1/R signal to the counter which compares the number of signals coming from N1 with the preset value of N revolutions. FF1 remains energized as long as the number of signals from N1 is less or equal to N. Since FF1 sends a constant binary[1] to N3, it will transfer all the 72/R pulses to MS8. MS8 is energizing the drive device which creates a 10 volt signal of 1 μsec duration each time there is a 72/REV signal. After 15 revolutions have been counted the process stops, all the FF's are reset, and the system awaits the new initiating signal from PB.

In the tape mode the interface has a dual purpose, one in the record mode and the second in the reproduction mode.

In the record mode SW is in the same position as is the computer mode and the inputs 1/R and 72/R are the same. The A/D triggering is disconnected and one channel of a FM analog tape recorder is connected to tape out. The process is the interface is similar to the computer mode operation, except that now, the signals from N1 and N2 are flowing to MS8 and MS9 respectively. Then MS8 creates, thru G1, a 10V pulse representing a 1/REV signal, and MS (creates, thru G2), a 5V pulse representing a 5 degree increment in rotor rotation. In addition the operation of the tape is con-trolled by the interface. After the operator has pushed PB the tape is operated forward and after 0.5 sec delay

Figure C-1 Interface Generalized Block Diagram

122

the recording starts. The reset signal from the COUNTER energizes MS7 which stops the tape completely.

In the reproduction process the fourth channel of the tape recorder is connected to TAPE IN and SW is switched to tape mode. C2 is adjusted to react only to the 10V signals and C4 reacts to the 5V signals. The A/D output of the interface is connected to the triggering of the ADS. When the operator pushes PB the same process occurs as explained in the computer mode. In addition the tape is operated in the manner explained in the recording mode.

Figure C-1 is a generalized block diagram of the interface, and does not include fine details of the design which were needed to make the system work.